INFORMATION TO USERS

This manuscript has been reproduced from the microfilm master. UMI films the text directly from the original or copy submitted. Thus, some thesis and dissertation copies are in typewriter face, while others may be from any type of computer printer.

The quality of this reproduction is dependent upon the quality of the copy submitted. Broken or indistinct print, colored or poor quality illustrations and photographs, print bleedthrough, substandard margins, and improper alignment can adversely affect reproduction.

In the unlikely event that the author did not send UMI a complete manuscript and there are missing pages, these will be noted. Also, if unauthorized copyright material had to be removed, a note will indicate the deletion.

Oversize materials (e.g., maps, drawings, charts) are reproduced by sectioning the original, beginning at the upper left-hand corner and continuing from left to right in equal sections with small overlaps. Each original is also photographed in one exposure and is included in reduced form at the back of the book.

Photographs included in the original manuscript have been reproduced xerographically in this copy. Higher quality 6" x 9" black and white photographic prints are available for any photographs or illustrations appearing in this copy for an additional charge. Contact UMI directly to order.

UMI

University Microfilms International
A Bell & Howell Information Company
300 North Zeeb Road Ann Arbor, MI 48106-1346 USA
313/761-4700 800/521-0600

Order Number 9510744

Cloning and characterization of fibrillin 2, a new extracellular matrix protein

Zhang, Hui, Ph.D.

City University of New York, 1994

U·M·I
300 N. Zeeb Rd.
Ann Arbor, MI 48106

CLONING AND CHARACTERIZATION OF FIBRILLIN 2, A NEW EXTRACELLULAR MATRIX PROTEIN.

by

Hui Zhang

A dissertation submitted to the Graduate Faculty in Biomedical Sciences in partial fulfillment of the requirements for the degree of Doctor of Philosophy, The City University of New York.

1994

This manuscript has been read and accepted for the Graduate Faculty in Biomedical Sciences in satisfaction of the dissertation requirement for the degree of Doctor of Philosophy.

8/14/95
Date

Francesco Ramirez, Ph.D.
Chair of Examining Committee

Date

Terry A. Krulwich, Ph.D.
Executive Officer

James Bieker, Ph.D.

Sandra Masur, Ph.D.

Robert Mecham, Ph.D.

Mark Taubman, M.D.

Supervisory Committee

The City University of New York

ABSTRACT

CLONING AND CHARACTERIZATION OF FIBRILLIN 2, A NEW EXTRACELLULAR MICROFIBRIL COMPONENT.

by

Hui Zhang

Adviser: Professor Francesco Ramirez

Microfibrils are incompletely characterized structures of the extracellular matrix (ECM), that in association with elastin participate in the formation of the elastic fibers. The gene coding for the major component of microfibrils, fibrillin, has recently been cloned. This fibrillin gene (FBN1) has also been shown to be responsible for Marfan syndrome (MFS), a connective tissue disorder with skeletal, cardiovascular and ocular manifestations. During the cloning of FBN1, a structurally homologous gene (FBN2) was unexpectedly identified. Genetic linkage analysis revealed that FBN2 is tightly linked to an MFS-related disorder, congenital contractual arachnodactyly (CCA). It was therefore proposed that FBN2 produces a protein product that is structurally and functionally related to that of FBN1. The main goal of this thesis project was to test this hypothesis by characterizing the FBN2 product.

First, the FBN2 transcript was cloned in its entirety, and the deduced amino acid sequence was shown to be structurally related to the FBN1 product. Second, antibodies raised against a peptide with FBN2 specific sequence identified the protein encoded by the FBN2 gene (Fib2) in the extracellular microfibrils. The antibodies also revealed that Fib2 is preferentially located in elastin-rich areas of the connective tissues. To confirm and

extend this observation, murine FBN1 and FBN2 cDNA probes were used to establish the pattern of fibrillin expression during mouse embryogenesis by in situ hybridization. These revealed that the FBN1 and FBN2 genes are differentially expressed, both in term of developmental stages and tissue localization. The differential expression of the fibrillin genes strongly suggests that there are differences in microfibril composition and function in various developmental stages and tissues. The postulated differences are consistent with the distinct pathologies resulting from defects in the two fibrillin proteins. This work lays the foundation for more in depth studies elucidating the function and regulation of the fibrillins, and clarifying the role of these proteins in microfibril assembly and elastic tissue formation.

This thesis is dedicated to the memory of my mother,
whose courage, wisdom, and selfless love
inspired me to achieve my goals.

ACKNOWLEDGMENTS

I would like to express my appreciation to the members of my thesis committee for agreeing to serve on the committee, and for their time and effort spent on my behalf: Dr. James Bieker, Dr. Sandra Masur, Dr. Mark Taubman, and especially Dr. Robert Mecham, for his wise scientific and philosophic advises.

A special debt of gratitude is owed to my thesis adviser, Dr. Francseco Ramirez, for his understanding during difficult periods of my life; and for providing the opportunity and guidance to accomplish this project.

I would like to thank Dr. Robert Lazzarini for providing an excellent research environment at Brookdale Center for Molecular Biology; and other faculty members for sharing their knowledge and resources, particularly, Dr. Victor Friedrich, Dr. Thomas Lufkin, Dr. Kevin Kelley, and Dr. Ronald Kohanski.

I would also like to thank all my friends who have shared my happiness and difficulties, and have given me their sincere support over the years. Among them I would like to specifically mention: Dr. Brendan Lee, for introducing me to the world of molecular biology from teaching me how to use a pipetman and what an Eppendorf tube is; Ms. Wei Hu, for her excellent technical assistance; Dr. Lygia Pereira, for being the friend that no one could ever replace; and Yiqin Xu, my dearest friend who always has an ear for my complaints.

I am also grateful to my family in China for giving me love, understanding, and support. I hope my completion of the thesis will be of some reward to them.

Finally, to the very special person in my life, Stephen Apfelroth, I thank him for helping me in every possible way, and standing by me whenever I need.

TABLE OF CONTENTS

LIST OF FIGURES

INTRODUCTION

The proteins of the extracellular matrix (ECM) together with the cells that produce them, form the connective tissue which provides the structural integrity for all tissues and organs of the body. The main fibrous scaffolding of the matrix is provided by the collagens and elastic fibers. Filling the space between the cells and the fibers are soluble precursors of the fibrous proteins, proteoglycans, structural glycoproteins and other molecules secreted by the cells or filtered from the plasma. Elastic fibers confer elasticity to all connective tissues and are therefore present in a wide variety of tissues, especially those under specific and periodic stress. Elastics fiber consist of a highly hydrophobic protein, elastin, and a morphologically distinct microfibrillar component. The gene for one of the microfibrillar proteins, fibrillin, has recently been cloned and shown to cause Marfan syndrome (MFS) when impaired. This work also led to the preliminary identification of another fibrillin-like gene linked to an MFS-like condition, congenital contractural arachnodactyly (CCA). The original aim of this investigation was to verify the existence of this putative microfibrillar protein, and to establish its structural-functional characteristics.

I. Elastic Fibers

Elastic fibers are present in tissues normally subject to stretching and expansile forces, including arteries, pleura, lung, certain ligaments (ligamenta flava of human, and ligmentum nuchae of ruminants), auricular cartilage, vocal cords, and the skin. The reversible elasticity of elastic fibers allows the tissues to recoil after they have been dilated, expanded, or stretched. Such elastic recoil ability is part of the physiological basis for phonation, respiration, and the maintenance of continuous pressure in the circulatory system.

Depending on the strength and direction of the forces exerted on the tissues, elastic fibers may vary in thickness, length, or arrangement in different tissues. With the help of special stains, such as Verhoeff's stain and Weigert's resorcin-fuchsin, elastic fibers can be visualized in histological preparations for light microscopy. In arteries, elastic fibers form thick concentric lamellae, with some interlaminar connecting fibers dispersed radially throughout the media of the vessel. Very large, highly branched elastic fibers are observed in elastic cartilage, such as the auricular cartilage. Thin, rope-like, scattered fibers are seen in the lung tissue outlining the course of the respiratory tree. Similar thin fibers are also observed in elastic ligaments oriented roughly parallel to the axis of the ligament. In skin, the long and branched elastic fibers form a loose network mainly in the deep dermis (Goldberg and Rabinovitch, 1988).

Electron microscopic examination of elastic fibers has shown that while their diameters may vary from 35-50 nm to greater than 100 nm, they all have the same organization (Dempsey and Lansing, 1954; Hall et al., 1955). The major component of the elastic fiber is a cement-like amorphous core of elastin without observable periodicity. At the periphery of this amorphous core is a microfibrillar component with a diameter of about 10 nm. During elastic tissue morphogenesis, these microfibrils appear before elastin in the form and orientation later assumed by the elastic fibers. They are therefore believed to serve as "scaffold" proteins that direct elastic fiber assembly (Cleary and Gibson, 1983).

The soluble precursor of elastin, tropoelastin, is cross-linked by oxidative deamination (via lysyl oxidase) of lysine residues into desmosine and isodesmosine. This polymerization reaction insolublizes the tropoelastin monomers on the pre-existing microfibrillar structure, creating the elastic fiber. Elastin deposits along the microfibrillar bundles eventually embedding some of the bundles within, and displacing others to the peripheral region where microfibrils are seen in the mature fibers.

II. Elastin

Electron microscopic studies of purified elastic fiber using negative staining suggested a fibrillar substructure of the elastin core, consisting of 5 nm filaments (Gotte et al., 1974). This finding was supported by optical diffraction and low angle X-ray scattering analyses (Serafini-Fracassini et al., 1976). The freeze-fracture cryotechnique revealed a 6-7 nm granular structure in bovine ligamentum nuchae in the relaxed state, and quasi-parallel filaments when stretched (Pasquali-Ronchetti and Fornieri, 1984). Quick-freeze, deep-etch electron microscopy was recently used to obtain a three-dimensional surface view of the elastin component in a minimally altered state. This revealed a densely packed, randomly arranged network of fine filaments, 7nm in diameter, as the main structural feature of elastin. This observation was supported by the finding that purified tropoelastin monomers appear as 5-7 nm spheres when examined using freeze-etching and rotary shadowing techniques. The authors therefore proposed that tropoelastin molecules join together in three dimensions to form the filamentous network revealed by freeze-etch electron microscopy (Mecham and Heuser, 1992).

Tropoelastin was first isolated from the aorta of copper-deficient swine (Sandberg et al.,1969). The avalability of peptide sequence from porcine tropoelastin, and cross-species sequence homology allowed cloning of tropoelastin cDNA from human (Indik et al 1987), bovine (Raju and Anwar 1987, Yeh et al 1987), chick (Bressan et al 1987; Tokimitsu et al., 1987), and rat (Deak et al 1988) sources. These cloning experiments confirmed the porcine peptide sequence; they also showed that the primary structure of tropoelastin consists of alternating hydrophobic and cross-linking domains. The hydrophobic regions of different species are variable in both the number and the content of the amino acids. In contrast, the alanine-rich cross-linking domains are highly conserved, particularly in the number of the alanine residues positioned between the lysines. Lysines are always separated by two or three alanines; never by one or more than three. Measurements of circular dichroism indicated that the alanine-rich cross-linking regions are

in an α-helix conformation (Foster et al., 1976). Such secondary structure would bring lysines separated by two or three alanines to the same side of the helix, facilitating the cross-linking reactions (Mecham and Heuser, 1992). Separation by one or four alanines would situate the lysine side chains on opposite sides of the helix where they would unlikely contact one another for a subsequent condensation reaction (Fig.1).

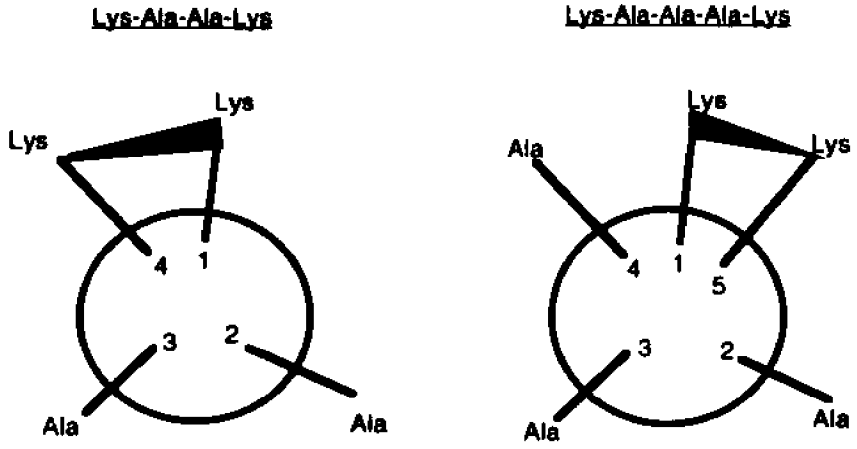

Figure 1: Cross-sectional view of the elastin crosslinking region drawn as an α-helix. Numbers indicate the positions of amino acids, and bars represent the side chains of amino acids extending outward in a helical array. Lysines at position 1 and 4, or 1 and 5 are close to each other and may possibly form intra-molecular cross-links.

Data from a variety of species have indicated that the basic carboxyl-terminus of tropoelastin is highly conserved. The only two cysteines of tropoelastin are found in this part of the molecule. They can form a disulfide bond that stabilizes a positively charged pocket suitable for binding the acidic microfibrils (Brown et al., 1992). This region may be one of the mediators for interactions between elastin and microfibrillar proteins during elastic fiber assembly.

Tropoelastin synthesis takes place in the rough endoplasmic reticulum of elastogenic cells with little post-translational modifications. Once translated, the protein is transported to specific locations within the infoldings of the cell membrane for fiber assembly (Serafini-Fracassini, 1984). The exact process of tropoelastin secretion is poorly understood. Available evidence indicates that a 67-kDa galactose lectin serves as a "chaperon" protein for tropoelastin secretion (Mecham and Heuser, 1992). The affinity of this 67-kDa protein for tropoelastin is minimized upon interaction with sugar (Hinek et al., 1988; Barondes., 1988). It is possible that the sugar groups on the highly glycosylated microfibrillar proteins could serve as the trigger for releasing tropoelastin into the matrix (Mecham et al, 1991). Immediately after secretion, the lysine residues of the tropoelastin crosslinking domains are oxidatively deaminated into allysine through the action of the copper-dependent lysyl oxidase enzyme. The aldehyde residues of allysines and the ε-amino group on lysine side chain are then condensed into desmosine and isodesmosin (Fig. 2, Paz et al., 1982). About 70% of the lysine residues in elastin are involved in these interactions (Mecham and Heuser, 1992).

Mature elastin is an inert macromolecule with two major characteristics, insolubility and elasticity. It is highly resistant to protein solvents and hydrolysis with dilute acids or alkali. More than 60% of the amino acids in elastin are neutral. The content of glycine, proline, alanine and valine is particularly high. The preponderance of hydrophobic residues explains in part the high insolubility of elastin. The lysine cross-links between the soluble protein monomers are, however, the main contributors to the insoluble nature of the elastin polymer. The presence of hydrophobic amino acids also leads to lipid and Ca^{++} deposition on the mature elastic fiber during aging and atherosclerosis (Labat-Robert, et al. 1990). This deposition may result in progressive loss of elasticity and early degradation of the protein. Finally, the low content of charged amino acids in elastin accounts for the poor staining of this protein by ionic dyes.

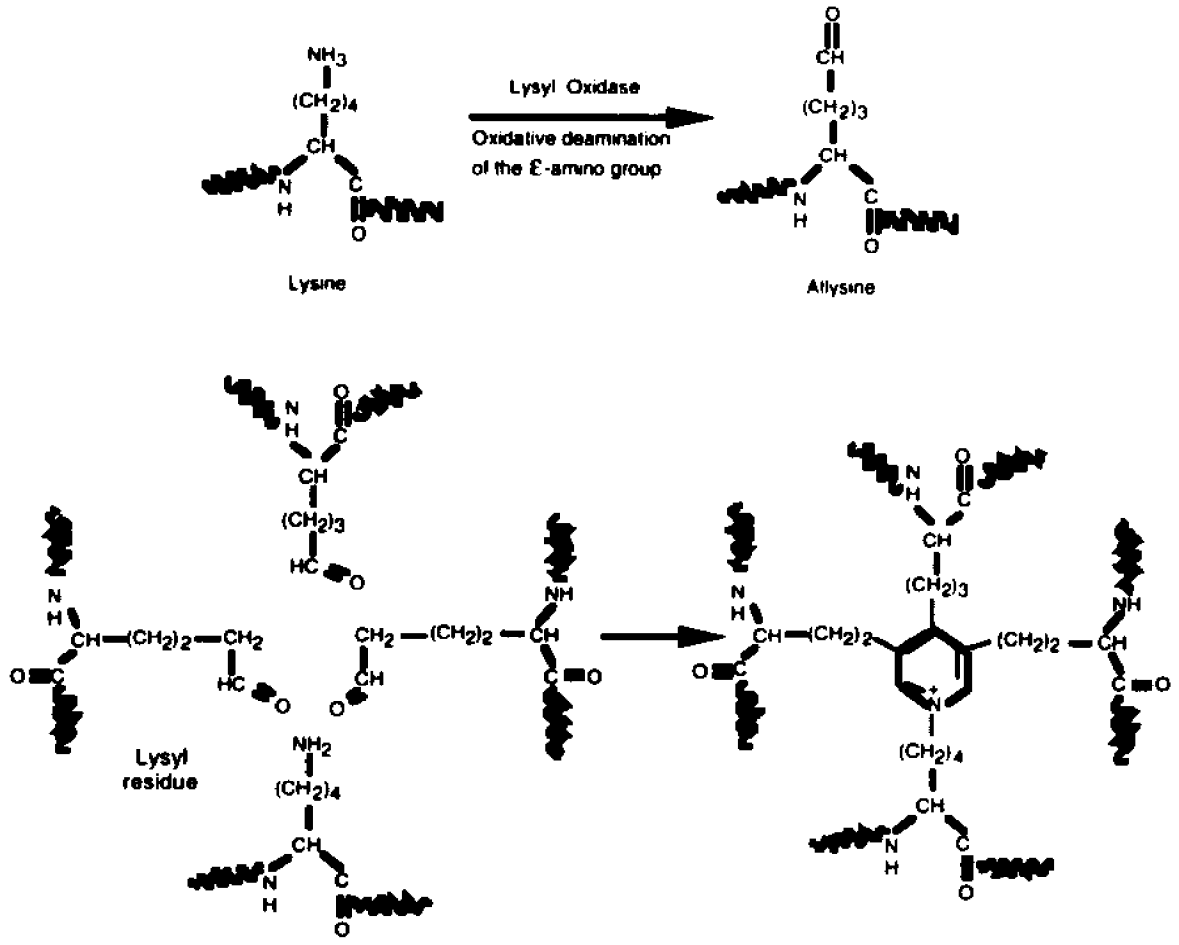

Figure 2: Schematic representation of four lysine residues forming desmosine, and potentially linking four elastin chains.

Elastin is responsible for the characteristic property of elastic fiber recoil. Since elastin has a half-life similar to the lifespan of the animal, its elasticity is believed to derive from an entropy-driven mechanism, rather than from the stressing of chemical bonds expected to result in a faster turn over of the protein (Lefevre and Rucker, 1980; Shapiro et al., 1991). The proposed "rubber" model describes elastin as a three dimensional network of randomly coiled chains joined by covalent cross-links. Upon stretching, the chains would extend in the direction of the force applied, resulting in a more orderly state. This decreases the conformational entropy of elastin which in turn generates the elastic restoring force (Hoeve, 1974). There are however differences in the thermodynamics of elastin

compared to that of rubber (Urry, 1984). Although elastin exists predominantly in a random coil network, some physico-chemical studies suggested a β-spiral conformation in which β-turns connect the suspended segments (Urry,1984). Supported by these observations, the author proposed a liberational entropy mechanism viewing elastin as a syncytium of easily deformable globular or fibrillar corpuscles behaving as interconnected springs. While these models differ in the details of molecular conformation, they all agree that the free energy is the source of the elastromeric force. This free energy contained in an orderly low entropy state in stretched tissue is released upon recoiling to a disordered maximum entropy state.

The interaction between the hydrophobic regions of elastin and the surrounding water may also play a significant role in elasticity (Weis-Fogh and Andersen, 1970; Gosline, 1979a). Consistent with the idea, dehydration of elastic tissue greatly compromises its elasticity (Gosline, 1978b). It is therefore likely that the water-hydrophobic interaction acts in conjunction with the entropy effect to confer elastin with the ability to reversibly deform upon exertion of force.

III. Microfibrils

Identification

During the original purification of elastin, investigators noted that the elastic fiber was tightly cross-linked to an elastase-resistant polysaccharide material identified as a "mucoprotein-containing" outer-coat (Hall et al., 1952). Karrer (1958) showed the first convincing images of fibrils 11 nm in diameter situated both at the periphery of the amorphous elastic fibers and within them. This fibrillar structure was given its present name, microfibril; at that time this morphological term defined all extracellular filamentous structures less than 20 nm in diameter and lacking the characteristic collagen banding (Low, 1962).

That microfibrils are distinct ECM proteins is indicated by their characteristic pattern of enzyme sensitivity and staining affinity. Microfibrils are readily digested by trypsin or chymotrypsin proteases but they are resistant to elastase; in contrast, elastin is susceptible to elastase but resistant to the other proteases. Like elastin, microfibrils are resistant to collagenase, hyaluronidase and β-glucuronidase (Ross and Bornstein, 1969). These characteristics exclude collagen fibers and proteoglycan filaments as potential components of microfibrils (Frederickson and Low, 1971; Hay, 1978; Mayer et al., 1981). The current definition of microfibrils is limited to 11-14 nm unbranched filaments, as seen mostly in elastic tissue (Cleary and Gibson, 1983). These elastin-associated microfibrils exhibit high affinity for cationic uranyl-acetate and lead citrate stains, which do not stain elastin. Conversely, elastin is readily stained by anionic phosphotungstic acid (PTA), which stains microfibrils poorly (Greelee et al., 1966). The use of PTA staining was the standard procedure at the time of the original electron microscopic studies of elastic fibers; this substantially delayed the recognition of the microfibrillar component of elastic fibers.

The affinity of microfibril for cationic stains, including ruthenium red, was considered indicative of possible glycoprotein (negative charge) content (Yu and Lai, 1970). This possibility was further examined by electron microscopy using the periodic acid-alkaline bismuth stain (analogous to the periodic acid Schiff stain for glycoprotein in light microscopy) and the concanavalin A (Con A) binding test. Positive reactions of the microfibrillar component of elastic tissue with both procedures supported that microfibrils were composed of, or closely associated with glycoproteins (Fanning and Cleary, 1985).

Tissue distribution

Microfibrils have been identified by electron microscopy in all the tissues where elastin is found. The 10 nm fibrous structure is seen in association with amorphous elastin in elastin-rich tissues, such as the aorta and other blood vessels, ligamentum nuchae, the elastic cartilage of external ear and epiglottis. Microfibrils are also recognized in tissues

where elastic fibers are less abundant, including the lung (from trachea to alveolar ducts), uterus, periosteum, perichondrium, intervertebral disk, periphery of the thymus, and the capsule of the hip joint (reviewed by Cleary and Gibson, 1983).

While elastic fibers are never seen without the microfibrillar component, a structure morphologically indistinguishable from microfibrils has been observed without association to immunogenically identifiable elastin. In skin, for example, the elastic fibers are described mainly in the deep dermis, or reticular dermis. However, the microfibrillar bundles of these elastic fibers extend up through the papillary dermis, connecting themselves to the fibrous structure arranged as a candelabra at the dermal-epidermal junction (Cotta-Pereira et al., 1976, 1978). If the tissue sections are subjected to prior oxidization, these "elastin-less" fibrils stain like elastic fiber with aldehyde fuchsin, resorcin fuchsin, and orcein stains, and they are therefore called "oxytalan" fibers (Fullmer and Lillie, 1958). Fibrils with the same staining characteristics are also found in the peridontal ligament of some teeth, tendons, ligaments, fasciae, periosteum, the adventitial layer of blood vessels, and in the connective tissue sheaths of dermal appendages and nerve fibers. Some papillary dermal microfibrils and fibrils in tendon, periostium, mucosa, and fibro-cartilage can be stained with orcein without prior oxidation. Electron microscopic examination has revealed that these fibrils are associated with small amounts of elastin. They are named "elaunin" fibers as part of the elastic fiber system (Gawlik, 1965).

Morphologically identical microfibrils totally devoid of elastin are also observed electron-microscopically in the ciliary zonules of the eye (Raviola, 1971), and in the mesangium of the renal glomerulus (Farquhar et al., 1961, Hsu and Churg, 1979). These microfibrils were futher demonstrated as immunologically related to the elastin-associated microfibrils. Kewley et al. (1977a) developed an antibody against nuchal ligament microfibril extract which gave several immunoprecipitin lines on immuno-diffusion against the antigen. The most prominent line was isolated from the gel and used to generate a second "monospecific" antibody in rabbit. This antimicrofibril antibody not only revealed

antigen on the surface of elastic fiber, as it was intended to, but also demonstrated positive staining on the basement membrane of the tubules and glomeruli of the kidney (Kewley et al., 1977b). Similarly, antibodies developed against sonicated zonules stained the microfibrils of nuchal ligament and aorta in the same periodic fashion as seen in zonule fibrils (Streeten et al., 1981). This finding implicated similar structural components in zonule microfibrils and in aortic elastin-associated microfibrils. It also suggested for the first time the possible linkage between microfibrils and MFS, since this condition is characterized by dissecting aortic aneurysm and dislocation of the lenses.

In summary, the study of microfibrils has indicated that morphologically identical and antigenically similar microfibrils are present in all tissues which contain elastin, and in many which do not. It is unclear though, whether all the microfibrils are truly identical in composition. Answer to this question requires full knowledge of the different components of the microfibrils.

Ultrastructure

After appropriate cationic staining, microfibrils appear in the electron microscope as multiple thread-like individual filaments. Higher magnification resolves these structures into consecutive beads in cross section, and tubules in longitudinal section (Fig. 3, Cleary and Gibson, 1983; Inoué and Leblond, 1986; Wright and Mayne, 1988; Mecham and Heuser, 1992). Upon closer examination, the 10-12 nm tubular structure has a beaded appearance with a hollow center. This inner electron-lucent lumen of the tubule is surrounded by a 1 nm thick electron dense wall, with spikes projecting from its surface. There is also a small dot in the middle of the lumen which is referred to as the spherule (Inoué and Leblond, 1986).

The more recent technique of rotary shadowing involving minimal tissue processing has confirmed the ultrastructure of microfibrils as beads connected to one another by multiple filaments extending out from the bead surface (Wright and Mayne, 1988;

Fleischmajer et al., 1991; Ren et al., 1991; Keene et al., 1991). The distance between one bead to the next can vary from 22 nm to over 100 nm, depending on whether the tissue examined is under tension at the time of fixation. The filaments joining the beads appear to bow outward, giving a shorter bead-to-bead distance when tissue samples are in a relaxed state; but they become straight, extending the distance between the two connecting beads when the samples are stretched (Ren et al., 1991; Keene et al., 1991). These stretching experiments have demonstrated a unique extension-contraction mechanism of the microfibrils accomplished by adjusting the distance between the beads. The study of Keene et al. (1991) indirectly confirmed that the microfibrils are stretchable by showing under transmission electronmicroscopy that the beaded appearance is more identifiable in stretched samples than in non-stretched ones. This is probably due to the increased distance between the beads upon stretching. The extendability of microfibrils allows for flexibility of the structure, but at the same time, the covalent links between the beads provide a limit to this extendability. Also noted in stretched samples are two cross-striation bands on the filaments between two beads (Wright and Mayne, 1988; Ren et al., 1991). The authors postulated that this structure may play a role in organizing the overlapping filaments of the beads.

Function

The function of microfibrils has never been clearly defined, but the limited extendability suggested by ultrastructural studies seems to indicate a role of microfibrils in enhancing the stregth of flexible structures. Unlike elastin, microfibrils can stretch without deforming. The presence of microfibrils in tissues that are subjected to multi-directional stretching and tension further supports the hypothesized role of providing strength and structural integrity.

For instance, in an elastic tissue like the aorta, microfibrils surround the elastic fiber limiting the maximum dilatation by their limited extendability. The microfibrils in the aortic

adventitia, where elastin is scarce, provide additional support for the vessel. Microfibrils in the nonelastic ciliary zonule not only anchor the lens, but also adjust the thickness of the lens by effectively conducting tension from muscular movement of the ciliary body.

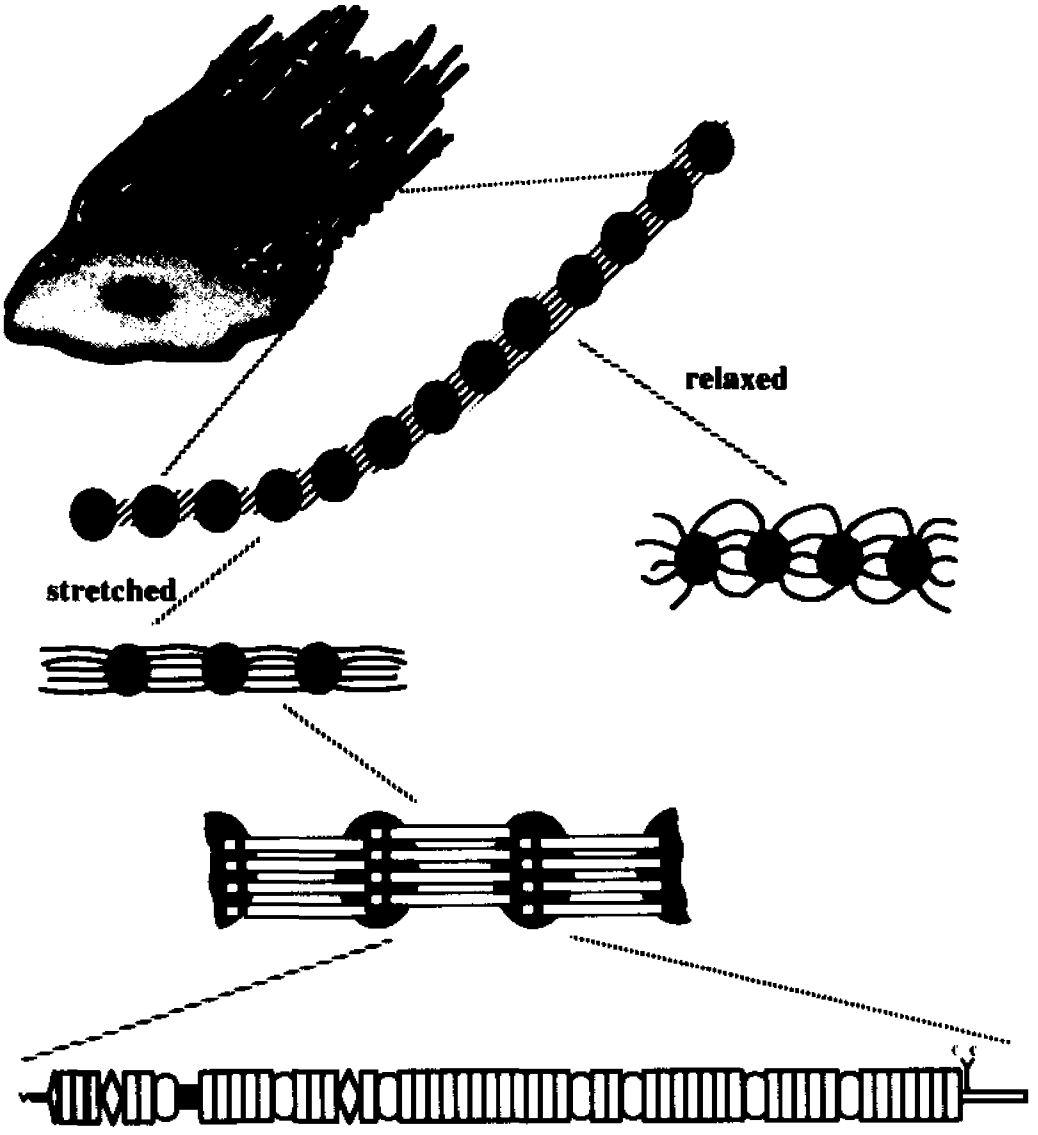

Figure 3: Diagramatic illustration of elastic fiber assembly. Note the "beads on string" microfibril structure and how the distance between beads may increase at stretched state.

Another widely postulated function of microfibrils is in directing elastic fiber formation. Microfibrils are the element first observed in all developing elastic tissues,

including in vitro cell culture systems (Cleary and Gibson, 1983). It is believed that the orientation of these microfibrils determines that of the mature elastic fibers. Some of the microfibrils are embedded within elastin during its deposition, whereas others remain at the periphery of the elastic fiber. It is unclear whether or not the microfibrils within elastin and the ones around it are different; it is also unknown how exactly microfibrils direct elastin deposition.

Composition

Resolving the biochemical composition of microfibrils has proven to be a difficult task due to their complexity and highly insoluble nature. Microfibrils can only be dissolved under reducing conditions after repeated extractions with guanidine hydrochloride (Ross and Bornstein, 1969). Materials like collagen type VI and amyloid P were once believed to be microfibrillar components because they were found physically adherent to elastic fibers and present in microfibrillar extracts (Gibson and Cleary, 1985; Breathnach et al., 1989). Despite these difficulties, a number of putative structural components of microfibrils have been identified over the last decade.

Fibrillin is the most abundant structural protein of the microfibril. This macromolecule will be discussed more extensively in the next section. Another important protein, MAGP (microfibrillar associated glycoprotein) has been shown to be associated with microfibrils by immunogenic and biochemical means (Gibson et al., 1986, 1991). MAGP is present in all tissues containing microfibrils, irrespective of the amount of associated elastin (Kumaratilake et al., 1989). This 31-kDa protein has an acidic amino-terminus, and a basic carboxyl-terminus where the thirteen cysteines of the molecule are located. These cysteines may form disulfide bonds with other microfibrillar proteins during fiber assembly.

Emilin (elastin microfibril interface located protein) was originaly isolated from chick aorta. It has a molecular weight of 115 kDa, and is apparently located in microfibrils

that are in close contact with elastin (Bressan et al., 1983, 1993). The involvement of emilin in elastogenesis was suggested by its detection at elastogenic sites prior to elastin deposition, and was supported by the interference of anti-emilin antibodies with elastic fiber formation in cell cultures (Bressan et al., 1993).

Using an antibody against zonule microfibrils, Horrigan et al. (1992) cloned the gene coding for a 32-kDa protein which was specifically localized to microfibrils in a variety of tissues. This protein was named associated microfibril protein (AMP). Its high content of acidic amino acids (23% glutamate and 6% aspartate) makes it possible to interact with basic tropoelastin during elastic fiber assembly. Lysyl oxidase (Serafini-Fracassini et al., 1981; Kagan et al., 1986) and a 36-kDa glycoprotein from porcine aorta (Kobayashi et al., 1989) have also been reported to be associated with the microfibrils.

Detailed data on the tissue distribution of these putative microfibrillar proteins are not available. It is not clear whether they are present in all microfibrils, and whether all microfibrils have the same composition. The individual expression and function of these candidate microfibrillar proteins, and their relationships to one another are yet to be fully defined.

IV. Fibrillin

Distribution and morphology

As already mentioned, the best characterized microfibrillar component is fibrillin. This 350-kDa protein was originaly identified from the supernatant of human fibroblast cultures, using a monoclonal Ab (mAb) raised against pepsin-digested tissue rich in microfibrils (Sakai et al., 1986). The mAb demonstrated that fibrillin localizes to the same tissues where microfibrils are found. These include the skin, lung, vasculature, cartilage, tendon, kidney, cornea and cilliary zonule. Immuno-electron microscopy further confirmed this point by showing that fibrillin is a component of the elastin-associated and elastin-less microfibrils (Sakai et al., 1986).

Fibrillin was also shown to be a glycoprotein through metabolic labeling with [^{3}H]glucosamine. Increased gel mobility under non-reducing conditions indicated the presence of intramolecular disulfide bonding in fibrillin (Sakai et al., 1986). In fact, about 14% of the amino acids of fibrillin are cysteines, two-thirds of which are reducible in fibrillin monomers, suggesting their possible involvement in intrachain disulfide bonding (Sakai et al., 1991).

Under electron microscopy, purified fibrillin appears as a 148 nm long and 2.2 nm wide extended molecule, an observation that is consistent with results from velocity sedimentation experiments (Sakai et al., 1991). Pepsin digestion of amnionic microfibrils yielded a crab-like structure in addition to the short rod-shaped fibrillin fragments (Maddox et al., 1989). This crab-like structure has six to eight flexible arms surrounding a central dense region, and corresponds to the bead on a microfibril beaded-string. This conclusion is based on the finding that a mAb (m69) against the part of fibrillin molecule contained in this structure (most likely the amino-terminus) decorates the beads on microfibrils (Sakai et al., 1991). Furthermore, m69 and mAbs against other segments of fibrillin decorate microfibrils with constant periodicity. This characteristic periodicity implies a "head-to-tail" model of fibrillin fiber assembly in microfibrils, as opposed to a "head-to-head" assembly which would result in an alternating periodicity (Sakai et al., 1991). The bead structure is probably where "heads" and "tails" (amino- and carboxyl- termini) interact with each other and possibly with other microfibrillar proteins.

Primary structure

The primary structure of fibrillin has been deduced from the cloned cDNAs isolated using information derived from partial peptide sequences. Fibrillin is a gene product mostly composed of multiple cysteine-rich repeats resembling those found in epidermal growth factor (EGF) precursor, and transforming growth factor-β binding protein (TGFβ-bp) (Maslen et al., 1991; Lee et al., 1991; Pereira et al., 1993; Corson et al., 1993). The

protein can be divided into five structural/functional domains (Fig. 4, Pereira et al., 1993). Domain A is a cysteine-poor, basic domain located at the amino-terminus immediately after the signal peptide. Domains B and D consist of cysteine-rich repeats and are separated from each other by a proline-rich domain C. The prolines in domain C have been proposed to introduce a hinge in fibrillin, possibly allowing the bending of the fibrillin molecule in the relaxed state (Pereira et al., 1993). Domain E is the lysine-rich carboxyl-terminus of the molecule. It contains several stretches of consecutive lysines, and two cysteines that may form links between fibrillin molecules and/or other microfibrillar proteins.

The most often seen cysteine-rich repeat in fibrillin is an EGF-like repeat which has the following average amino acid composition:

$$DXD/NXCX_6CX_4CXD/NX_4F/YXCXCX_{12}CX.$$

The spacing of the cysteine residues and the conserved amino acids D, D/N, D/N, F/Y at specific positions indicate that these EGF-like repeats belong to the Ca^{++} binding subclass (EGF-CB). In other proteins, the disulfide bonding between the cysteines of a EGF-CB motif brings the conserved amino acids together and produces a signal for the hydroxylation of the third conserved amino acid, D/N, forming a high affinity Ca^{++} binding site (Dahlbäck et al., 1990; Handford et al., 1991; Selander-Sunnerhagen et al., 1992). Corson et al. (1993) reported that fibrillin has a calcium binding ability that can be diminished by reducing agent. This result indicates that disulfide bonding is necessary for the fibrillin protein to bind calcium. Binding of calcium by EGF-CB- repeats can stabilize protein secondary structure and help mediate protein/protein interactions, as for example in the Vitamin K-independent protein C (Ohlin et al., 1988; Davis, 1990), human factor IX (Rees et al., 1988) and the Drosophila Notch gene product (Rebay et al., 1991).

The second kind of motif is homologous to the TGFβ-bp sequence that contains eight cysteines, three of which are consecutively clustered together (Kanzaki et al., 1990). In fibrillin, these motifs are interspersed among the EGF-like repeats with their consecutive cysteines being the likely candidates to mediate covalent intermolecular interactions. In

fact, one-third of the cysteines in soluble fibrillin monomers from tissue culture medium appear to be in the free reactive sulfhydryl form that can potentially form intermolecular disulfide bonds (Sakai et al., 1991).

The third kind of cysteine-rich motif, characterized by the presence of two consecutive cysteines, has been so far identified only in fibrillin. Called the Fib motif (Pereira et al., 1993) or the hybrid motif (Corson et al., 1993), this sequence is believed to have arisen from the fusion of an EGF-like repeat and a TGFβ-bp repeat. Studies of the genomic structure of the FBN1 gene have shown that most repeats are encoded by single exons, resulting in a cassette-like organization of the gene (Pereira et al., 1993). Such intron/exon arrangement has prompted the speculation that the gene for fibrillin might have evolved from duplication of an ancestral EGF-like coding unit.

Although the transcription start site of FBN1 is still controversial, the location of the first methionine codon in the FBN1 gene is generally agreed upon (Periera et al., 1993; Corson et al., 1993). Despite the absence of an in-frame upstream stop codon, the following indirect lines of evidence suggest that this ATG codon is indeed the translational start site. First, it is within the context of a Kozak consensus sequence (Periera et al., 1993; Corson et al., 1993); second, there is an abrupt decrease in sequence homology between the murine and the human genes upstream to it (Yin et al., 1994); third, the peptide encoded by the sequence immediately 3' to it conforms to the structural criteria of a leader sequence (Periera et al., 1993); finally, expression of only the ATG containing exon disrupts microfibril assembly in cultured cells (Dietz, personnal communication). This last result indicates that the putative signal peptide can direct fibrillin secretion, and that the very amino-terminus of the protein can participate in fibril assembly. More importantly, the data also imply that the ATG codon is used as the start site of translation.

Relationship to MFS

The original cloning of the fibrillin gene (FBN1) also led to the demonstration of a causal association between mutations in this gene product and MFS. MFS is an autosomal dominant disorder with an estimated incidence of 1 in 10,000. About 15-20% of the cases are de novo mutations (McKusick, 1956; Pyeritz and McKusik, 1979). The three most commonly affected systems in MFS patients are the musculoskeletal, the ocular, and the cardiovascular systems. The abnormalities involving the musculoskeletal system include arachnodactyly (long, spidery fingers), dolichostenomelia (limbs are disproportionately long compared with the trunk), high narrow palate, excessive height (exceeding the 95th percentile for age), hyperextensible joints, pectus deformities, vertebral column deformities, and pes planus (flat foot). Ectopia lentis (dislocation of the lens) and myopia are the major clinical features involving the ocular system. Dilatation of the ascending aorta is the key symptom in the cardiovascular system. It can lead to dissection of the vessel which is the major cause of death in MFS patients. Mitral valve prolapse is also seen in about three quarters of the patients. The symptoms and signs progress as the patients age. Without effective medical intervention, half of the affected men survive to age 40, and half of the women to age 48 (Pyeritz, 1990).

The first direct evidence that a microfibrillar abnormality is associated with MFS came from the immunological studies showing deficient fibrillin content in both the skin and cultured fibroblasts from MFS individuals (Hollister et al., 1990; Godfrey et al., 1990). At the same time, genetic linkage studies in different ethnic groups localized the MFS locus to a region of chromosome 15, 15q15-21.3, subsequently identified as the fibrillin locus. (Tsipouras et al., Kainulainen et al., 1990, 1991; Lee et al., 1991; Maslen et al., 1991; Dietz et al., 1991a). The identification of fibrillin mutations in MFS patients conclusively established defective fibrillin as the cause of MFS (Dietz et al., 1991b). Metabolic studies of the fibrillin protein supported the conclusion by demonstrating

defective synthesis, secretion, and matrix assembly of fibrillin in cultured fibroblasts of MFS patients (McGookey et al., 1992).

Since then, additional fibrillin mutations have been characterized in MFS patients (Deitz et al., 1992, 1993; Godfrey et al., 1993; Hewett et al., 1993 Kainulainen et al., 1992, 1994). The majority of the fibrillin mutations are missense mutations that alter amino acids believed to be involved in maintaining the hypothetical secondary structure, or in confering the calcium binding property to the protein. A less frequent group of mutations generates shorter peptides either by in-frame deletion of one or more exons, or by generating premature termination codon. These mutations presumably affect the alignment of the fibrillin molecules during polymerization, thus resulting in defective and weaker fibrils. It is yet to be established whether or not there is a third group of fibrillin mutations that reduces the production of structurally normal fibrillin, and causes the MFS phenotype.

Genetic heterogeneity

The genetic heterogeneity of fibrillin was unexpectedly discovered during the search for the MFS gene (Lee et al., 1991). Briefly, this cloning work identified two distinct groups of genomic clones that hybridize to a fibrillin cDNA fragment. The first group was shown to correspond to the gene located in the same region of chromosome 15 as the MFS locus. The second group of clones was found to contain three putative exons coding for EGF-like sequences similar to those of fibrillin. This fibrillin-like gene was mapped to chromosome 5 at q23-31, and thus named Fib5 or FBN2 to distinguish it from the FBN1 gene on chromosome 15. Moreover, genetic linkage analysis associated this fibrillin-like gene to an MFS-related condition, CCA, with a LOD score of 6.2 at zero recombination fraction (Lee et al., 1991; Tsipouras et al., 1992).

CCA is a rare, dominantly inherited, connective tissue disease that bears some clinical resemblance to MFS. CCA shares with MFS skeletal signs such as

dolichostenomelia, scoliosis, and arachnodactyly, but is characterized by congenital and symmetrical contractures of the joints, in contrast to the generalized joint laxity of MFS. Such contractures are maximum at birth, and improve spontaneously with age and use. A distinctively shaped abnormal external ear is recognized as a characteristic sign of CCA. Lack of ocular and cardiac involvement also distinguishes CCA from MFS (Beals et al., 1971).

Using an oligonucleotide specific for the EGF-like sequence of the FBN2 genomic clone, a placental cDNA clone, MF23, was isolated (Lee, et al., 1991). Aside from containing the three EGF-like repeats of the genomic clone, the deduced amino acid sequence of MF23 revealed that the encoded protein is structurally related to the FBN1 gene product. It is mostly composed of the same EGF-CB motifs as FBN1 with TGFβ-bp and Fib-motif sequences interspersed among them. However, the homology between these two gene products ends abruptly in the middle of the fibrillin sequence (Lee et al., 1991; Maslen et al., 1991). In place of additional cysteine-rich motifs, the MF23 encoded product has a short carboxyl terminus followed by a 3' untranslated region (UTR) (Lee et al., 1991). Northern analysis using MF23 as a probe indicated that the size of FBN2 transcript was about the same as that of FBN1, implicating a possible same size protein as Fib1. Although it was not clear at the time how FBN2 might be related to FBN1, the appearent similarities between the two genes and their asssociation with two phenotypically overlapping genetic conditions raised the possibility that FBN2 might produce a fibrillin-like protein product.

However, fibrillin heterogeneity was not supported by the data in the literature. Previous ultrastructural studies had reported differences in the thickness of microfibrils in various tissues at different developmental stages, though there were inconsistencies among the reports (reviewed by Cleary and Gibson, 1983). Additionally, differences in tissue preparation could cause variations in microfibril diameter (Fanning et al., 1981). There was no biochemical indication of the existence of a 350-kDa microfibrillar protein other

than Fib1. The limited sequence homology between Fib1 and the peptide coded by MF23 provided little assurance that the FBN2 gene might indeed produce a bona fide fibrillin-like protein.

Despite the uncertainty, the presence of this high level sequence homology corroborates the genetic linkage of CCA to the FBN2 locus, and could not be accounted for by mere coincidence. Therefore, we proposed that FBN2 encodes for a distinct microfibrillar component of the fibrillin family, and it is associated with pathology different from that of FBN1. This thesis project was undertaken to test this hypothesis. Accordingly, the following three specific aims were to be accomplished:

1. To establish the primary structure of the Fib2 transcript.

2. To identify the Fib2 protein.

3. To characterize the spatio-temporal expression of the FBN2 gene.

In achieving these aims, we could elucidate the primary structure of Fib2 protein, and establish its structural relationship to Fib1. The sequence information could then be used to generate specific polyclonal (p) Abs in order to demonstrate the existence and distribution of the Fib2 protein. Using the cDNA clones and pAbs, we could then compare the spatio-temporal pattern of expression of the fibrillin genes, as a first step towards understanding the potential relationships between the fibrillins. Confirmation of our original hypothesis would set the stage for future experiments aimed at detailing the differential pathogenic potentials of the different fibrillins.

MATERIALS AND METHODS

I. Nucleic Acid Analysis

cDNA library screening

Two cDNA libraries were used to clone the FBN2 transcript. One was a commercial λgt11 placental cDNA library (Clontech), whereas the other was prepared with RNA from MG63 cell line using the λZapII vector (Stratagene). The libraries were plated at a density of 20,000-50,000 plaques/150 mm plate with the appropriate bacterial host (Y1090 for λ gt11, XL1-Blue for λZAPII), and incubated overnight. Plaques were transferred in duplicates onto nitrocellulose filters (Millipore). After baking at 80°C in a vacum oven for 1-2 hr, both sets of filters were pre-hybridized for 5 hr and then hybridized to the probe of interest. The hybridization solution used with oligonucleotide probes contained 6x SSC (1x SSC: 0.15 M NaCl and 15 mM sodium citrate, pH 7.0), 1x Denhart's solution (50x Denhardt's: 1% Ficoll, 1% polyvinylpyrrolidone and 1% bovine serum albumin), 0.05% sodium pyrophosphate, 0.1% sodium dodecyl sulfate (SDS) and 50 μg/ml salmon sperm DNA (ssDNA). The hybridization temperature varied from 40 to 55°C depending on the Tm of the oligonucleotide used (Tm, melting temperature, was calculated at 1 M Na^+ concentration, Sambrook et al., 1989). Filters were washed with 6x SSC, 0.5% sodium pyrophosphate, 0.1-1% SDS with increasing temperatures up to 10°C below the hybrid's calculated Tm. Hybridizations using cDNA probes were performed at 42°C in 50% formamide and 5x SSC. The washing stringency was determined according to the degree of homology between the hybridizing sequences. We used 0.5x SSC at 50°C as the highest washing stringency for cross-hybridization between the FBN1 probes and FBN2 cDNAs, and between the human and murine cDNAs.

DNA from the positive λgt11 clones was prepared by the liquid culture method according to Sambrook et al. (1989). Purified DNA was subsequently subcloned into the

pUC vector for sequence analysis. Positive λZAPII clones were conveniently excised from phage arms and re-circularized into the phagemid pBluescript following the manufacturer's recommendations (Stratagene).

Sequence analysis

The dideoxynucleotide chain termination on denatured plasmid DNA was employed to determine the sequence of fibrillin clones (Sanger et al., 1977, USB-Sequenase V2.0). The DNA for sequencing was prepared either by CsCl gradient centrifugation (Sambrook et al 1989) or by the Magic mini-preps DNA purification system (Promega). Sequences were analyzed using the computer program MacVector (International Bio Technologics).

RNA purification

RNA was purified from cultured MG63 cells by guanidine isothiocyanate lysis followed by LiCl precipitation (Sambrook et al., 1989). Briefly, cells were lysed using 5M guanidine isothiocyanate, 10 mM EDTA, 50 mM Tris-HCl, pH 7.5, and 8% v/v β-mercaptoethanol. The lysate was precipitated overnight with 7 volumes of 4 M LiCl at 4°C, after passing it a few times through a 18 G needle in order to shear genomic DNA. The next day, the lysate was pelleted at 11,000 rpm in a Sorvall centrifuge and washed with 3 M LiCl to minimize DNA contamination. After resuspending it in TE (10 mM Tris-HCl pH 8.0, 1 mM EDTA) containing 0.1% SDS, the pellet was extracted three times with phenol and chloroform before ethanol precipitation. The resulting RNA was resuspended in diethyl pyrocarbonate-treated water (DEPC-H_2O) and quantitated by UV spectrophotometry. The quality of the RNA was verified on a freshly prepared agarose gel. The presence of sharp 28 S and 18 S rRNA bands at approximately a 2:1 ratio was used as an indicator of undegraded RNA. About 500 μg of RNA in 400 μl volume was loaded onto an oligo dT column (Stratagene) to select for polyA$^+$ mRNA according to the supplier's instructions.

Northern analysis

Total RNA was used for Northern analysis (Sambrook et al., 1989). About 10 µg of RNA was dissolved in 50% formamide, 1x formaldehyde gel-running buffer (0.02 M 3-[N-morpholino]propanesulfonic acid (MOPS) pH 7.0, 5 mM sodium acetate, 1 mM EDTA pH 8, and 2.2 M formaldehyde). After heating at 68°C for 5 min and rapid chilling on ice, the sample was loaded onto a formaldehyde denaturing 0.8% agarose gel in 1x formaldehyde gel-running buffer, and electrophoresed at 5 V/cm. RNA size markers (BRL) were included on the gel and stained with ethidium bromide. The gel was then capillary blotted overnight onto a Hybond N^+ nylon membrane (Amersham) in 20x SSC. The RNA was crosslinked to the membrane by a brief exposure to UV-light. After a rinse in 2x SSC, the membrane was pre-hybridized at 42°C for at least 6 hr before addition of the probe. The hybridization buffer contained 5x SSC, 1x Denhart's, 50 µg/ml ssDNA, 50% formamide, 25 mM sodium phosphate, 0.1% SDS, and 10% dextran sulfate. Probes were labeled with [γ-^{32}P] dCTP by nick-translation to a specific activity greater than $3x10^8$ counts per min(cpm)/µg. For each hybridization, we routinely used 1-$3x10^6$ cpm/ml of probes. Stringent washing conditions (0.1x SSC, 0.5-1% SDS at 65°C) were used for all Northern blot hybridizations.

Construction of cDNA libraries

Both random primed and oligo-dT primed libraries were constructed from 4 µg of MG63 polyA^+ RNA. Double stranded cDNA was synthesized using Amersham cDNA synthesis System Plus following the manufacturer's protocol. A small amount of [γ-^{32}P] dCTP was included in the reaction to estimate the amount of cDNA obtained. The blunt-ended double stranded cDNA was phenol/chloroform extracted three times before two precipitations with 2M ammonium acetate and 2.5 volumes of ethanol to remove

unincorporated dNTPs. The subsequent steps of EcoRI linker ligation, size fractionation and kinase treatment were accomplished using the Amersham cDNA cloning system.

The cDNA molecules with EcoRI adapters were cloned into the EcoRI site of the λZAPII vector (Stratagene). After performing test ligations to chose the most efficient insert/vector ratio, 2.5-5 ng cDNA was ligated to 100 ng phage arms and packaged with GIGAPACK II gold packing extract (Stratagene). Primary libraries were plated with XL1-Blue host and amplified. The random and oligo-dT primed libraries contained about $4x10^5$ and $6x10^5$ independent clones, respectively.

Rapid amplification of 5' cDNA ends

Various RACE (for rapid amplification of 5' cDNA ends) protocols were tested in order to obtain the 5' end of the FBN2 transcript. We found the Clontech modified method SLIC (single-stranded ligation to single-stranded cDNA) to be the most successful one. About 2 µg of polyA$^+$ MG63 RNA was reverse transcribed using the 3' primer MF129 (Figs. 4 and 6) following the 5'-AmpliFINDER RACE protocol (Forhman et al., 1988). After hydrolysis of the template RNA, the first strand cDNA was column purified with GENOBIND sepharose beads supplied in the kit and precipitated with 0.2 M sodium acetate and ethanol. A single stranded oligonucleotide anchor with a 5' phosphate group and a 3' amino group (to block self-ligation) was ligated to the 3' end of the cDNA using T4 RNA ligase. This modification avoided homopolymeric tailing with the deoxyribonucleotide transferase enzyme, which could have interfered with specific annealing of the primers in the subsequent PCR amplification. A portion of the anchored cDNA was then amplified with a primer complementary to the anchor, and the nested gene-specific primer MF140 (Fig. 4 and 6). The PCR products were hybridized to a primer located further 5' to confirm their specificity, and then cloned into pCRII vector using TA cloning kit (Invitrogen).

Primer extension

For the primer extension experiment, the 20mer MF129 was synthesized and end labeled with [γ-^{32}P]ATP using T4-polynucleotide kinase. MF129 is located 151 nucleotides downstream from the 5'end of clone A06-4 (Figs.4 and 6). Following labeling, the reaction product was precipitated with 2 M ammonia acetate and ethanol to eliminate unincorporated nucleotides. The pellet was resuspended in deionized formamide and the specific activity measured with a scintillation counter. About 1 ng of the labeled primer (with a specific activity of 5-10x10^8 cpm/ug) was annealed to 1 µg of poly A^+ RNA in 30 µl of annealing buffer (80% formamide, 40 mM PIPES [piperazine-N, N' bis(2-ethane-sulfonic acid)] pH 6.4, 1 mM EDTA pH 8.0, 0.4 M NaCl) overnight at 30°C. The RNA used in these experiments was prepared from cell lines MG63 and NT2/D1. The annealed primer-RNA complex was precipitated with 0.3 M sodium acetate and ethanol, and reverse transcribed at 42°C for 1 hr using 12.5 U of AMV reverse transcriptase (Promega). The product was extracted with phenol/chloroform, and ethanol precipitated. The pellet was resuspended in gel loading buffer (95% formamide, 20 mM EDTA, 0.05% bromophenol blue, 0.05% xylene cyanol), and loaded onto a 5% sequencing gel after heat denaturation at 94°C for 3 min. Primer extension products were visualized by autoradiography.

II. Protein Analysis

Antibody generation

We raised pAbs against recombinant antigenic peptides expressed by a commercial bacterial based expression system (Novagen). Nucleotide oligomers for both strands of the fibrillin sequence to be expressed were synthesized after being adapted into E. coli codon usage. The oligomers were ligated into pET-3xa vector which contains the strong bacteriophage T7 promoter and the T7 translation signals. In order to ensure plasmid stability, the recombinants were propagated in a host E. coli strain (HB101) that lacks the

T7 polymerase gene . After confirming the reading frame and the sequences, the plasmids were transformed into a lysogenic strain BL21(DE3) which contains a chromosomal copy of the T7 polymerase gene. The T7 RNA polymerase can be activated by induction with isopropyl-β-D-thiogalactopyranoside (IPTG), which in turn initiates the transcription of pET-3xa plasmids. After 2-4 hr induction with 1.4 mM IPTG, more than 50% of the total proteins produced by the bacteria is the fusion protein (Studier et al., 1990). The fusion protein was then collected as insoluble inclusion bodies following Bruggemann's procedure (1991). Briefly, the bacterial pellet was resuspended in TNE (50 mM Tris-HCl pH 8.0, 1 mM EDTA, 100 mM NaCl) and lysed at room temperature with 1 µg/ml of lysozyme. The lysate was pelleted, then resuspended and incubated for 30 min in TNE with 0.1% deoxycholate (DOC), 10 µg/ml DNase, 10 µg/ml RNase, and 8 mM $MgCl_2$ to further eliminate the nucleic acid and bacterial protein. This mixture was repeatedly pelleted and resuspended by sonication with cold TNE + 0.5% Triton. The last pellet was washed with cold PBS + 0.5% Triton, and resuspended with cold PBS by sonication. We estimated that more than 90% of this suspension represented the fusion protein inclusion bodies. After further purification on an SDS-polyacrylamide gel electrophoresis (SDS-PAGE), the antigen proteins were sent to Mount Sinai's Hybridoma Core Facility for rabbit immunization. The initial titer was 1:500 for both antibodies for Fib1 and Fib2 against the fusion proteins. The titer was boosted with subcutaneous injection of 10 µg of antigens periodically, and antisera were collected two weeks after each boost.

Immunoprecipitation

Confluent MG63 cells cultured in 35 mm dishes were washed twice with PBS to clear any residue from serum before being placed in 700 µl of serum-free, cysteine-free Dulbecco's modified Eagle medium. After 2 hr starvation, 50-100 µCi of ^{35}S cysteine (Amersham) was added and the cells were incubated for 12-16 hr. The collected medium was placed on ice and proteinase inhibitors were immediately added at the following

concentrations: 5 mM EDTA, 50 μM N-ethylmalimide, and 50 μM PMSF (phenylmethlsulfonyl fluoride). After clearing cell debris by centrifugation, 20 μl of either anti-Fib1 (Ab-f1C) or anti-Fib2 (Ab-f2C) antisera were added to 230 μl of the supernatant, together with 50 μl of 15% proteinA beads (Pharmacia). The mixture was shaken for 3 hr at 4°C. The beads were then centrifuged at 4°C, washed repeatedly with cold PBS, then washed twice with RIPA buffer (150 mM NaCl, 1% NP-40, 0.5% DOC, 0.1% SDS, 50 mM Tris pH 8.0), and finally rinsed again in PBS. After draining out PBS, the pellet was resuspended in 2x gel loading buffer (1x: 5% glycerol, 2.5% β-mercaptoethanol, 1% SDS, 0.38% Tris, 0.01% bromphenol-Blue) and boiled for 5 min before loading on a 4% SDS-PAGE. The gel was dried and autoradiographed to visualize the precipitated proteins.

Silver staining

The amount of the immunoprecipitated unlabeled protein was estimated by silver staining using a commercial kit (Boehringer Mannheim). Unlabeled serum-free overnight culture medium was collected and immunoprecipitated with fibrillin pAbs at 1:50 pAb: media ratio. About 3 ml of media was used to precipitate Fib1, while as much as 24 ml was used to obtain a similar amount of Fib2. The immunoprecipitates were separated in 4% SDS-PAGE. After fixing the gel with isopropyl alcohol and acetic acid, the gel was soaked in a sensitizer solution for 5 min before transferring into silver stain solution for 20 min. The staining was visualized by two 1 min changes of developer followed by a third 5-10 min change. The first two quick changes in the developer helped minimize the background, so that the gel could be left in the third change until the desired staining showed. The developed gel was then photographed.

Western blotting

Equivalent amounts of Ab-f1C and Ab-f2C immunoprecipitates (as verified by silver staining) were loaded on a 4% SDS-polyacrylamide gel, separated, and transferred

onto a nitrocellulose membrane (Millipore) in a gel running buffer containing 20% methanol. The membrane was then washed with TBST (10 mM Tris-HCl pH 8.0, 150 mM NaCl, 0.05% Tween 20) and blocked with 3% BSA in TBST for 2 hr at room temperature or overnight at 4°C. The primary antibody (Ab-f1C) was diluted 1 to 100 with blocking solution and incubated with the membrane for 2 hr at room temperature. After washing with TBST a few times for 10 min each, the secondary antibody Anti-rabbit IgG (Fc) alkaline phosphatase conjugate (Promega) was incubated with the membrane at the supplier's recommended dilution. The membrane was washed with TBST as before, and transferred into a color development solution prepared by adding 66 µl of NBT and 33 µl of BCIP solution to 10 ml of substrate buffer (100 mM Tris-HCl pH 9.5, 100 mM NaCl, 5 mM $MgCl_2$). The purple color was developed until the desired intensity was reached and the reaction was stopped by rinsing the membrane in deionized water.

Immunohistochemistry and immunofluorescence

The samples used in our studies were discarded human tissues obtained from the Departments of Pathology of New York University Medical Center, and Mount Sinai School of Medicine. Formalin-fixed tissues were either snap-frozen with OCT (Tissue TEK) embedding medium for immunofluorescent analysis or paraffin embedded for immunohistochemistry. Consecutive sections about 8-10 µm thick were prepared for the staining of both antibodies. Paraffin sections were de-waxed with xylene and rehydrated with a graded series of ethanol. Intrinsic peroxidase activity was blocked by immersing the slides in a solution of 3% hydrogen peroxide in methanol for 10 min. The slides were then blocked with 10% goat serum for 2 hr at room temperature. Frozen slides were taken straight out of the freezer for blocking. Primary antibodies (diluted 1:100 with blocking solution) were incubated on the slides overnight at 4°C. After washing with PBS for 1 hr with 4-5 changes, biotinylated goat anti-rabbit IgG (Zymed) was added to the slides for 1 hr. The slides were then washed with PBS before developing the signals. For

immunohistochemistry, streptavidin-peroxidase and the chromagen AEC supplied with the Zymed Histostain-SP kit were used as instructed. Steptavidin-rhodamine (Amersham) was used for immunoflourescent studies. Stainings were viewed and photographed with a Zeiss Axiophot microscope. All experiments included pre-immune serum as control.

Immunoelectron microscopy

This work was accomplished in collaboration with Dr. Elaine Davis at the department of Cell Biology and Pathology of Washington University Medical Center, St.Louis MO. Fetal bovine tissues were fixed in 7% paraformaldehyde in 0.1M Sorensen's buffer (pH 7.4) for 4-6 hr at 4°C and processed for reductive denaturation according to Gibson et al. (1989). Specimens were dehydrated in a graded series of methanol to 90% at progressively lower temperatures from 4°C to -20°C. Samples were then infiltrated and embedded with Lowicyl K4M (SPI supplies) which was subsequently polymerized by UV illumination for 24 hr at -35°C and an additional 48 hr at -10°C. Thin sections of tissue were cut with a diamond knife on a Reichert ultra-cut microtome and placed on formvar coated nickel grids. After blocking with 1% BSA in 100 mM NaCl and 50 mM Tris-HCl (pH 7.4) for 15 min, the grids were incubated with primary antibodies diluted in blocking solution overnight at 4°C. Following extensive washing and a second blocking step, the grids were incubated with goat F-(Ab')2 anti-rabbit IgG conjugated to 10 nm colloidal gold (BioCell Research Lab) at 1:30 dilution for 1 hr at room temperature. Immunolabeled sections were counter-stained with methanolic uranyl acetate for 2 min followed by lead citrate for 30 sec. Controls included non-immunized rabbit serum and omission of primary antibody.

III. In Situ Hybridization

Tissue preparation

Mouse embryos from different developmental stages were dissected and quickly fixed in fresh 4% paraformaldehyde dissolved in PBS at 4°C overnight. Embryos older than 16.5 days post-coitus (d.p.c.) were fixed for 2-5 days and decalcified by adding 5% EDTA to the paraformaldehyde solution. The embryos were dehydrated by a series of immersions in graded ethanol (30%, 50%, 70%, 80%, 90%, 100%) at room temperature for 30 min each, and cleared with 2 changes of xylene for 30 to 60 min each, before embedding them at 60°C in Paraplast plus (Fisher) for 2 hr with 3 changes of wax. Embryos were oriented into the desired positions with a hot metal probe. About 6-8 µm thick sections were cut and spread onto Superfrost/plus slides (Fisher). Slides were stored at 4°C until use.

Before hybridization, the appropriate sections were selected and deparafinized with Americlear (a xylene substitute, Scientific Products), and rehydrated by immersing the slides through a graded series of ethanols quickly followed by a 5 min rinse in DEPC-H_2O. Hydrated slides were fixed for 10 min in 4% paraformaldehyde before treatment with 1 µg/ml proteinase K (Boeringher Mannheim) for 30 min at 37°C in 0.1 M Tris-HCl pH 8, and 50 mM EDTA. The slides were rinsed with the same Tris-EDTA buffer followed by treatment with 0.1 M glycine pH 8 in 0.2 M Tris-HCl pH 8 at room temperature for 10 min. The slides were acetylated to absorb positive charges after a brief rinse with DEPC-H_2O and 0.1 M triethanolamine-HCl pH 8.0. The acetylation procedure was performed by first adding 0.5 ml of acetic anhydride to a dry staining dish, and then simultaneously adding the slides and 200 ml of 0.1 M triethanolamine. After dipping the slides up and down to mix the buffer, they were left in the mixture for 10 min in a fume hood. The acetylation buffer was rinsed off with 2x SSC and the slides were dehydrated with graded ethanol. Finally, the slides were dried in a dust-free location and stored for hybridization.

Preparation of the cRNA probes

A murine FBN1 probe covering 840 bp of the 3' UTR was obtained from Dr. Bonadio's laboratory at the University of Michigan, Ann Arbor, MI. The clone was linerized with restriction enzyme SpeI for antisense cRNA probe transcription. The murine FBN2 probe was isolated from a mouse 10.5 d.p.c. embryonic cDNA library (kindly provided by Dr. Lufkin, Mount Sinai School of Medicine) using the human cDNA clone 3'A as a probe (Fig. 4) . The resulting 880 bp murine clone encompassing the 3'UTR of FBN2 was linearized for antisense transcription using the restriction enzyme PstI.

The linearized plasmids were transcribed with T7 polymerase using MAXI-Script kit (Ambion) following the supplier's protocol and with ^{35}S-UTP (NEN) as the labeling substrate. After removal of the DNA template with DNase (RNase free), the probes were hydrolysed to 100-150 nucleotide long fragments by incubating them in 0.1 M sodium carbonate buffer pH 10.2 at 60°C for 40-50 min. Free nucleotides were removed by passing the probe mix through a G-50 Sepharose column. The elutriate was ethanol precipitated and the pelleted probe was resuspended in a small volume of TE with 10 mM DTT and stored at -80°C.

Hybridization and autoradiography

Hybridizations were performed in a buffer containing 50% formamide, 0.3 M NaCl, 20 mM sodium acetate, pH 5.0, 5 mM EDTA, 10% Dextran sulfate, 1x Denhardt's solution, 500 µg/ml of yeast tRNA and 0.1 M DTT. About 40,000 cpm of probe was added to each µl of the hybridization mix. About 5 µl/cm^2 of such mix was added to the tissue sections which were then covered with clean cover slips. Hybridizations were carried out at 50°C in a humid chamber for 16 hr. The slides were then washed with 4 changes of 4x SSC and 10 mM DTT at 50°C for 2 hr (the cover slips would float off in the first wash), followed by 2 hr wash at 50°C with 50% formamide, 2x SSC and 10 mM DTT. After rinsing with NTE buffer (0.5 M NaCl, 10 mM Tris-HCl pH 8.0, and 1 mM EDTA)

for 10 min, the slides were digested with 20 µg/ml of RNaseA and 1 U/ml of RNaseT1 in the NTE buffer for 40 min at 37°C. This was followed by a wash with NTE buffer containing 10 mM β-mercaptoethanol at 37°C for 30 min, a wash in 2 x SSC with 10 mM β-mercaptoethanol at 37°C for 15 min, and a final wash in 0.1 x SSC with 10 mM β-mercaptoethanol for 10-20 min at 50°C. The slides were then rinsed in 0.1x SSC with 10 mM β-mercaptoethanol at room temperature and dehydrated with increasing concentrations of ethanol in 300 mM ammonium acetate. After drying, the slides were dipped into NBT-2 photographic emulsion (KODAK) at 42°C in the dark room, and autoradiographed in a light tight box at 4°C for 4 to 7 days. The slides were then developed with KODAK D-19 developer for 3.5 min at 15°C and fixed in KODAK fixer for 6 min at room temperature. After counter-staining with hematoxylin (Diagnostic Solutions Inc.) for 20 sec, the slides were dehydrated and mounted. The results were viewed with a Zeiss microscope and photographed in both bright and dark fields.

RESULTS

I. Primary Structure of Fibrillin 2

Introduction

The search for the genetic defect of MFS identified not only the fibrillin gene (FBN1) on chromosome 15 but also a structurally homologous gene (FBN2) on chromosome 5q23-31 which was linked to the MFS-related disorder CCA (Lee et al.,1991). This linkage suggested that the FBN2 locus produced a protein product, although there was no direct biochemical evidence for the product. The original FBN2 clone, MF23, was isolated from a λgt11 placental cDNA library; it contains a 2.2 kb open-reading-frame (ORF) and a 0.6 kb 3' UTR (Fig. 4). The ORF has 81% overall amino acid homology to Fib1, and bears the same structural characteristics. The 13 EGF-CB repeats of MF23 are highly homologous to the 6th through the 18th EGF-like motifs of domain D of Fib1 (Fig. 4, Pereira et al., 1993). Like Fib1, these EGF-CB motifs are interrupted by TGFβ-bp and Fib motifs (Fig. 4). Despite this strong homology, the deduced amino acid sequence of MF23 has a short 16 amino acid carboxyl terminus with a termination codon after its 13th EGF-like repeat (corresponding to the 18th EGF-like repeat of Fib1/domain D; Lee et al., 1991).

Previous unpublished Northern blot analysis using MF23 as a probe identified a 10-11 kb transcript in MG63 cells (osteogenic sarcoma cell line). If a protein product were translated from this transcript, it would have been similar in size to Fib1. However, there was no suggestion of such a protein in the original isolation of fibrillin (Sakai et al.,1986). In addition, the early termination codon of MF23 limited the homology of this putative fibrillin-like protein to the amino-terminal portion of Fib1. To resolve the nature of FBN2 locus, we first screend for additional sequence of the FBN2 transcript in both the 5' and the 3' directions from the MF23 clone.

Cloning of the full length FBN2 transcript

The Clontech placental library was initially screened with oligonucleotides corresponding to both ends of MF23. The resulting clones were further selected by PCR amplification with nested primers and primers in the vector phage arm to identify the longest clone for subcloning and sequencing. For example, clones that were positive for oligonucleotide probe MF58 were amplified with the complementary primer MF69 and the λgt11 primers flanking the cloning site (see Fig. 4 for positions of primers). Clone A1 (Fig. 4) produced the longest PCR product, extending 1.6 kb further 5' from MF23. The DNA of this phage clone was subcloned and sequenced. This information allowed us to synthesize new oligonucleotide probes to continue the cDNA "walking". As a result, we identified clone A06-4 extending the 5' coding sequences for another 0.5 kb (Fig. 4). Screening of 3' sequence was carried out using the MF90 oligonucleotide (from nucleotide [nt] 2740 to 2761 as in Lee et al., 1991, Fig. 4) as a probe. Only one clone, B2, was identified; unfortunately, it ends 30 nt 5' to the 3' end of MF23.

Overall, the new clones extended the ORF of MF23 about 2.1 kb in the 5' direction. The amino acid translation of these cDNAs retained the structural similarity to the amino terminus of Fib1. The cloning work also revealed that most of these placental library clones have different 3' UTRs. For example, the 3' portion of clone A1 is identical to the coding segment of MF23 from nt 1 to nt 298, but continues into an unrelated 480 bp fragment containing several in-frame stop codons. Similarly, the 390 bp 3' portion of A06-4 is identical to the 5' end of A1, but is followed by a 126 bp unrelated UTR. It was unclear whether these clones represent functional products, or abortive transcripts. This raised the possibility that the original Northern data might represent a cross-hybridization signal between MF23 and the FBN1 mRNA, and that the actual FBN2 transcript and protein were not as large as believed.

To confirm the transcript size, we performed Northern analysis on MG63 RNA using the unique 3'UTR of MF23 rather than the entire clone as the probe. Despite

numerous attempts, no hybridization signal was ever detected with this probe. We then used the 1 kb EcoRI fragment of one of the new clones (A1, Fig. 4) that has only 40% nucleotide homology to the corresponding FBN1 sequence. Under stringent hybridization conditions, this probe identified a transcript of about 10-11kb (Fig. 5). The same size message was detected by the same probe in RNA from a teratocarcinoma cell line, NT2/D1 (data not shown). Re-hybridization of the filter to the 3'UTR of FBN1, detected a slightly smaller transcript (Fig. 5). Based on this evidence, we concluded that FBN2 produces a 10.5 kb transcript.

To estimate how much 5' sequence remained to be cloned, a primer extension experiment was performed using primer MF129 (151 nt downstream from the 5' end of clone A06-4, Fig. 4 and 6) and RNA from cell lines MG63 and NT2/D1. This yielded a primer extension product of about 495 nt in length from both RNA sources, thus suggesting that there were about 345 nt yet to be cloned in order to reach the 5' end of the FBN2 transcript (Fig. 7).

The estimated size of the transcript together with the result of the primer extension seemed to indicate that FBN2 contains a 5 to 6 kb long 3' UTR. However, sequencing of the genomic regions containing the cDNA sequences coding some of the carboxyl ends showed that both these short ORFs and the continuing 3' UTRs correspond to intron sequences (data not shown). This information gave us reason to suspect that some of the cDNA clones, including MF23, might represent partially spliced transcripts, and a properly processed FBN2 transcript would contain a longer 3' ORF. Indeed, we later confirmed that the carboxyl terminus coding sequence and the 3'UTR of MF23 represent an unspliced intron. This result also explained our failed attempts to identify FBN2 transcript using the 3'UTR of MF23 as a probe.

In our search for additional 3' coding sequence, we screened 240,000 clones of the Clontech placental cDNA library with an oligonucleotide (MF132, Fig. 4) from within the last EGF-CB repeat of MF23. More than one hundred positive clones were identified; they

were further selected for the ones that did not hybridize to an oligonucleotide probe from the 3'UTR of MF23 (MF63, Fig. 4; nt. 2385 to nt. 2366, Lee et al., 1991). Five such clones were identified, but none of them produced new sequence information as they had shorter versions of the same 3'UTR as MF23.

We then realized that full term placenta might not be an appropriate source for FBN2 mRNA, and decided to construct a cDNA library from the MG63 cell line where we had demonstrated the presence of the 10.5 kb transcript. Random-primed and oligo dT-primed cDNA libraries were constructed from MG63 poly A^+ RNA to ensure cloning of both the 5' and 3'-ends of the 10.5 kb FBN2 transcript. The λZapII vector was chosen for easy manipulation of the cDNA insert. The primary libraries were again screened with the double selection of MF132 and MF63 probes. One of the two resulting clones, 4J, was found to have sequence identical to nt 967 to 2215 of MF23 (Fig. 4). Nucleotide 2216 is where the sequence encoding the non-EGF carboxyl terminus of MF23 begins. In its place, clone 4J contains a continuing 0.4 kb ORF whose deduced amino acid sequence extends the homology to Fib1. The other clone, RP08, overlaps with the 3' portion 4J for 0.5 kb and extends the ORF towards 3' for another 0.3 kb (Fig. 4). This additional 0.3 kb sequence maintains the strong homology to FBN1. Thus, the MG63 cell line proved to be a better source for the cloning of a full-length FBN2 transcript.

Subsequent screening of the MG63 cDNA library was carried out using oligonucleotide probes or low stringency hybridization to FBN1 probes. As a result, clones covering the entire carboxyl-terminal half of Fib2 were identified (Fig. 4). Using oligonucleotide MF150 (positioned at the 3' end of RP08; Fig. 4), a 3.5 kb long clone, 15061, was isolated and characterized. Clones 3'A and 3'B were identified by low stringency hybridization to the 3'end fragment of FBN1 (F-3.3, Pereira et al., 1993). Clone 3'B is 1.3 kb in length and overlaps with both clone 15061 and clone 3'A. Together, these three clones extended the ORF of MF23 towards its carboxyl-terminus for another 4.3 kb. Clone 3'A contains a 2 kb insert, 1.4 kb of which is 3' UTR with a poly A

tail, following the putative polyadenylation signal AAUAA. The poly A tail was verified as a genuine post-transcriptional addition by its absence in the correspoding genomic fragment (data not shown).

The search for further 5' sequence by library screening failed to produce new cDNA clones, probably because of poor representation of the 5' end of such a large transcript. As an alternative, we decided to take the RACE approach (Forhman et al., 1988). We chose the modified SLIC protocol that allows specific priming in the PCR amplification step (Dumas et al., 1991). Poly A^+ RNA from MG63 cell line was reverse transcribed by priming with oligomer MF129 (Figs. 4 and 6). After ligation to the AmpliFINDER anchor, the resulting cDNA was amplified with nested primer MF140 (Figs. 4 and 6). Following subcloning, recombinants positive for an oligonucleotide (MF130) located further 5' to MF140 were sequenced. Although most clones ended around the 5' end of clone A06-4, one of them, RC1, extended the sequence for 43 nt further 5'. This allowed us to synthesize a new primer for PCR amplification of the anchored first strand cDNA. We sequenced all of the resulting clones that contained inserts long enough to extend the sequence. The longest clones extended the sequence 347 nt further 5' to A06-4, thus reaching the estimated end of the primer extension products. The additional sequence contains an in frame methionine codon 201 nt downstream of its 5'end. Although no stop codon was identified in the preceding sequences, this methionine is followed by a potential signal peptide. Moreover, the amino terminal sequence has some structural homology to FBN1. We therefore concluded that we had completed the cloning of the FBN2 transcript.

Theoretical structure of the FBN2 encoded protein

The ORF of the overlapping FBN2 cDNA clones translates into a 2911 amino acid polypeptide which has an overall 80% homology to the Fib1 protein. The theoretical product of the FBN2 locus was therefore named fibrillin 2 (Fib2). The Fib2 protein is

mainly composed of cysteine-rich repeats homologous to the EGF, EGF-CB, TGFβ-bp, and the Fib motifs arranged in the same order as in Fib1 (Fig. 4). Because of this, the amino acid sequence of the Fib2 protein can be aligned to that of Fib1 and divided into the same five structural domains (A to E) (Pereira et al., 1993; Fig. 4). Domains B and D are cysteine-rich, whereas domains A, C, and E are cysteine-poor regions that correspond to the amino-terminus, the connecting region, and the carboxyl-terminus.

Although only 19% homologous to each other, domain A of Fib2 and Fib1 contains a putative signal peptide composed mostly of non-polar amino acids. In Fib2, the tri-peptide "AGQ" introduces a β-turn in this sequence at the carboxyl end of the signal peptide, making the sequence a good candidate for the putative cleavage site (MacVector; Pealman and Halvorson, 1983). The amino terminus is as basic as that of Fib1 with an estimated pI of 11.7. Only in Fib2 this region contains a stretch of prolines immediately after the postulated signal peptide cleavage site (Fig. 8).

Domains B and D are composed of the same cysteine-rich repeats as the Fib1 protein (Corson et al., 1993; Pereira et al., 1993). Domain D has 47 EGF-like repeats, all but one of which belong to the calcium binding subgroup. Six TGFβ-bp motifs as well as one Fib motif are interspersed among these EGF-repeats. There are three EGF-like motifs and two EGF-CB motifs in domain B, with one TGFβ-bp and one Fib motif among them. All the cysteine-rich sequences are arranged in the exact same manner in Fib2 as in Fib1 (Fig. 4). The amino acid conservation within these repeats of Fib2 has retained all of the putative N-glycosylation sites and the one RGD cell attachment site of Fib1 (An additional cell attachment site is found in the second TGFβ-bp repeat of domain D/Fib2, Figs. 4 and 8). The resulting high degree of homology between Fib1 and Fib2 is 87% for domain B, and 81% for domain D.

Region C connects the two cysteine-rich domains and is mostly made of glycine residues. This is in striking contrast to the high proline content in the corresponding region of Fib1 (Fig. 8). Although region C of Fib2 has no homology to that of Fib1, we

nevertheless believe that the glycines of Fib2 may also provide flexibility to allow bending in the same manner as previously proposed for the proline-rich region of Fib1 (Pereira et al., 1993). Regardless of the validility of the hypothesis, the amino acid difference of region C was used to generate Abs specific to each fibrillin.

The carboxyl-terminus of Fib2, region E, has the same number of amino acids as Fib1 and a homology of 50%. Despite the relatively low degree of homology, there are some noticeable features that are conserved in the two proteins. The only two cysteine residues of this region are conserved within the context of 14 identical amino acids (Fig. 8). As previously discussed, these residues may potentially mediate protein-protein interactions through disulfide bonding. Moreover, this region of Fib2 has a high lysine content like Fib1, and one of the three possible glycosylation sites of Fib1.

In conclusion, the experiments described in this section determined the primary structure of Fib2. They also explained the unusual structure of the original clone MF23. More importantly, they provided the means to perform the next set of experiments aimed at excluding the possibility that FBN2 was just a pseudogene producing abortive transcripts.

II Characterization of the Fibrillin 2 Protein

Introduction

To identify the Fib2 protein, we generated specific pAbs. Since the two fibrillins are highly homologous, it was critical to choose epitopes in the most divergent sequence of the fibrillins, region C. We expressed a 45 amino acid segment from this region of Fib1, and a corresponding 43 amino acid peptide of Fib2 in a bacterial expression system (sequences illustrated on Fig. 8 in italic). Gel-purified bacterial fusion proteins were then used to immunize rabbits. The resulting antisera identified the Fib2 protein as a microfibrillar component in a three-step approach. First, we proved that the Fib2 protein was made in the same MG63 cell line where the FBN2 transcript had been detected by Northern analysis. Then we demonstrated that Fib2 is present in tissues known to contain

microfibrils. Lastly, we localized Fib2 epitope on to the elastin-associated microfibrils using immunoelectron microscopy.

In vitro identification of the Fib2 protein

To identify the fibrillin proteins in the MG63 cells, antisera against each fibrillin were used to immunoprecipitate the radioactively labeled culture media supernatant of this cell line. Following electrophoresis, the precipitates were visualized by autoradiography. The precipitate of Fib2 Ab (Ab-f2C) migrated for about the same distance as Fib1, indicating similar molecular weight. In contrast to the equivalent mRNA levels observed on the Northern blot, the Fib2 protein was substantially less abundant than Fib1 (Fig. 9A).

To verify the specificity of Ab-f2C, a Western blot analysis was performed on its immunoprecipitate using anti-Fib1 pAb (Ab-f1C). Immunoprecipitate of Ab-f1C was included as a positive control. Equal amounts of both precipitates, as estimated by silver staining (Fig. 9B), were separated by SDS-PAGE. After transferring the proteins from the gel to a nitrocellulose membrane, they were incubated with Ab-f1C. A positive signal was seen only in the lane loaded with Ab-f1C immunoprecipitate (Fig. 9C). This experiment demonstrated that the immunoprecipitation product of Ab-f2C was not the result of a cross-reaction with Fib1. This result, together with the obervation of the expected molecular weight, led to conclude that the cultured cells secret the Fib2 protein.

In vivo distribution of Fib2

In addition to establishing the tissue locolization of Fib2, immunohistochemical studies showed a difference in the distribution of the two fibrillins that may be indicative of distinct functional roles. Initially, we examined a number of adult human tissues, including skin, aorta, muscle, ligament and tendon. These are the same tissues that Sakai et al. (1986) reported to contain fibrillin. Although we could reproduce those results using our anti-Fib1 pAb, we barely detected Fib2 protein in the same tissues.

The spontaneously resolving nature of the CCA contractures suggested to us that the protein might be primarily expressed in fetal tissues. We first tested this idea on some fetal skin tissue. We found not only the presence of the Fib2 protein, but also quantitative and qualitative differences in the expression of the two fibrillins (Fig. 10). Skin is composed of two parts, the epidermis and the dermis connected by the dermal-epidermal junction. The dermis contains the dermal appendages, such as hair follicles and sweat glands. The dermis is also where the elastic fibers of the skin are located. Likewise, the connective tissue sheath of the hair follicle has a high content of "oxytalan fibers" (Fullmer and Lillie, 1958). Fib2 staining, although not detectable in adult tissue, was seen in fetal skin as discrete fibers in the dermis, particularly around the hair follicles (Fig. 10B). Ab-f1C showed a discrete fibrous staining which extends from dermis to epidermal junction in both fetal and adult skins (Fig. 10A, C). The dermal appendages did not have particularly stronger staining with this pAb. In contrast, a distinctive candelabra-like structure was noted at the epidermal junction where no Fib2 was detected. Based on these results, we then performed a more systematic immunohistochemical analysis of the fibrillins in human tissues at 20 week gestation. Fib2 was detected in the ECM of a wide variety of tissues. The overall pattern was similar to that of Fib1, but the expression level was generally lower except in tissues rich in elastic fibers.

The aorta has three distinct cellular layers from the lumen outward: the intima, the media, and the adventitia. In fetal aorta, Fib2 staining was most abundant in the medial layer (Fig. 11B). As shown by Verhoeff's staining, this is the vessel layer where most of the elastic fibers are located (Fig. 11D). In contrast to Fib2, Fib1 staining was intense across the three layers with the adventitia being the strongest (Fig. 11A). It should be noted that the net amount of Fib1 staining detected in the media was still greater than Fib2.

Differences in Fib1 and Fib2 distribution were also seen in hyaline cartilages of the skeletal system. Cartilage is surrounded by a fibrous sheath, the perichondrium, which is composed of an outer dense connective tissue layer, and an inner cellular layer that has the

potential to differentiate into chondrocytes. The chondrocytes at the periphery of the cartilage are less differentiated and still dividing while the cells in the interior of the cartilage are more mature and have stopped dividing. Ab-f2C detected accumulation of Fib2 protein in the matrices of the peripheral areas of the cartilage (Fig. 12D), and the perichondrium (Fig. 12F). A diffuse staining of Fib1 was however seen in the entire cartilaginous matrix (Fig. 12C) with a relatively more elevated level of accumulation in the hypertrophic zone of the osteogenic cartilage (Fig. 12E). These results suggested that Fib2 might be produced earlier than Fib1 in the less differentiated chondrocytes.

The staining of elastic cartilage of the fetal ear dramatically demonstrated the differential localization of the fibrillins, and the preferential distribution of Fib2 in elastic matrices. While the fibrillar staining of Fib1 was mostly seen in the connective tissue surrounding the cartilage (Fig. 12A), the elastic cartilage core itself and the perichondrium directly adjoining the core were intensely stained with Fib2 Ab (Fig. 12B).

The expression of fibrillins was also examined in the developing eye. Both proteins were detected in the sclera and the cornea. Anatomically, the latter is a transparent extension of the sclera at its most anterior portion. Fib2 expression was seen evenly distributed throughout the sclera (Fig. 13E), but was restricted to the morphologically distinctive anterior third of the Descemet's membrane of the cornea (Fig. 13B). Descemet's membrane is an acellular connective tissue layer situated just posterior to the corneal stroma. Consistent with previous findings, Ab-f1C reproduced the intense staining in the full thickness of Descemet's membrane (Fig. 13A, Sakai et al., 1986). Fib1 staining in the sclera was predominantly in the outer layer and the inner vascular choroid layer (Fig. 13D). Unfortunately, we could not compare the fibrillin accumulation in the delicate zonule fibers because our tissue preparation did not preserve them.

In the fetal kidney there was a similar staining pattern for both proteins in the basement membrane of the glomeruli and in the developing collecting ducts. Perhaps, there was a hint of greater expression of Fib1 in the tubular region, and of Fib2 in the glomeruli

(Fig. 13G, H). In the fetal lung, Fib1 staining was mainly located in the interlobular septa and the perivascular and peribronchiolar connective tissue with light staining of the alveolar matrix (Fig. 13J). In contrast, Fib2 showed minimum staining at this stage of lung development (Fig. 13K). Finally, we could not detect any convincing signal of either protein in the ligament and tendon samples from the same stage (data not shown).

In summary, our immunohistochemical and immunofluorescent analysis documented the presence of Fib2 in microfibril-rich connective tissue of the developing embryo, especially in the elastic fiber-containing regions.

Ultrastructural localization of Fib2

Despite the successful identification of the Fib2 protein in tissues, our results were not sufficient to define the exact relationship between Fib2 and microfibrils. To localize Fib2 in the matrix, we performed immuno-electron microscopy studies in collaboration with Dr. Elaine Davis using our Ab-f1C and Ab-f2C Abs. The immuno-labeling was performed in elastin rich fetal bovine ligamentum nuchae and aorta. The tissues were first incubated with primary pAbs and repeatedly washed. A gold-conjugated secondary Ab was used to visualize the fibrillin/anti-fibrillin-Ab complexes. The gold particles localized both Fib1 and Fib2 to the morphologically indistinguishable microfibrils of fetal bovine ligamentum nuchae (Fig. 14A, B). Such specific localization was also seen on microfibrils of elastic laminae in fetal bovine aorta (data not shown). This finding demonstrated that Fib2 is closely associated with, if not a component of the 10nm microfibrils.

III. Developmental Expression of Fibrillins

Introduction

The immunohistochemical studies suggested that morphologically identical microfibrils may be different in composition. The failure to detect Fib2 in adult tissues, and its relatively higher accumulation in fetal elastic matrices seemed to imply that the

distribution of microfibrillar components may change in time and space during development. The Fib2 protein is either degraded, or masked during the subsequent elastic fiber assembly and maturation. To further support this hypothesis, we decided to study the embryonic pattern of fibrillin expression using the in situ hybridization approach. We chose to examine the mouse embryos since our lab is currently involved in establishing transgenic mouse models for FBN1 and FBN2 mutations. Defining the spatial and temporal pattern of expression during normal development is a complementing first step toward understanding the function and pathogenic potential of fibrillins.

The 839 bp probe for murine FBN1 covers the 3'UTR from nt 8546 to nt 9384 (Yin. et al, 1994). To isolate the murine FBN2 probe, we screened a 10.5 d.p.c. embryo cDNA library using the 3' most human cDNA as a probe. Three overlapping clones mI, mJ, and mF were isolated and sequenced (Fig. 15). They span a 3.9 kb region that contains 2.8 kb ORF (Fig. 16). The deduced ORF shows 96% homology to the human Fib2 amino acid sequence (Fig. 17). In contrast, the amino acid homology of the murine Fib2 to human and murine Fib1 is 79.1% and 78.8% respectively. Clone mF covers a 876 bp segment of the 3'UTR (Fig.16) that is 73% homologous to the corresponding sequence of human FBN2 (from nt 8936 to nt 9811). It can not be aligned to either the human or the murine 3'UTRs of FBN1. This clone was chosen as the probe for specific detection of murine FBN2 transcripts. Additionally, we used as a control probe, the type II collagen gene which is specifically expressed in cartilage (Cheah et al., 1991). Riboprobes of equivalent specific activity were synthesized from each of these clones and used for in situ hybridizations on serial sections of mouse embryos collected at days 10.5, 13.5, and 16.5 p.c. This study confirmed and further delineated the differential expression of fibrillins in microfibril-containing tissues as first suggested by the immunohistochemical analysis. More importantly, it showed that FBN2 expression appears transiently and with a characteristic pattern. It peaks parallel to the formation of a given tissue and decreases (sometimes disappears) thereafter. In contrast, the accumulation of the FBN1 message

increases gradually as morphogenesis proceeds. The following is a description of fibrillin expression during mouse embryogenesis presented by organ systems.

Lungs

The developing lung represents the best example illustrating the differential spatial and temporal pattern of expression of the fibrillin genes. At 10.5 d.p.c., the lung bud is rapidly elongating and the primary bronchi are present as small tubes. A strong signal of FBN2 expression was detected in the epithelial layer of the budding main bronchi at 10.5 d.p.c., along with a weaker and diffuse signal in the primitive lung mesenchymal cells (Fig. 18A). A similar weak signal for FBN1 expression was seen in the mesenchymal cells but there was no signal in the bronchial epithelium (Fig. 18B).

As lungs develop, they subdivide into lobes where secondary lobar bronchi and tertiary segmental bronchi continue to branch. By 13.5 d.p.c., branching of the segmental bronchi is dominant. The levels of FBN1 and FBN2 message were comparable in the mesenchyme, but only the FBN2 transcripts were seen in the epithelium of the forming segmental bronchi, particularly on the lumen side (Fig. 18E,F). A weaker signal of FBN2 message was still detectable in the epithelium of the main bronchi at this stage (Fig. 19A).

At 16.5 d.p.c., the lungs are still compact, and terminal bronchi lined with cuboidal cells begin to appear. While segmental bronchi had little FBN2 expression at this point, the epithelial cells of the sprouting terminal bronchi were now the active sites of FBN2 expression (Fig. 18I). Except for an increased but still low level of expression in the mesenchyme, FBN1 expression was prominent only in the vasculature of the lung (Fig. 18J). The FBN1 message was never detected in the bronchial epithelium in embryos at any stages. Thus, lung tissue showed a developmentally specific and selective expression of FBN2 in bronchial epithelium during the formation of bronchi. Both fibrillins were expressed in the lung mesenchymal cells with progressively increasing ratio of FBN1 versus FBN2 message.

Kidneys

Dynamic changes in FBN2 expression were also noted in the developing kidney. The kidneys are undergoing rapid development around 13.5 d.p.c. The metanephric vesicles differentiate into primitive glomeruli and eventually move to their mature location in the cortical region, which itself differentiates from the metanephric cap tissue. Aside from the expression in the undifferentiated mesenchyme tissue, an increased amount of FBN2 message was seen in the metanephric vesicle and the metanephric cap tissue adjacent to the capsule of the kidney (Fig. 20A). At this stage, FBN1 expression was only seen in the renal capsules where FBN2 signal was also observed (Fig. 20B).

At 16.5 d.p.c., the undifferentiated metanephric cap tissue is still present just beneath the renal capsule, and the kidneys are more clearly divided into the peripheral cortical region and the central medullar region. At this stage, expression of FBN2 was seen mostly in the cortical region where the developing glomeruli are located (Fig. 20E, I). FBN1 message was mostly detected in the mesenchyme throughout the cortical and medullar regions (Fig. 20F, J). Expression of both fibrillins in the renal capsule was more apparent at this stage. Neither fibrillin was expressed in the collecting tubules (Fig. 20E, F) that develop from the metanephric diverticulum (ureteric bud), rather than the metanephric mesoderm as the rest of the kidney does. Thus, we observed expression of FBN2 in the renal mesenchyme at the location of the developing glomeruli. We also noted an increasing expression of FBN1 in the mesenchyme, but not particularly near the glomeruli. The results are in agreement with our immunohistochemical data suggesting that glomeruli have a greater accumulation of Fib2 protein.

Musculoskeletal system

The limbs at 10.5 d.p.c. are composed of primitive mesenchymal tissues. Cartilage starts to appear in the limbs at 13 d.p.c. Ossification occurs in skull and ribs around 15 d.p.c., but does not extend to the limbs until 16.5 d.p.c.

The fibrillin messages can be identified in the developing mesenchyme of the limb bud as early as 10.5 d.p.c., with FBN2 at a much greater intensity than FBN1 (Fig. 21A, B). By 13.5 d.p.c. the expression of FBN2 was seen in the perichondrium of the developing long bones (Fig. 22A, E), ribs (flat bone), and vertebral bodies (short bone, Fig. 19A), clearly defining the outline of the bone. FBN1 was also observed in the perichondrium but at a much lower intensity, as well as in the cartilage itself where FBN2 message was absent (Fig. 19B, and 22B, F). Such an expression pattern was even more clear in 16.5 d.p.c. embryos (Fig. 24) where FBN1 expression was now higher than 13.5 d.p.c. At this stage of development, an increased FBN1 signal was observed in the hypertrophic and calcifying zones compared with other areas of cartilage (Fig. 24B, J). Higher Fib1 accumulation around the more differentiated chondrocytes was also noted in our immunohistochemical study.

Expression of both fibrillins was seen in the ligaments surrounding the vertebral column and other joints at 13.5 and 16.5 d.p.c., with the FBN2 signal much stronger than that of FBN1 (Fig. 22, 23). In 16.5 d.p.c. embryos, active expression of FBN2 was observed in the ligamentum flava, an elastic ligament that forms after 14 d.p.c. Accumulation of FBN1 mRNA was also seen in the fibroblasts of this ligament but at a lower intensity than FBN2 (Fig. 24E, F). FBN2 was expressed in tendons as early as 13.5 d.p.c.(Fig. 22A, E), while FBN1 expression was barely detectable in this tissue even at 16.5 d.p.c. (Fig. 23B). The fibrocartilagenous intervertebral disc is another tissue that contains a moderate amount of elastic fibers. The expression of FBN2 in this structure was intense and more localized to the peripheral annulus fibrosis (Fig. 19A). A weaker and more diffuse signal of FBN1 was observed in the entire disc (Fig. 19B).

Well-developed muscle bundles are present in embryos at 16.5 d.p.c. Although the myocytes did not express FBN1, the fibroblasts of the perimysium showed an abundant accumulation of FBN1 mRNA (Fig. 24N). On the other hand, FBN2 expression was not only detected in the perimysial fibroblasts but also in the myocytes themselves (Fig. 24M). In summary, the results in the musculoskeletal system revealed that accumulation of FBN2 transcripts peaks earlier in development than FBN1; in turn, FBN1 accounts for an increasing portion of the fibrillin expressed by the differentiating tissues.

Larynx

The immunohistochemical staining of the auricular cartilage showed little Fib1 in the elastic cartilaginous core, but abundant Fib2 protein deposition. The in situ data of cartilaginous larynx confirmed the preponderance of FBN2 gene expression in elastic cartilage. At 13.5 d.p.c. the elastic epiglottis is separated by a discrete cleft from the rest of the larynx which is still pre-cartilaginous. The cartilaginous skeleton of larynx and trachea becomes well delineated by 15 d.p.c. Although the laryngeal structure was still poorly developed in the 13.5 d.p.c. embryo, an elevated level of FBN2 expression was already noted in the mesenchymal tissue that will eventually form the larynx (Fig. 25A, B). An intense signal of FBN2 message was observed in the elastic cartilage of the larynx, the epiglottis and the cuneiform cartilage in 16.5 d.p.c. embryos (Fig. 25D). The expression of FBN1 in these structures was no higher than in the surrounding matrix fibroblasts (Fig. 25B, E). The expression of both fibrillins in the hyaline cartilage of the larynx was mostly seen in the perichondrium, as was the case for cartilages of the skeletal system.

Cardiovascular system

At 10.5 d.p.c. the heart is still a single tube, inside which active morphogenesis of the aortico-pulmonary spiral septum and atrio-ventricular endocardial cushion tissue is taking place. By 13.5 d.p.c. the ascending aorta and the pulmonary trunk are distinct

vessels, and the valves and septa of the heart are in their primitive form. A continuous circulation starts around 14 d.p.c. when the communication between right and left ventricle is closed. The embryos of 16.5 d.p.c. have their heart and large vessels in the final prenatal configuration.

Expression of FBN1 in the cardiovascular system was an exception to the di-phasic pattern of fibrillin expression during embryogenesis. A high level of FBN1 message was detected as early as 10.5 d.p.c. in the aortic sac and the dorsal aorta (Fig. 26G, Fig. 21B). Intense signals continued to be seen at 13.5 and 16.5 d.p.c. in the full thickness of the aortic arch, pulmonary artery, and dorsal aorta (Fig. 27B, Fig. 28B, F). The level of FBN2 expression was lower in these structures (Fig. 26E, Fig. 27A, Fig. 28A, E), and the difference seemed to increase with the age of the embryo. The less intense signal of FBN2 message can be attributed in part to its more localized expression in the media layer, particularly the outer part of the elastic arteries and the muscular arteries.

Expression of FBN2 in the heart was seen uniformly in the myocardial cells (Fig. 26A, E, Fig. 27A), whereas FBN1 was mostly seen in the endothelial cells of endocardium and the epithilial cells of epicardium (Fig. 26B, F, G, Fig. 27B). Active transcription of both fibrillins was observed in the endocardial cushion tissue associated with the wall of the atrio-ventricular canal (which later forms the valves between atrium and ventricle, Fig. 26). FBN1 expression was noted in the forming aortico-pulmonary spiral septum (Fig. 26F). A significant amount of FBN1 message was detected in the arterioles of different tissues such the lung (Fig. 18J, D), the kidney (Fig. 20F) and the joints (Fig. 23B). As a result, the vasculature of the tissues was easily visible on slides hybridized to the FBN1 probe. FBN2 expression in small arteries was not particularly elevated.

Other tissues

The higher expression of FBN2 gene at earlier stages of development was in general observed in all mesenchymal tissues. At 10.5 d.p.c. the expression of FBN2 was

far greater than FBN1 (Fig. 21E, F); as the embryo developed, the level of FBN1 expression increased to give a signal comparable to, if not stronger than FBN2 at 13.5 d.p.c. By 16.5 d.p.c., FBN1 expression in the embryonic mesenchyme was clearly overriding that of FBN2, which was still reasonably strong (Fig. 23, 24).

The sclera of the eye represented another example of FBN2 expression preceding that of FBN1 during morphogenesis. The FBN2 message was detected in the sclera as early as 13.5 d.p.c. (Fig. 29A), while FBN1 signal was only seen in the 16.5 d.p.c. embryonic eye (Fig. 29E). Fibrillin expression was also detectable in the smooth muscle cells of the stomach and the intestines, with similar intensity for FBN1 and FBN2 (Fig. 29 T to O). A subtle difference was noted in the localization of the signal in the intestine. While FBN2 was expressed in the submucosa and lamina propria, FBN1 was found only in the submucosal cells (Fig. 29M, N). Expression of both fibrillins was seen in the capsule of the thymus, with FBN2 being relatively stronger and displaying an additional signal in the lobular septa (Fig. 19). The fibroblasts of the fibrous sheath of nervous tissue produced fibrillin messages. In contrast, the nervous tissue itself lacked any fibrillin expression and was used as the internal negative control (Fig. 19, Fig. 28E, F).

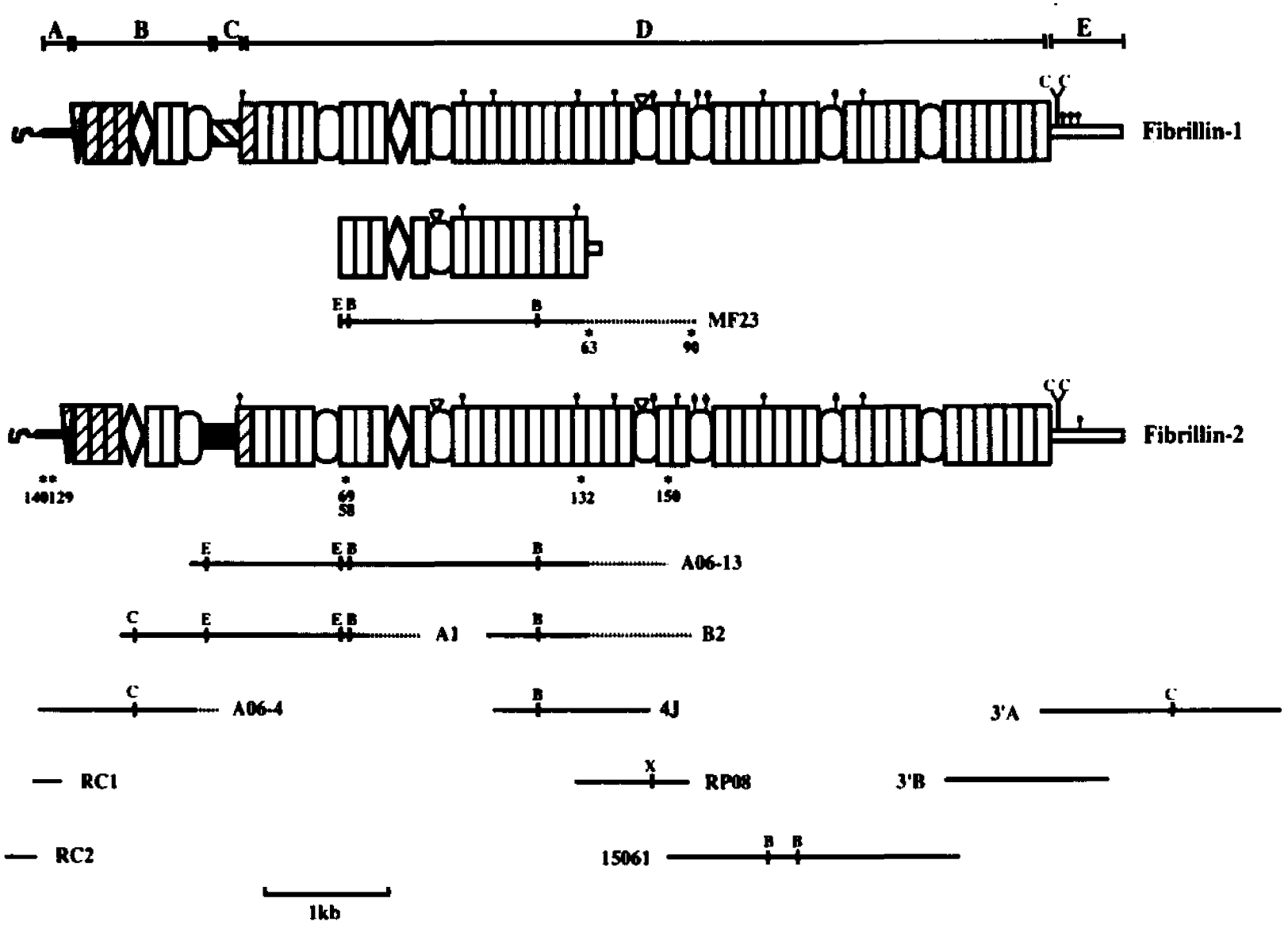
A
B
C
D
E
Fibrillin-1
MF23
63
90
Fibrillin-2
140129
69
58
132
150
A06-13
A1
B2
A06-4
4J
3'A
RC1
RP08
3'B
RC2
15061
1kb

Figure 4: (Previous page) Restriction map of FBN2 cDNAs with a schematic illustration of the Fib1 and Fib2 protein structure. Letters indicate the five structural regions. Symbols represent the following structural elements: signal peptide (wavy line); EGF-CB repeat (white rectangle); EGF repeat (hatched rectangle); TGFb-bp repeat (white ovals); Fib-motif (white diamond); putative glycosylation sites (black dots); potential cell-attachment signal (white triangle). Note that region C is depicted differently in two-fibrillins in order to emphasize its compositional difference. Asterisks indicate the positions of the oligonucleotide probes MF58, MF69, MF130 and MF150 used for the screening of the library; and primers MF129 and MF140 for the primer extension and RACE experiments. The dotted line on the restriction map indicate the unspliced intron sequences. Letters on the cDNAs indicate the following restriction enzymes: BamHI(B), ClaI(C), EcoRI(E) and XhoI(X).

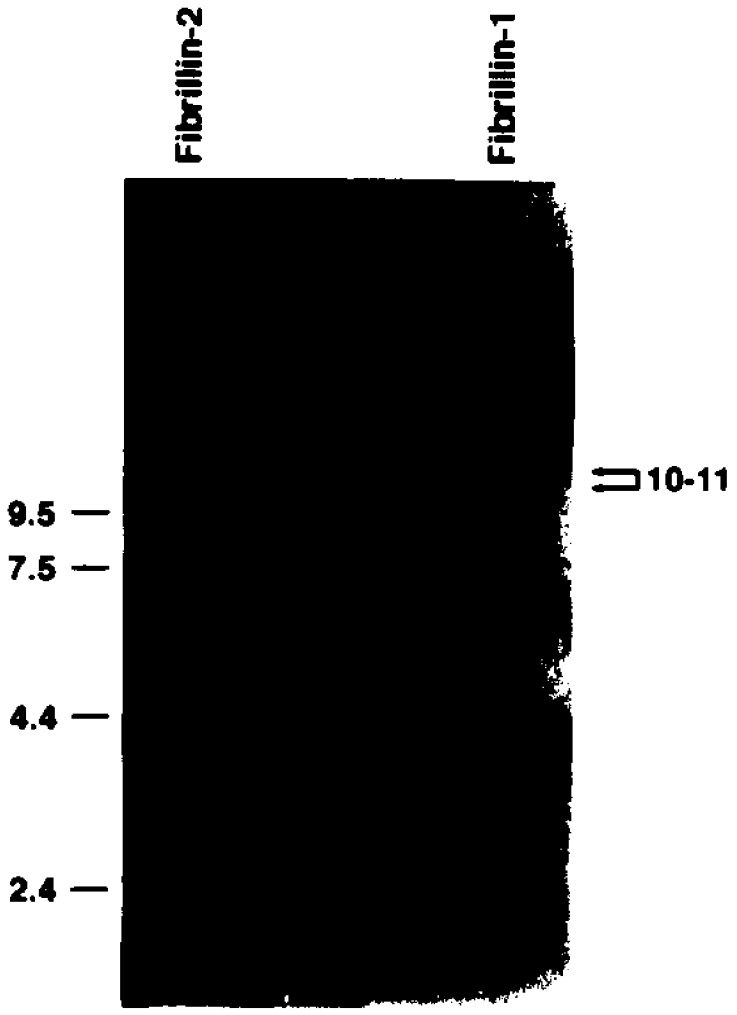

Figure 5: Northern blot hybridization of FBN1 and FBN2 specific probes to MG63 RNA . RNA size markers (in kb) are indicated on the left of the autoradiogram, while the estimated size range of the two transcripts is shown on the right.

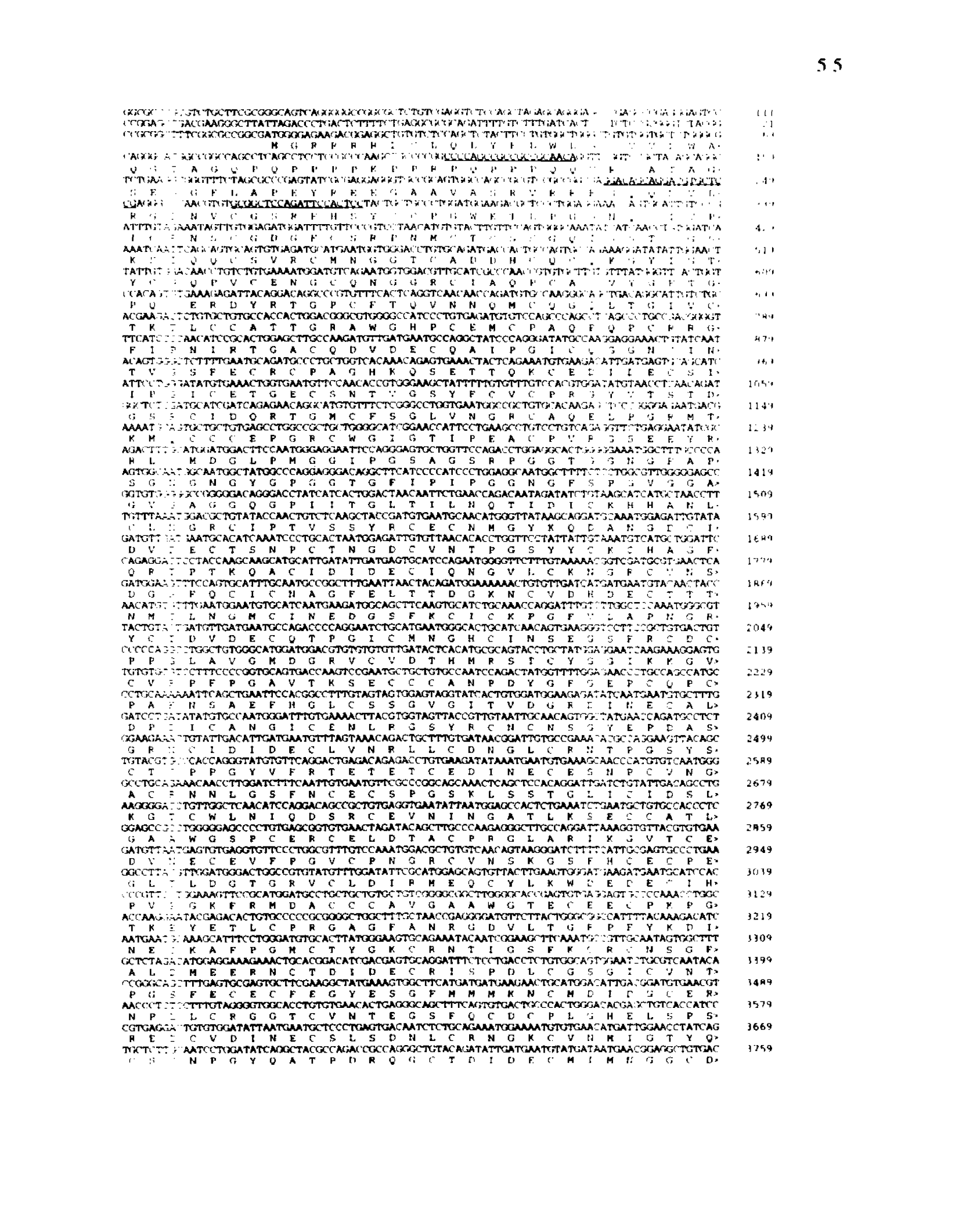

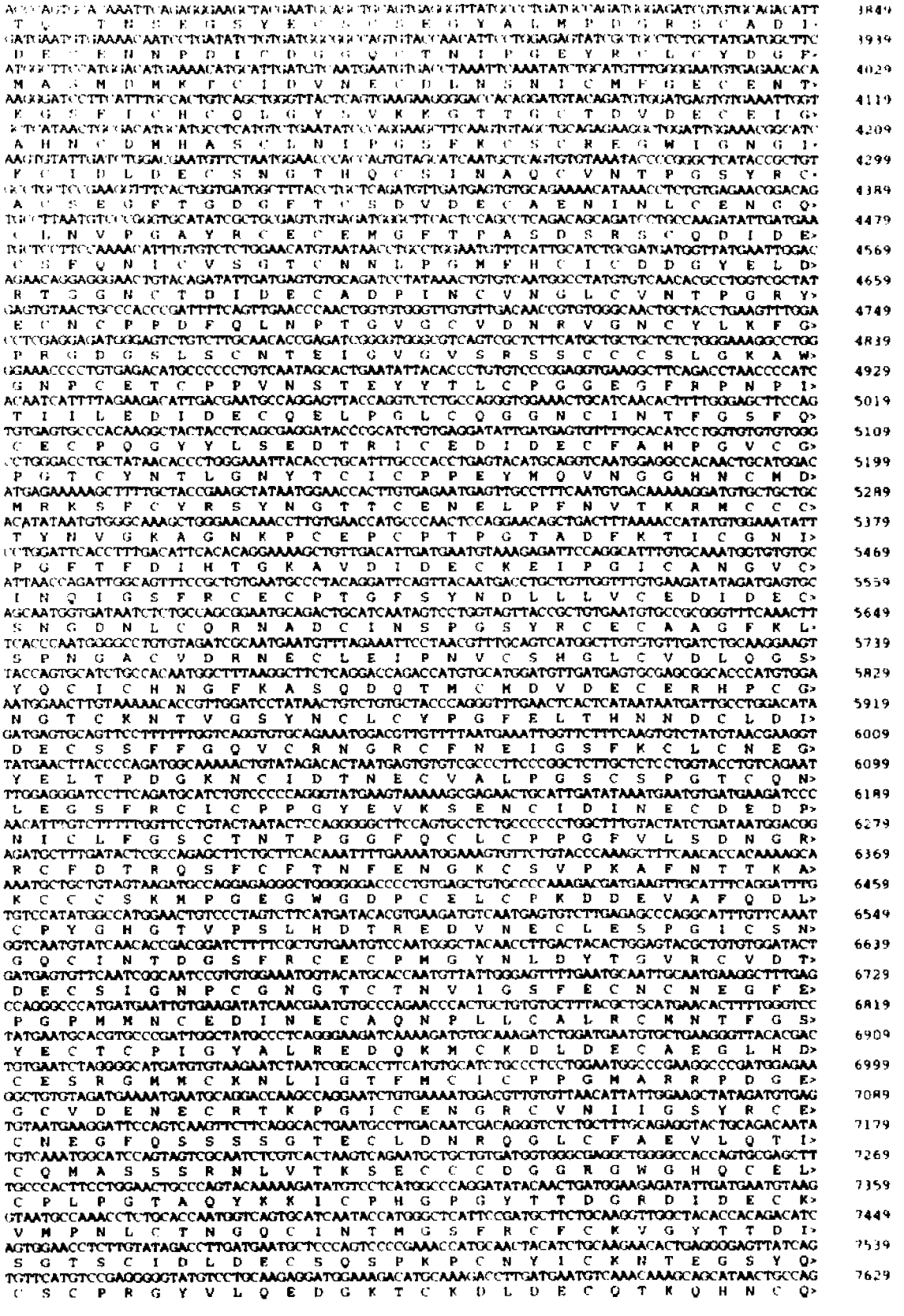

Figure 6: FBN1 cDNA sequence with amino acid translation. Numbering starts from the first ATG. Underlined sequences are primers used in primer extension and 5' RACE experiments. From 5' to 3', they are MF171, MF140 and MF129.

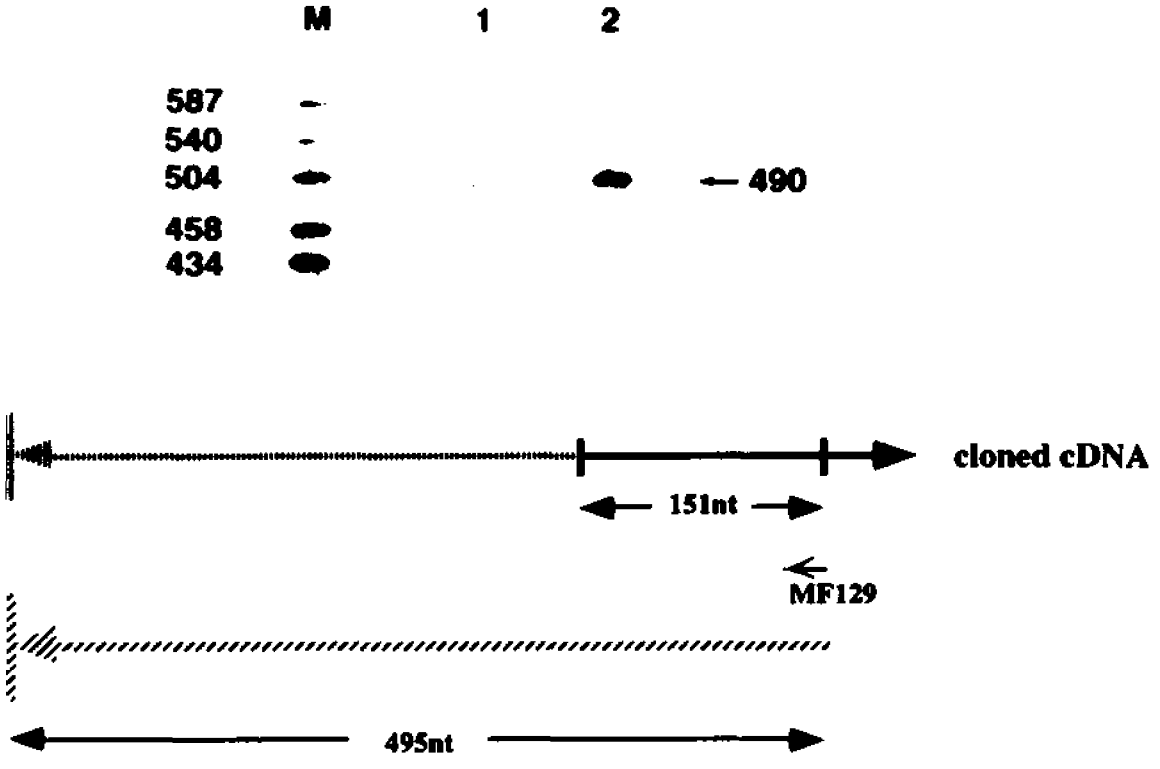

Figure 7: Primer extension using MF129 as primer (see Fig. 6). RNA from cell lines NT2/D1 (lane 1) and MG63 (lane 2). Marker sizes on the left are in nt, and the estimated product size is on the right.

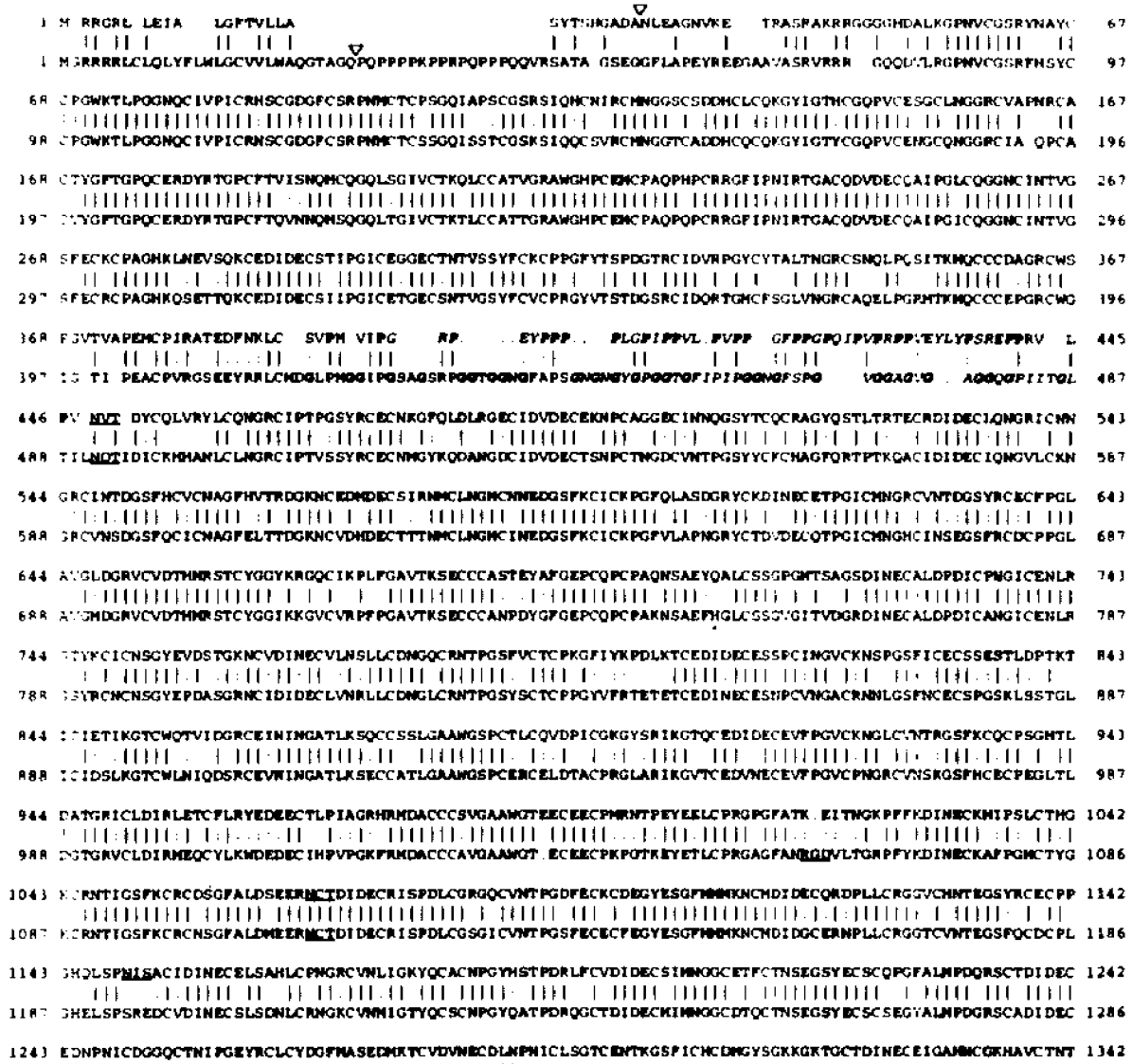

Figure 8: Comparison of the amino acid sequences of Fib1 (top) and Fib2 (bottom) with residues numbered according to Pereira et al. (1993). Identities and conservative changes are indicated by vertical bars, whereas one and two dots denote decreasing levels of evolutionary distance between amino acids calculated according to Gribskow and Burgess (1986). Dashes were introduced for best alignment. Glycosylation and cell-attachment sites are underlined. The sequence of the glycine- and proline-rich regions used for the generation of the antibodies are italicized with the glycine and proline residues indicated in bold characters. Triangles identify putative signal peptide cleavage sites and asterisks indicate the coding boundaries of MF23.

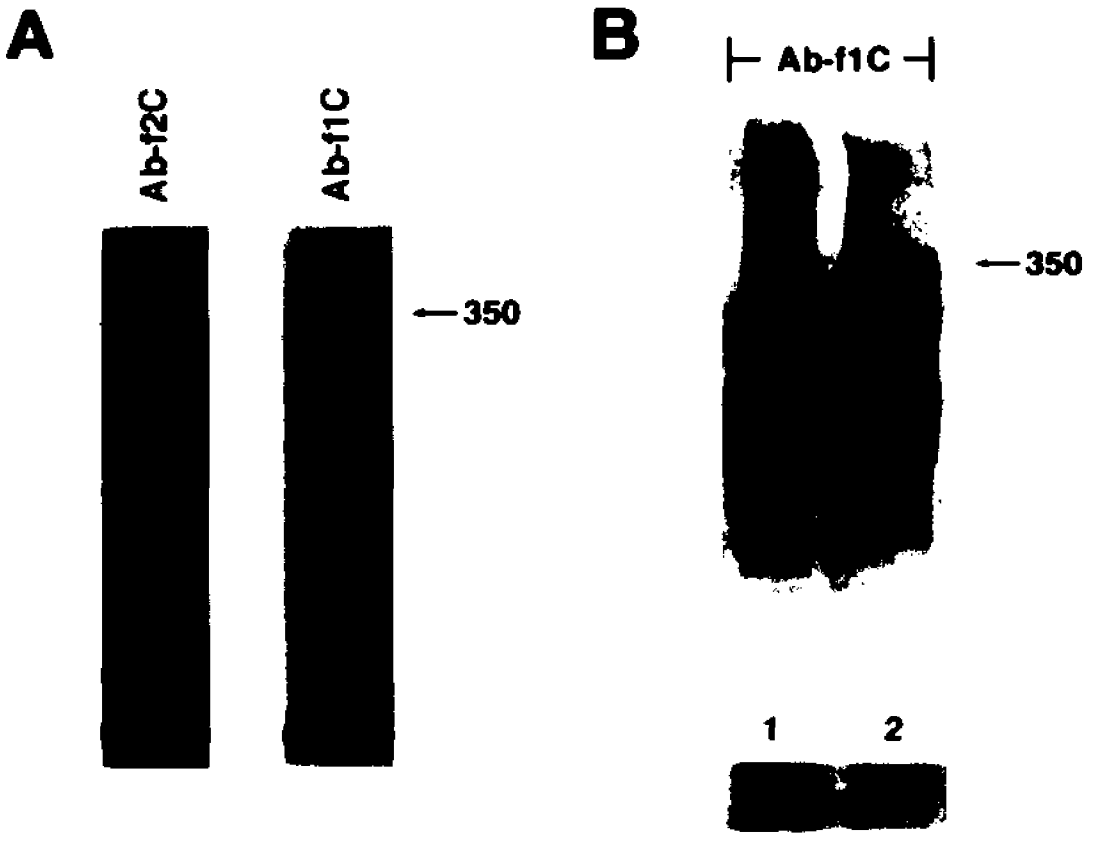

Figure 9: (A) SDS-PAGE of radioactively labeled immunoprecipitates obtained using Ab-flC or Ab-f2C antisera. (B) The unlabelled immunoprecipitates immunoblotted with Ab-flC. Underneath each lane is a silver staining of the gel showing equal loading of the two proteins. The estimated protein size is indicated on the right side of each panel.

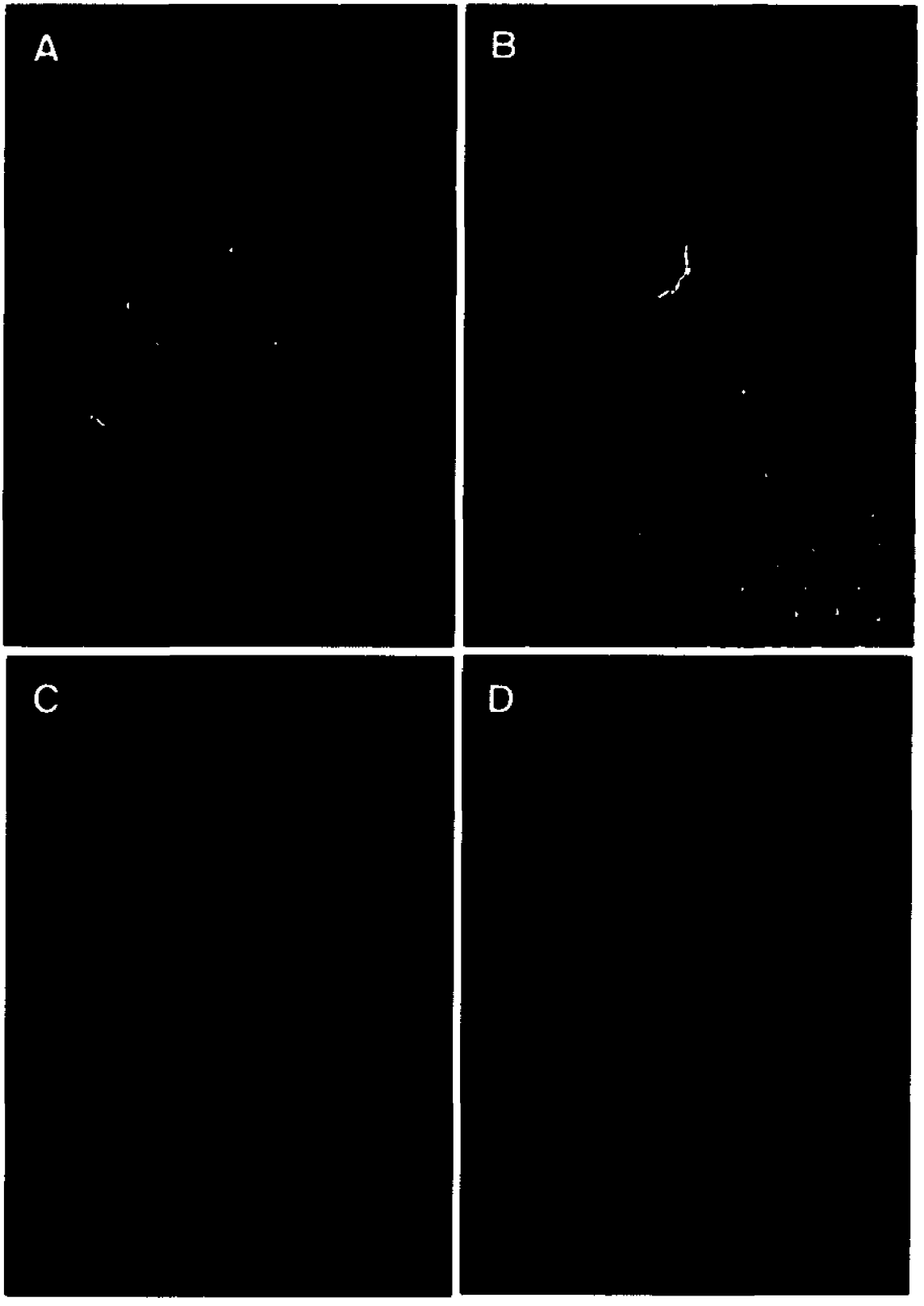

Figure 10: Indirect immunoflorescent localization of fibrillins in human skin. Staining of adult skin with Ab-f1C (A), Ab-f2C (C); and staining of fetal skin with Ab-f1C (B), Ab-f2C (D).

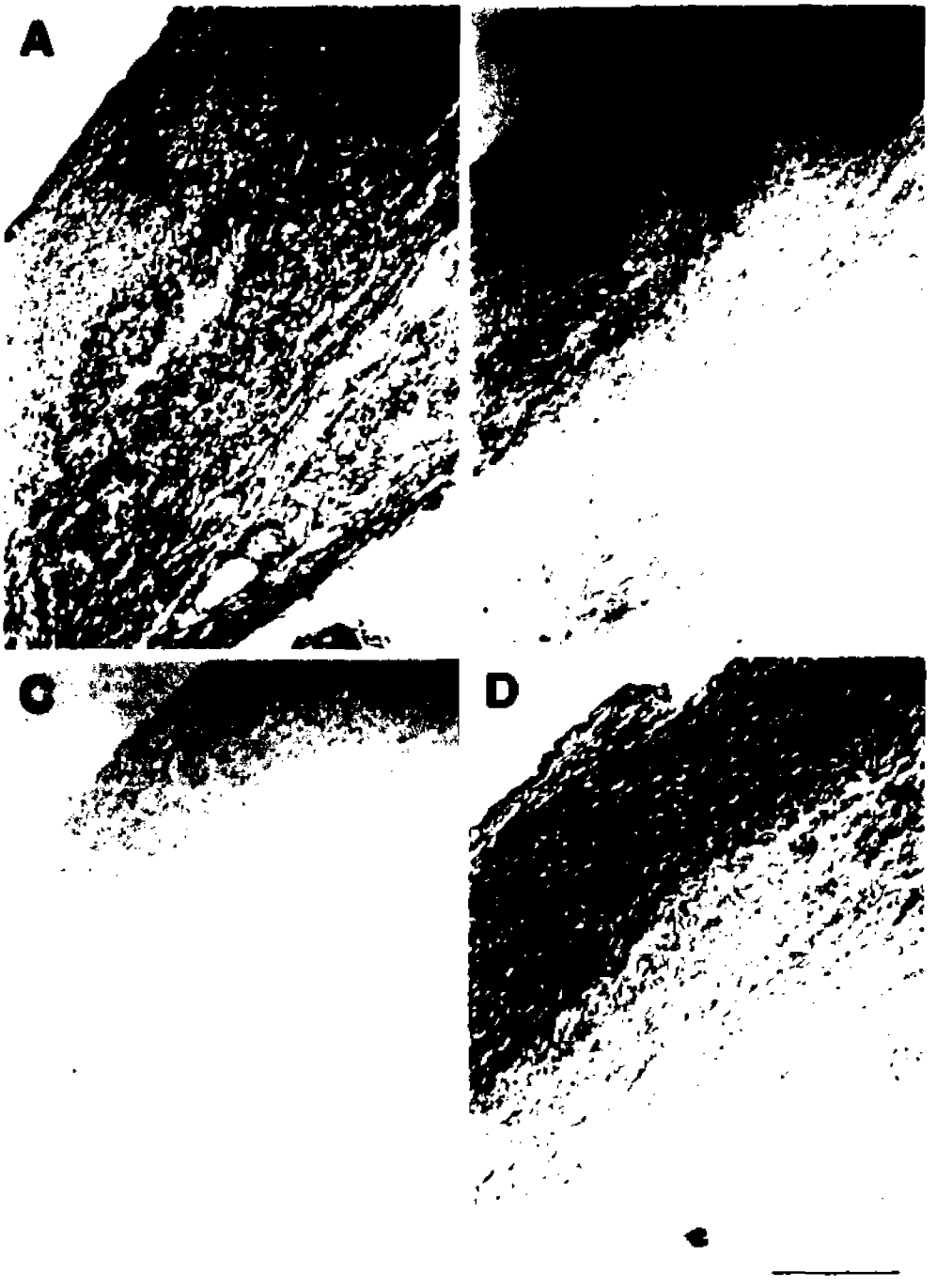

Figure 11: Immunohistochemical localization of fibrillins in human fetal aorta using Ab-f1C (A) and Ab-f2C (B) antisera. C shows sample treated with pre-immune serum, and D shows Verhoeff's staining for elastic fibers. Note that the lumen of the aorta is always at the top left corner. Bar = 200 μm.

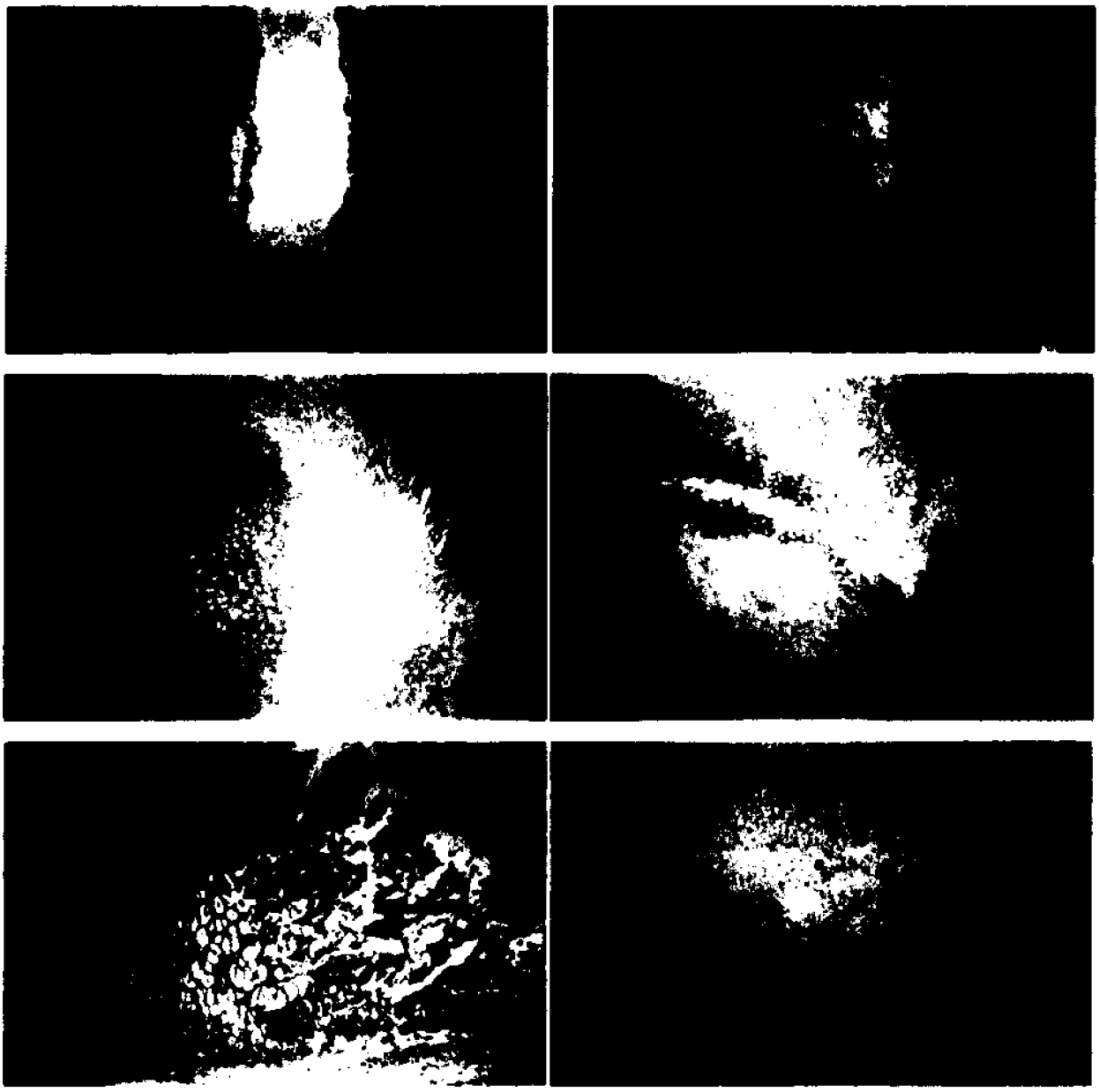

Figure 12: Immunohistochemical localization of fibrillins in human fetal ear (A and B) and toe (C to F) using Ab-f1C (A, C, and E) and Ab-f2C (B, D, and F) antisera. The arrows in B and F highlight the perichondrium, while the arrowheads point to the cartilaginous core in B, the peripheral areas of cartilage in D, and the hypertrophic zone in E. Staining with pre-immune serum was negative. Bar=100μm.


C
B
A
F

Figure 13: (Previous page) Immunohistochemical localization of fibrillins in human fetal ocular tissues (A-F), lung (G-I) and kidney (J-L) using Ab-f1C (A,D, G, and J) Ab-f2G(B, E, H, and K) antisera. C, F, I, and L show samples treated with pre-immune serum. The arrowheads highlight Descemet's membrane (A-C), the outer layer of the sclera (D-F), the interlobular septa of the lung (G-I) and the glomeruli of the kidney (J-L). In A-C, the arrow points to the anterior portion of the cornea, in which stained necrotic debris are noticeable, and in J-L the arrow points to the developing collecting ducts . Bars: (A-C) 10 μm; (D-L) 50μm.

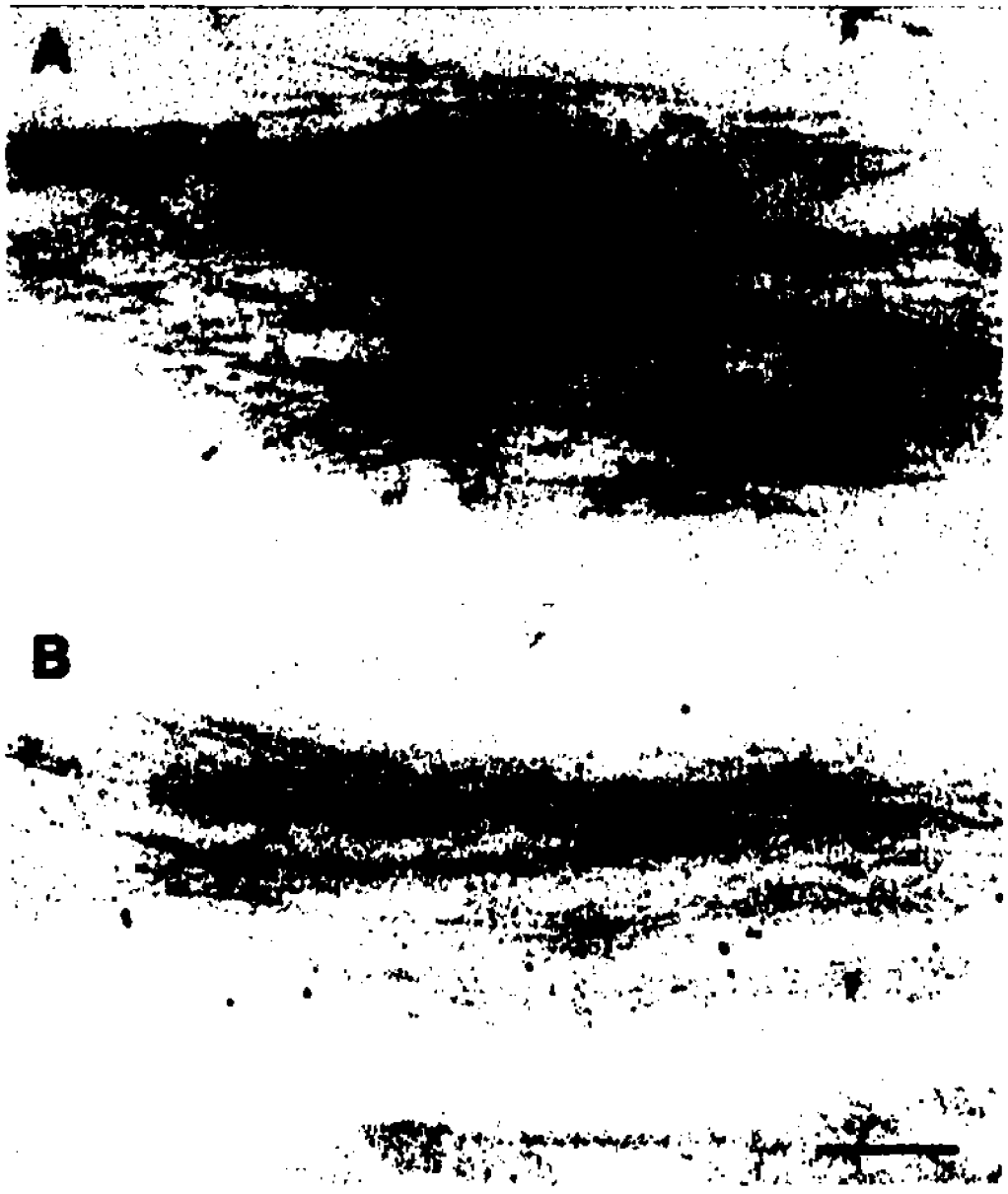

Figure 14: Immunolocalization of fibrillin-2 (A) and fibrillin-1 (B) on a developing elastic fiber in 170-d gestation bovine ligamentum nuchae. Gold particles label the peripheral mantle of microfibrils (MF) of the elastic fiber demonstrating the specific association of fibrillins with the microfibrils. Note that the central core of amorphous elastin (E) is devoid of label. Bar, 0.2 μm.

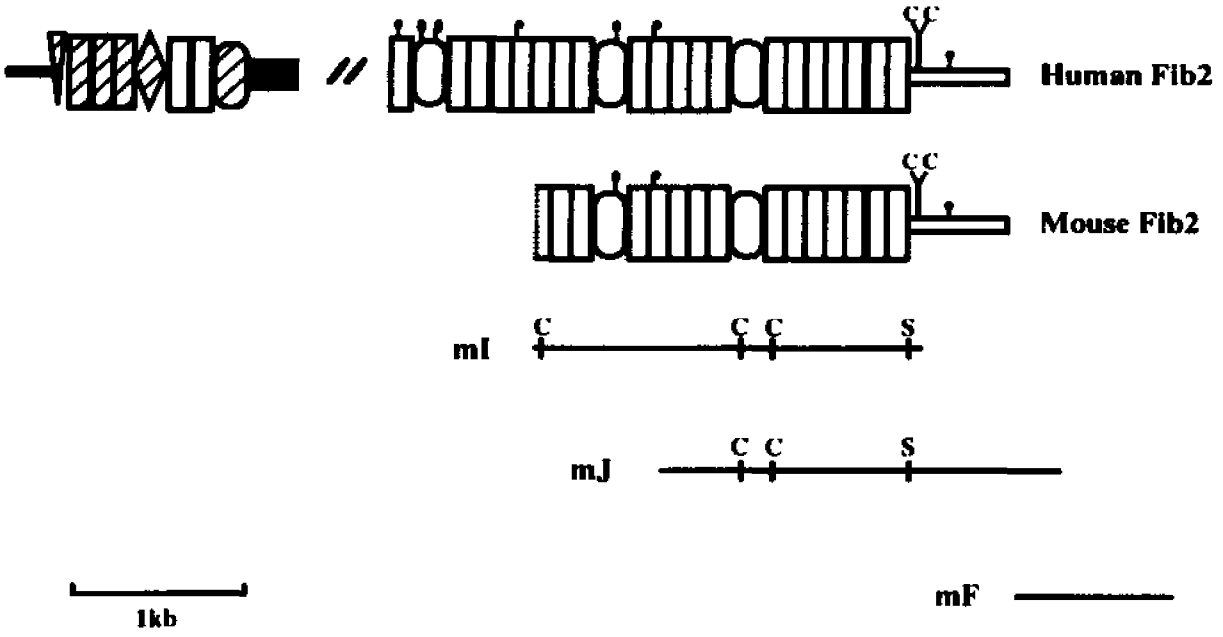

Figure 15: Restriction map of mouse FBN2 cDNAs and schematic comparison of the structure of murine and human Fib2. The symbols represent the same structures as in Fig. 4. Letters indicate the following restriction sites: ClaI (C) and SphI (S).

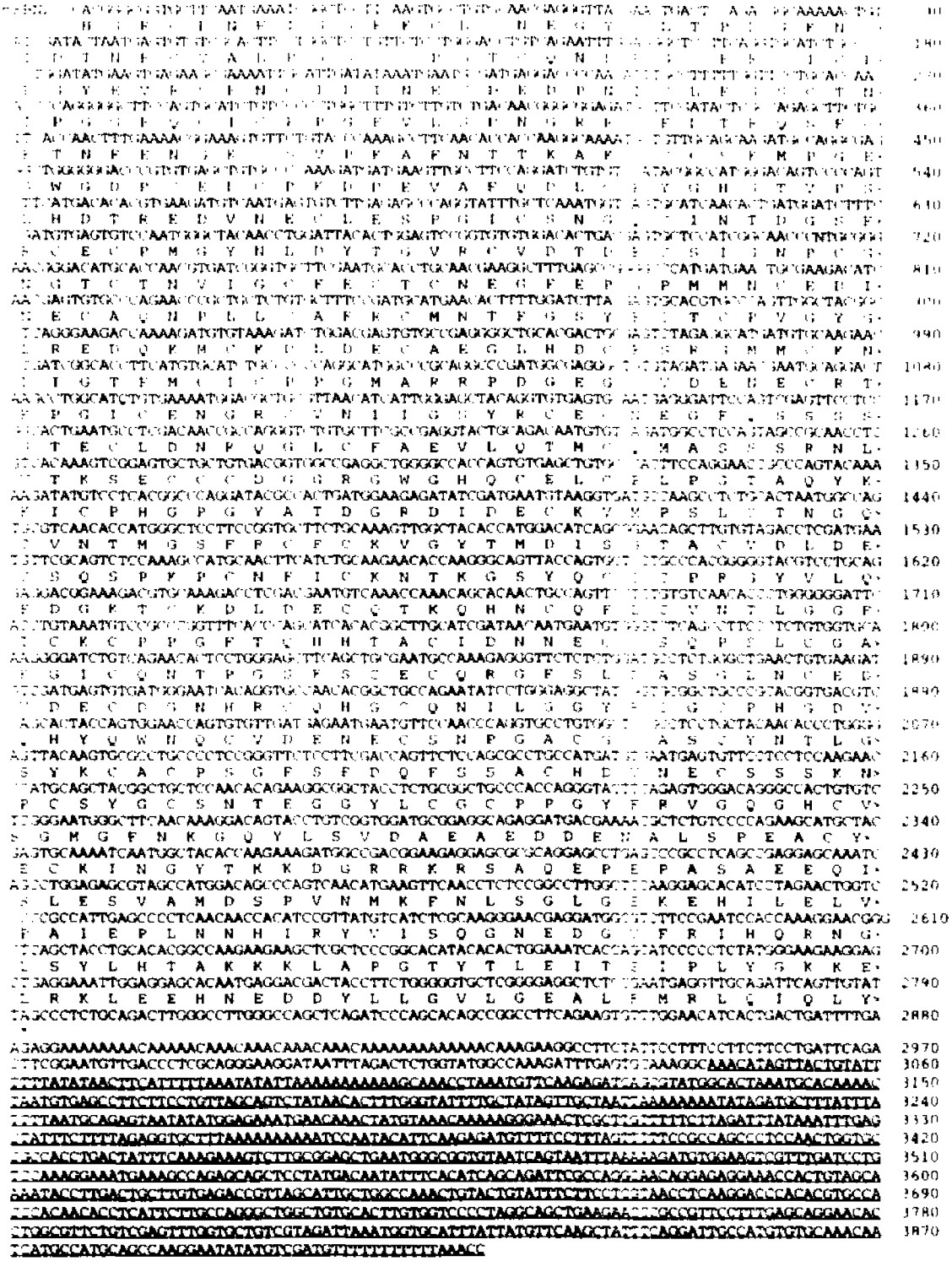

Figure 16: Mouse FBN2 cDNA sequence with amino acid translation. Underlined part indicate the fragment used as probe for in situ hybridization.

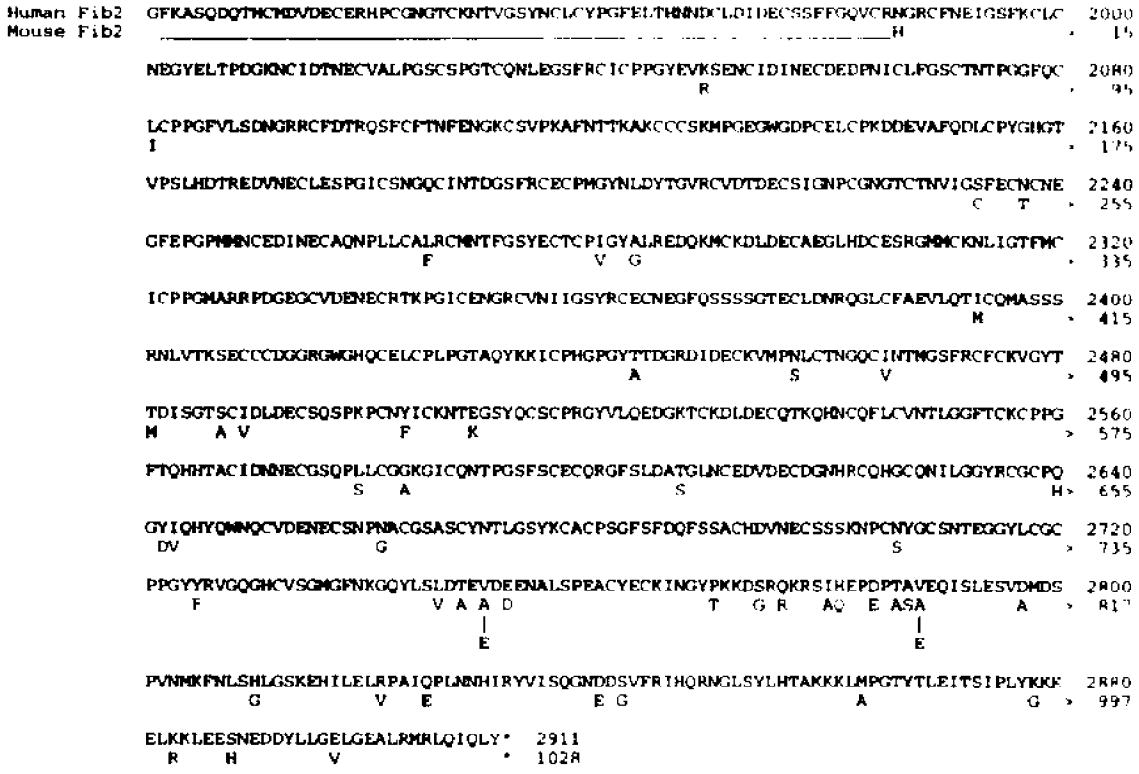

Figure 17: Comparison between human (upper) and mouse (lower) Fib2 primary structure. Only miss-matched amino acids are shown in the mouse Fib2.

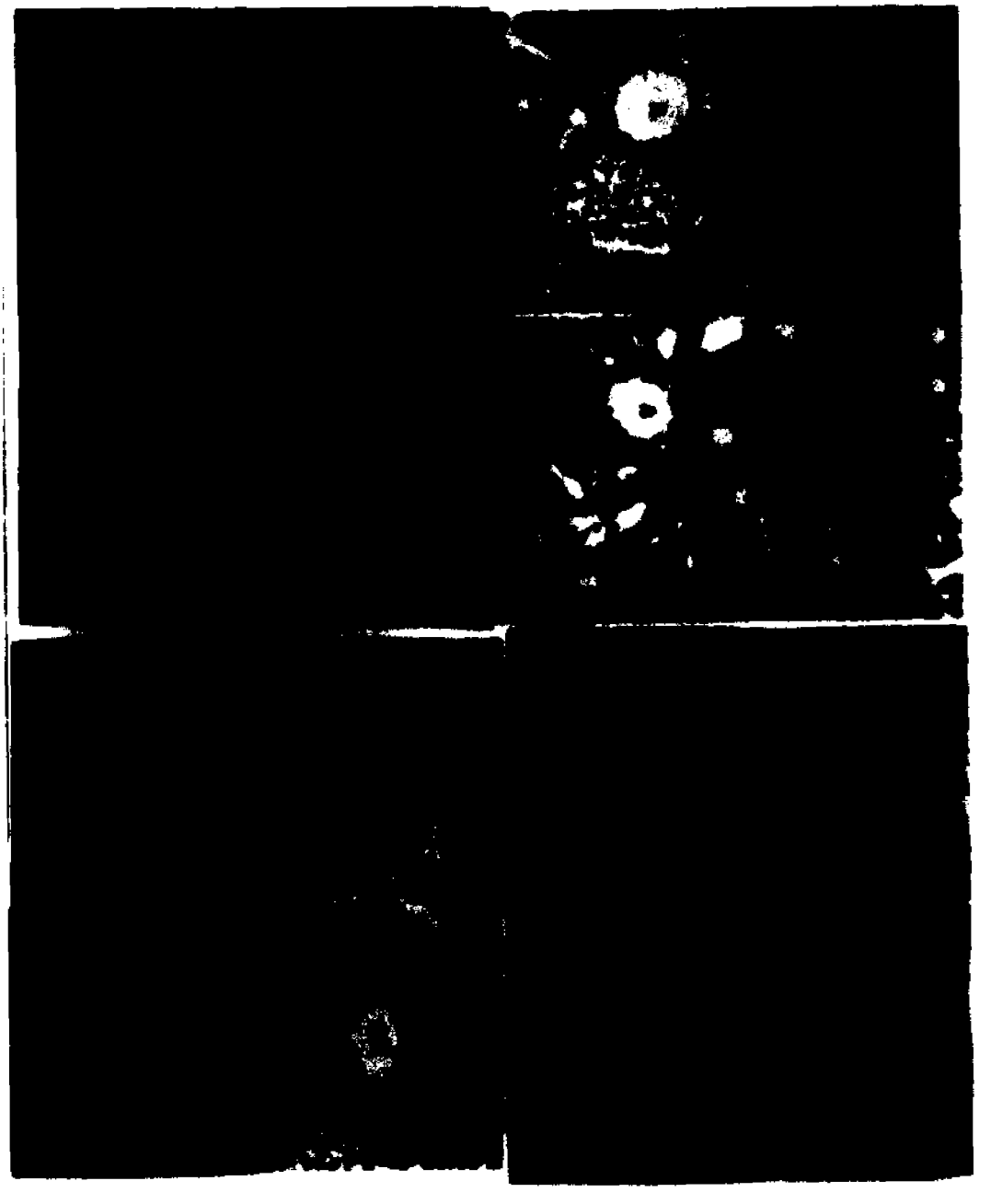

Figure 18: (Previous page) In situ hybridization of the lung bud at 10.5 d.p.c. (A-D), the developing lungs at 13. 5 d.p.c. (E-H) and 16.5 d.p.c. (I-L) using mouse FBN2 (A, C, E, G, I, K) and FBN1 (B, D, F, H, J, L) as probes. The epithelial cells of the main bronchi (mB), segmental bronchi (sB) and terminal bronchioles (tB) specifically express FBN2. Note the lack of FBN2 signal in the segmental bronchi at 16.5 d.p.c. (arrowhead) as compared to earlier stages. FBN1 expression at all stages is mostly in the lung parenchyma and arterioles (Ar). Bar = 50 nm.

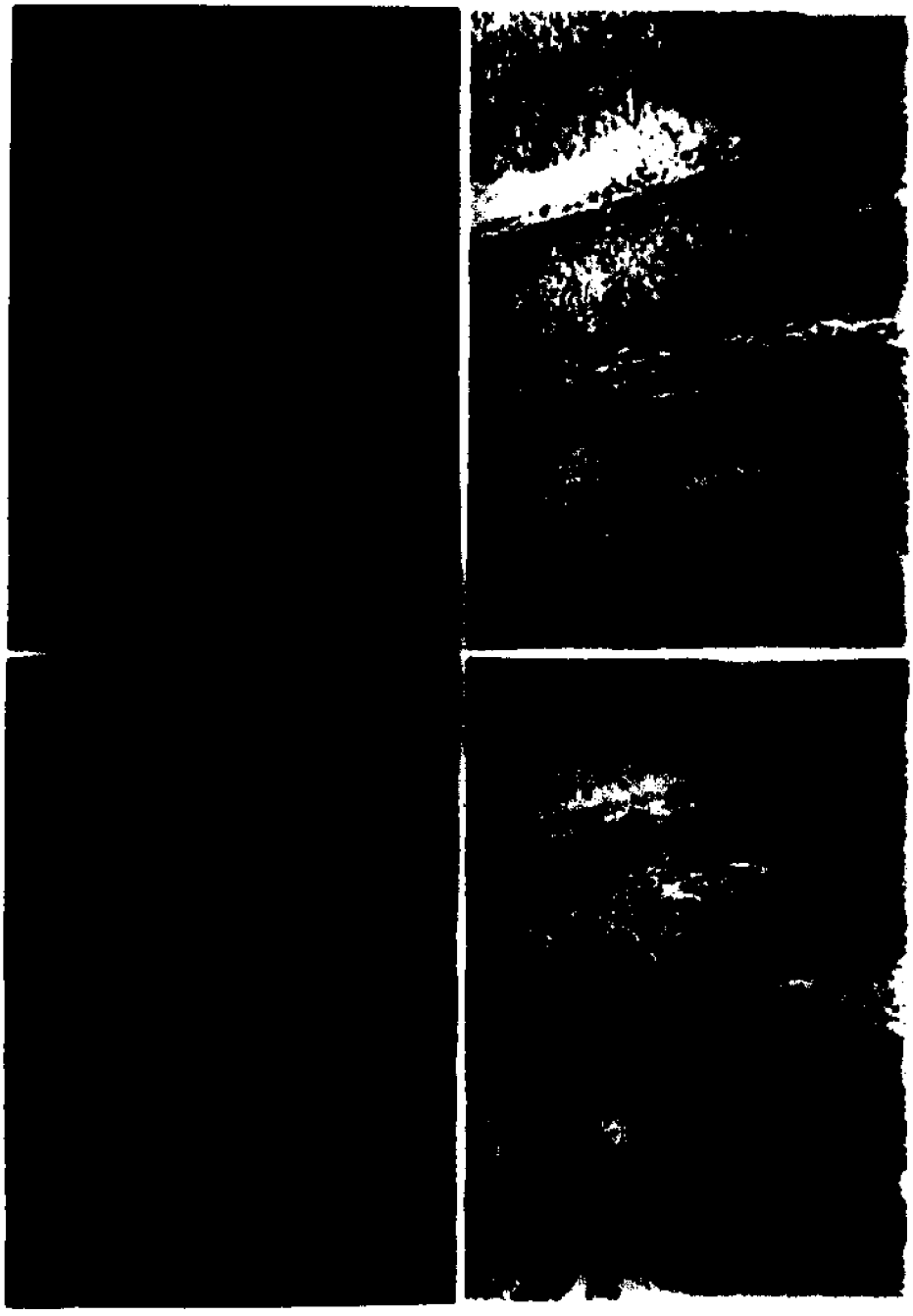

Figure 19: (Previous page) In situ hybridization of the main bronchi (mB), vertebral column (Vb), and the spinal cord (SpC) at 13.5 d.p.c. with FBN2 (A and C) and FBN1 (B and D) probes.

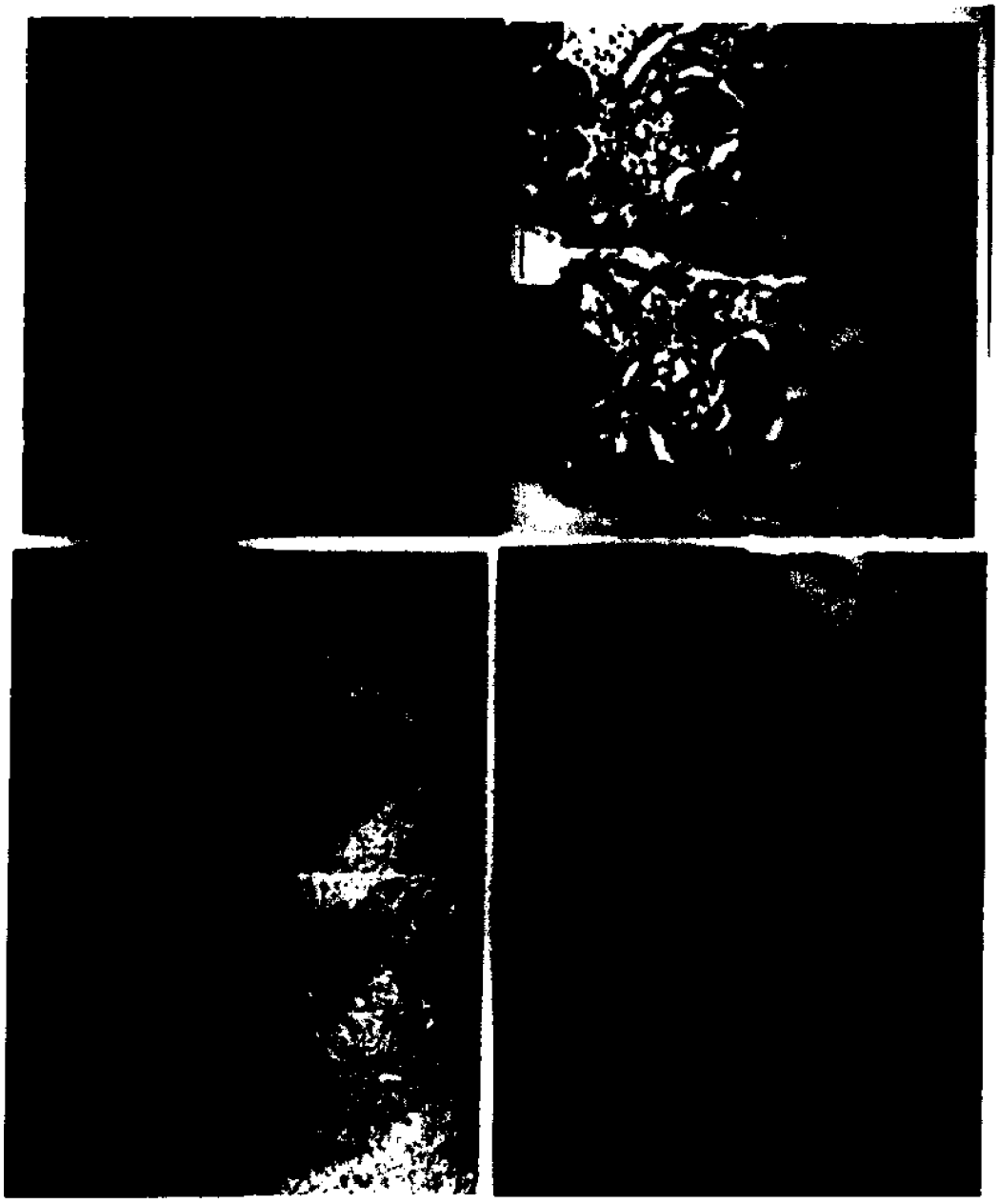

Figure 20: (Previous page) In situ hybridization of the kidney at 13.5 d.p.c. (A-D) and 16.5 d.p.c. (E-L) with mouse FBN2 (A, C, E, G, I, K) and FBN1 (B, D, F, H, J, L) probes. Open triangles point to the renal capsules and arrowheads to the developing glomeruli. Note the lack of firbrillin expression in the cells of collecting ducts (cd).

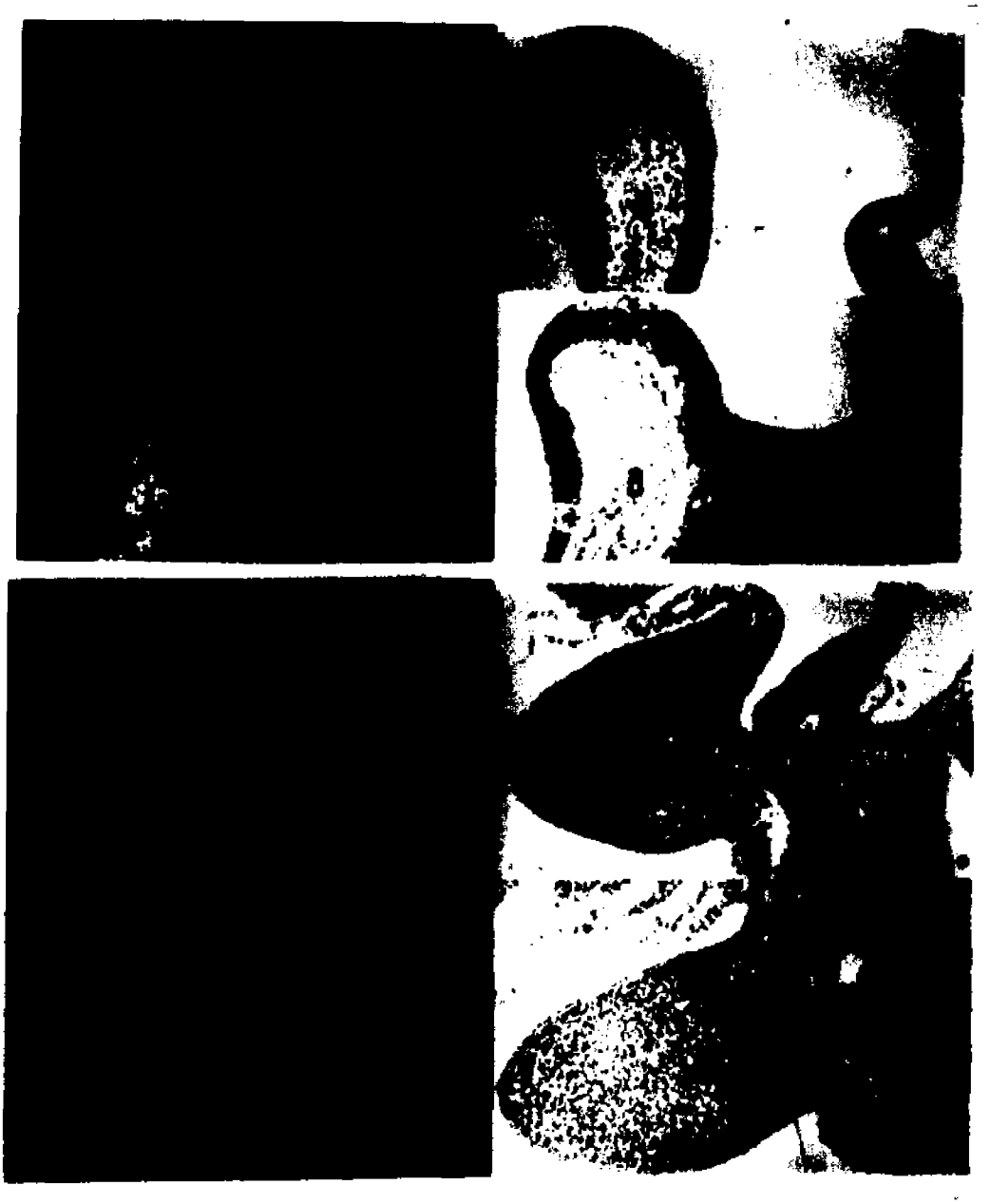

Figure 21: (Previous page) In situ hybridization of the 10.5 d.p.c. limb bud (Lb, A-D) and the cephalic mesoderm (CM, E-H), with FBN2 (A, C, E, G) and FBN1 (B, D, F, H) probes. The neuroectodermal cells (NEc) of the brain and spinal cord are not expressing either one of the fibrillins. Note the FBN1 signal in the cells of dorsal aorta (arrowhead).

Figure 22: Expression of FBN2 (A, C, E, G) and FBN1 (B, D, F, H) in joints of 13.5 d.p.c. mouse. Signals of the FBN2 message are prominent in the cells of perichondrinum (pCh), ligment (L), and tendon (T). FBN1 expression is widely distributed in the mesenchymal tissue with a slight increase in the perichondrium.

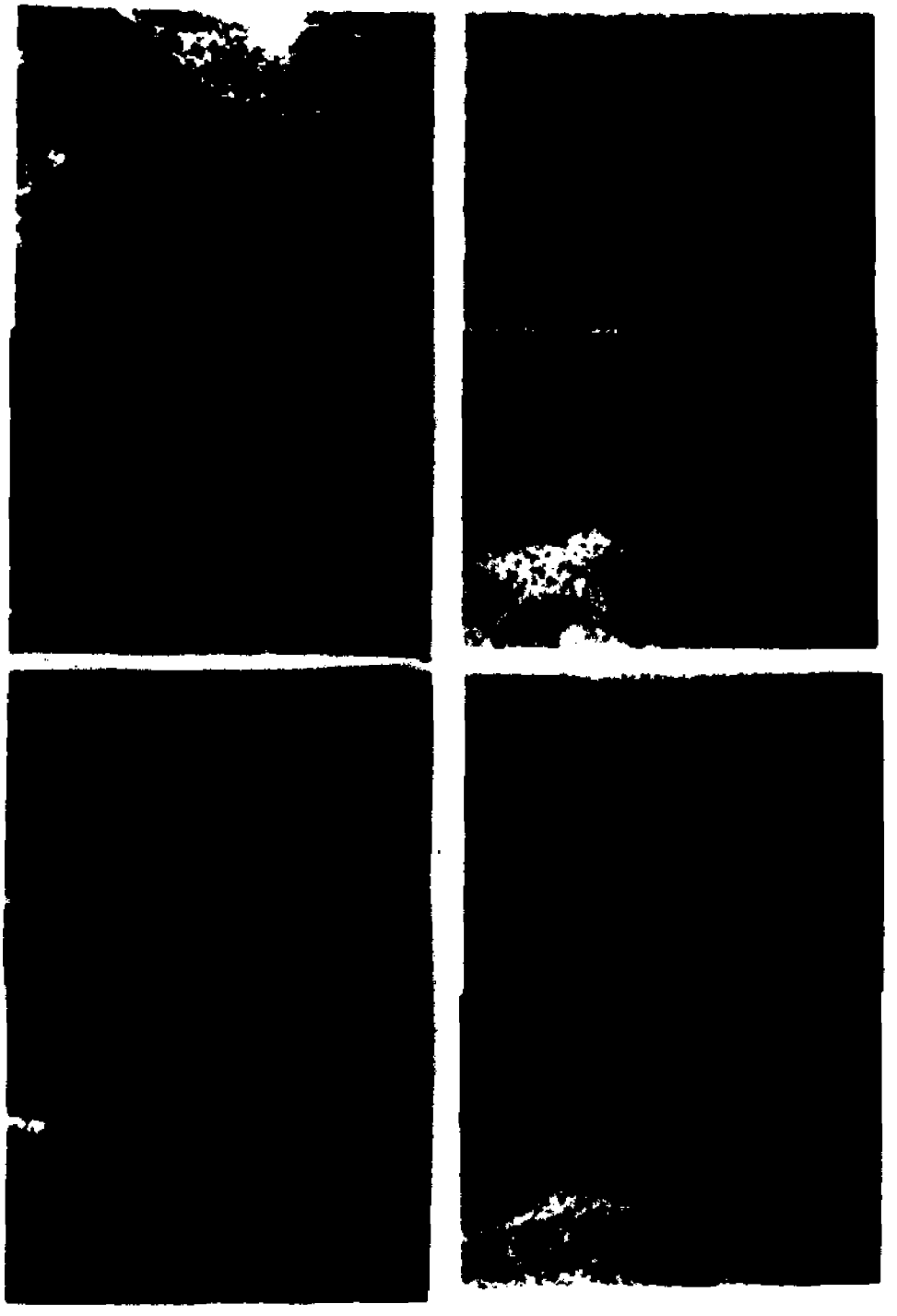

Figure 23: (Previous page) Expression of FBN2 (A, C) and FBN1 (B, D) in joints of 16.5 d.p.c. mouse. Intense FBN2 signals are noted in the cells of perichondrium (pCh), ligament (L), tendon (T), and the periphery of the cartilage (arrowhead). FBN1 expression is most notable in the vasculature around the joint capillaries (cp), and the cells surrounding the ligament and tendon. The signal of FBN1 in the mesenchymal cells (Ms) at this stage is more intense than that of FBN2.

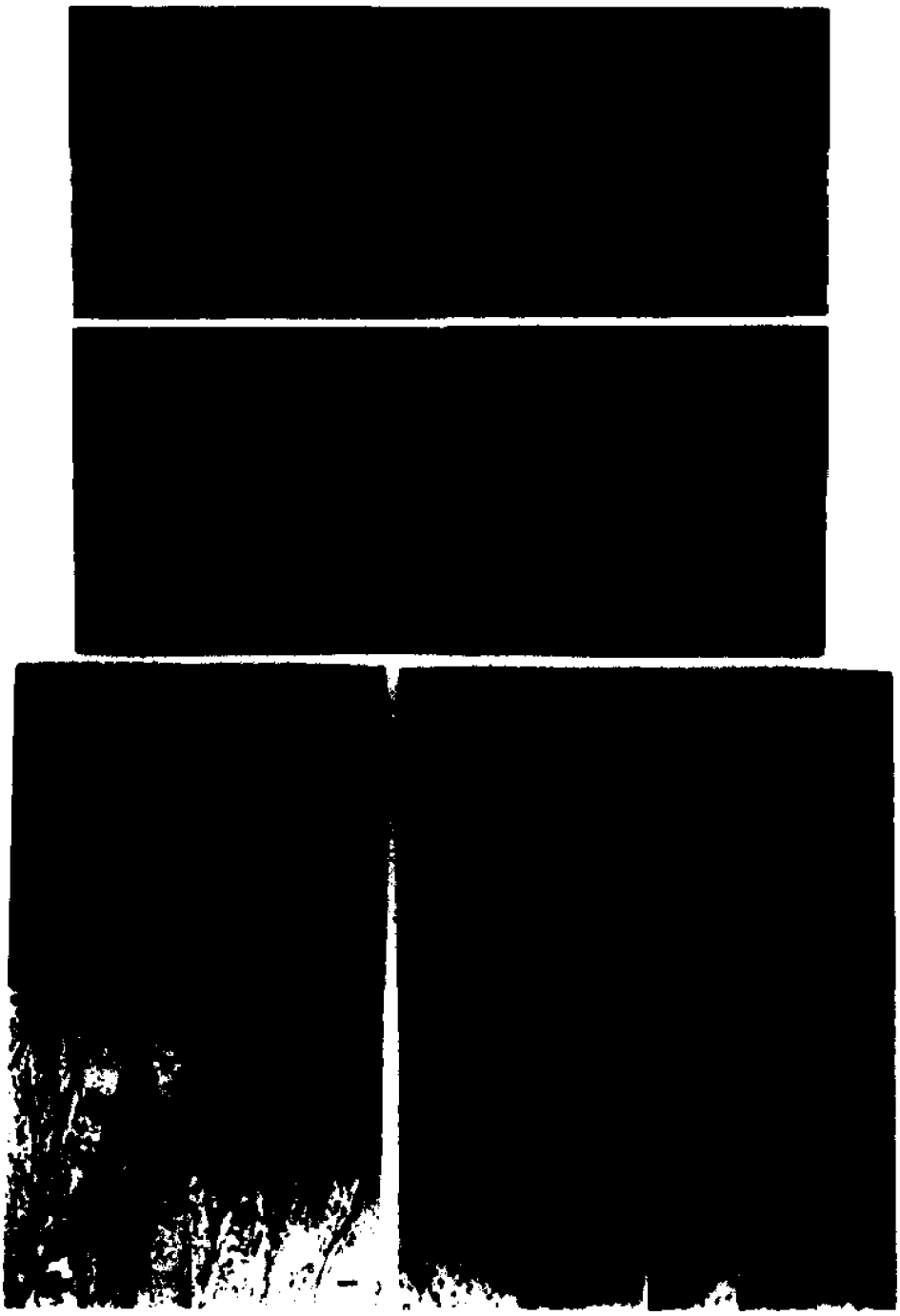

Figure 24: (Previous page) Expression of FBN2 (A, C, E, G, I, K, M, O) and FBN1 (B, D, F, H, J, L, N, P) in the long bone (A to D), ligamentum flava (E to H), rib (flat bone, I to L), and muscle (M to P) of 16.5 d.p.c.embryo. Intense FBN2 signal of is observed in the cells of perichondrium and growth plate (GP). Moderate expression of FBN1 is noted in the perichondrium, growth plate and the hypertrophic chondrocytes (hCh). The cells of the elastic ligamentum flava (LF) have a higher expression of FBN2 than FBN1 (E and F). Myocytes (M) accumulate FBN2 message, whereas perimysium cells (pM) express FBN1.

Figure 25: (Previous page) Expression of FBN2 (A, D, F) and FBN1 (B, C, E, G) in the laryngeal structures of 13.5 d.p.c. (A to C) and 16.5 d.p.c. (D to G) embryos. At 13.5 d.p.c., the mesenchymal cells (arrowhead) that later differentiate into the laryngeal structures have enhanced accumulation of FBN2 message. In 16.5 d.p.c. mouse, the elastic cartilages of the larynx, epiglottis (Ep) and cuneiform cartilage (Cn) have a high expression of FBN2. The signals for FBN1 in these structures are not particularly high. Esophagus (Es) and trachea (Ta) are indicated in the figure.

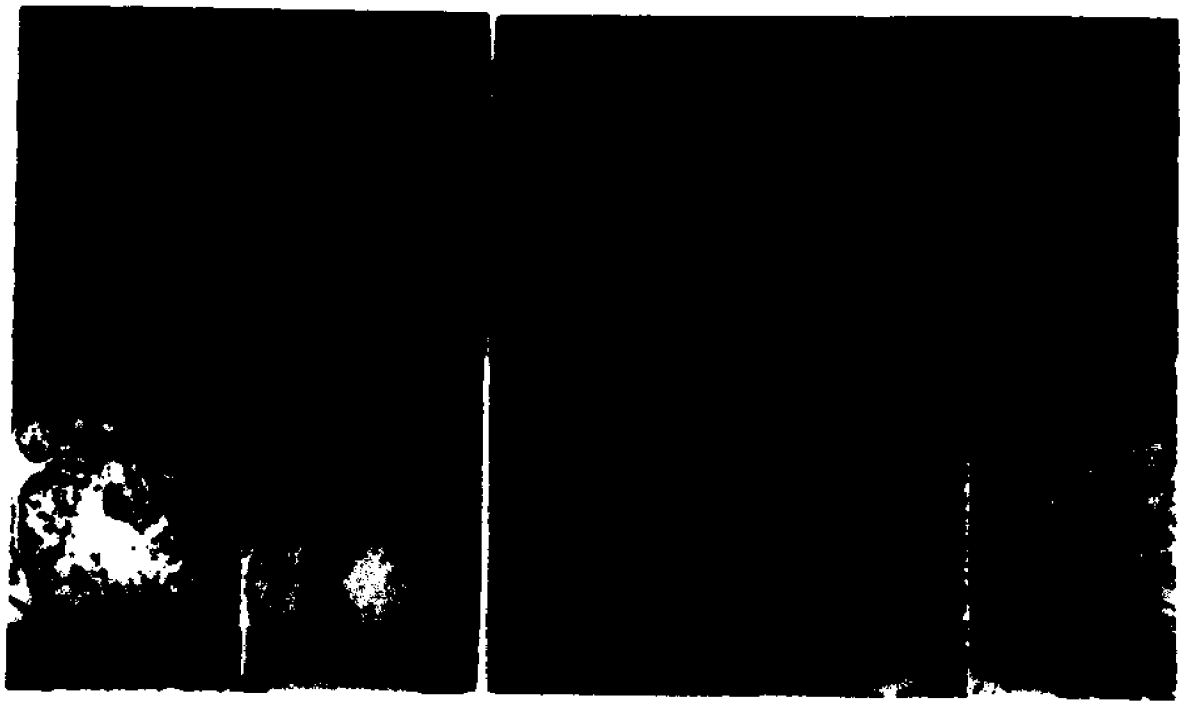

Figure 26: Expression of FBN2 (A, C, E, H) and FBN1 (B, D, F, G, I, J) in the 10.5 d.p.c. developing mouse heart. FBN2 signals are seen in the myocardial cells whereas FBN1 is expressed in the epi- and endocardial cells (arrowheads). The cells at the endocardial cushion (EnC) tissue express both FBN2 (A,E) and FBN1 (B, F). The truncus arteriosu region (tA), where the aortico-pulmonary spiral septum is forming, has a strong signal for FBN1 expression. The wall of the aortic sac (as) is expressing both fibrillins (E, G); note that only the edge of the aortic sac is on the section in E and H.

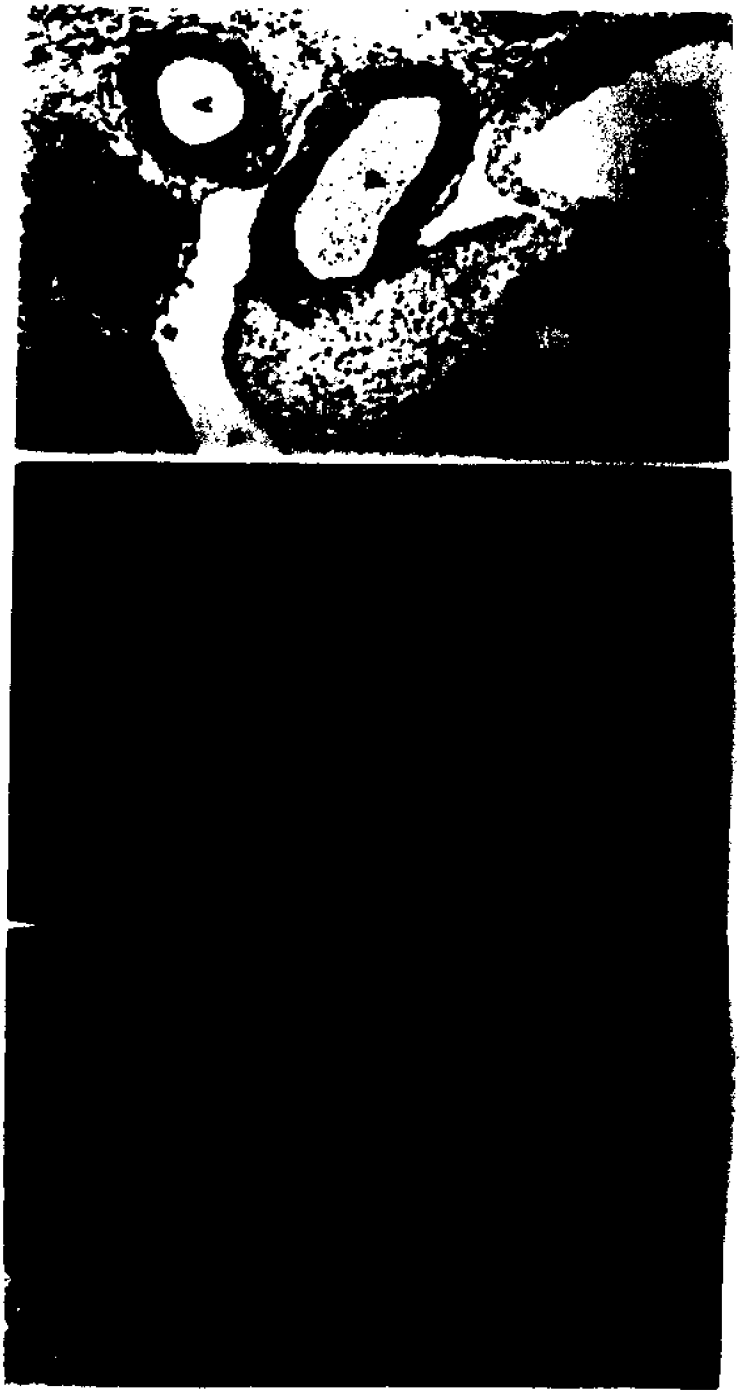

Figure 27: (Previous page) Expression of FBN2 (A) and FBN1 (B,C) in the heart (H) and elastic vessels of the 13.5 d.p.c. embryo. The entire walls of the pulmonary trunk (P) and aorta (A) have strong expression of FBN1, whereas the FBN2 message is observed mostly in the medial layer. The myocardial cells express the FBN2 gene, thus giving uniformly distributed signals in the heart. However, the expression of the FBN1 gene, most probably by the endothelial and fibroblast cells of the cardiac skeleton, gives a punctate signal pattern. The capsule and the septa of the thymus (T) also show fibrillin expression.

Figure 28: Expression of FBN2 (A, C, E, G) and FBN1 (B, D, F, H) in the large vessels of the 16.5 d.p.c. embryo. In the elastic arteries (A to D), FBN1 message is accumulated in the full thickness of the vessel wall, particularly in the intimal and adventitial cells (B, arrowheads). FBN2 signal is mostly seen in the medial layer and particularly, in the outer elastin rich part of the elastic arteries (A) and the muscular artery (E). Note the clearly negative background in the nervous tissue of the spinal cord (SpC).

Figure 29: Expression of fibrillins in the eye (A-F) and digestive system (G-O) of 13.5 d.p.c. (A to C, G to L) and 16.5 d.p.c. (D-F, M-O) embryos. Expression of FBN2 (A, D) is observed in the sclera (arrowheads) as early as 13.5 d.p.c., while FBN1 message is only seen on 16.5 d.p.c. sclera (E). Some expression of FBN2 can be noted in the retina cells (Rr) at 13.5 d.p.c., but no signal of either fibrillin mRNA can be detected in these cells at 16.5 d.p.c. The smooth muscle cells of the stomach (G-I) and the intestines (J-O) show accumulation of both fibrillin mRNAs. The lamina propia cells of the intestine also express FBN2, but not FBN1 (see arrowhead on M).

DISCUSSION

Results presented in this thesis conclusively demonstrate that fibrillin is not a monogenic product but a small group of matrix proteins with distinct patterns of expression and presumably, different functional roles. They also strongly suggest a differential fibrillin composition of morphologically similar microfibrils associated with elastin and unassociated. The compositional diversification of the microfibrillar networks probably results in distinct biochemical and physiological properties of various elastic and non-elastic tissues, both during embryonic morphogenesis and in adult organgenesis. The conclusions of this work have therefore provided an unexpected new perspective on microfibril biology, and as such, they lay the groundwork for future investigations aimed at testing the validity of several hypotheses. These conclusions and hypotheses will now be discussed together with a brief recollection of the most relevant experimental data.

I. Identification of the Full Length FBN2 Transcript

The first point clarified by this study was the nature of the FBN2 gene transcript identified originally through the cloning of the MF23 cDNA. As already mentioned, the sequence composition of the initial FBN2 clone MF23 suggested the following four alternatives: a) FBN2 is a pseudogene which does not encode a protein; b) FBN2 codes for a truncated version of a fibrillin-like protein; c) FBN2 codes for a protein of similar size, but only partially homologous to fibrillin; and d) FBN2 codes for a protein structurally and functionally related to fibrillin. The last two alternatives were indirectly supported by Northern blot hybridizations showing that the FBN2 and FBN1 transcripts are of comparable size. Unfortunately, this result was originally obtained using potentially cross-hybridizing probes. It should also be noted that the second and third alternatives would not necessary restrict the FBN2 gene product as being an ECM component. If this were true, it

might have meant that the genetic linkage between FBN2 and CCA was merely coincidental.

The initial phase of this work was therefore mostly devoted to confirming the sequence of the 3' end of the FBN2 transcript and, to a lesser extent, cloning its 5'end. This effort eventually lead to the demonstration that MF23 represents a partially processed mRNA whose carboxyl terminus coding region and 3'UTR correspond to part of an intron. The intronic nature of the 3' UTR of MF23 and the continued use of a placental cDNA library delayed the process of identifying the full-length FBN2 transcript. On the one hand, use of the carboxyl-terminus and/or 3'UTR probes of MF23 failed to give a positive Northern blot result. On the other, use of more upstream probes identified placental cDNAs extending further 5' the ORF of MF23, but also encoding truncated forms of fibrillin-like proteins. These initial findings strengthened the possibility that FBN2 might be a pseudogene that produces a variety of abortive transcripts. Fortunately, the availability of additional clones produced in this and a parallel study (Pereira et al., 1993) enabled us to use more discriminating probes in Northern blot analysis of RNA from different cellular sources. The results confirmed the 10.5 kb size of the FBN2 transcript in cell lines MG63 and NT2/D1. Convinced that FBN2 is transcribed and successfully processed at least in these cell lines, we constructed cDNA libraries from mRNA extracted from the MG63 cells. Characterization of clones isolated from these cDNA libraries provided structural evidence that FBN2 encodes a secretable protein of the same size as Fib1.

The choice of RNA from full-term placenta as a source for mature FBN2 mRNA was not a good one, in view of the subsequent evidence suggesting the transient expression of FBN2 during organgenesis. We speculate that Fib2 production occurs early in placental formation and ceases before the end of a pregnancy, and that the production of Fib2 protein is controlled post-transcriptionally by incomplete processing of the nuclear RNA. The production of non-globin proteins in mature erthyrocytes is an example of such a regulatory mechanism (Darnell et al.,1990). In these cells, non-globin transcripts constitute 99.95%

of the total nuclear RNA, but only 10-50% of the total mature mRNA. This apparent discrepancy indicates that, although transcription of non-globin genes continues throughout erythropoiesis, processing of non-globin transcripts and/or stability of most non-globin mRNA are substantially decreased in mature erythrocytes. Partially spliced FBN2 transcripts in placenta were probably collected along with poly A^+ mRNA due to the AT-rich nature of the intron, and subsequently reverse transcribed by priming at these regions with oligo-dT primers.

Although the MG63 cDNA libraries were instrumental in solving the Fib2 structure, they failed to yield the very 5' end of the FBN2 transcript. As an alternative, we used the RACE protocol to isolate the 5' end of the estimated 10.5kb transcript. In employing this approach we still had two major difficulties, the high GC content and the extensive secondary structure of the FBN2 mRNA. Appropriate tailing of the 3' end of first strand cDNA is critical for a successful PCR amplification which is in turn necessary for the subsequent cloning. The original procedure described by Forhman et al. (1988) utilizes terminal transferase to add homopolymers for the tailing reaction. In a highly GC-rich region, poly A (or poly T) primers have a substantial difference in Tm from the gene specific primers; while poly G (or poly C) primers can lead to miss-priming within the cDNA instead of priming at the added 3' homopolymer. As a result, both sets of primers will be unproductive for PCR. This complication was circumvented by ligating a single-stranded anchor oligonucleotide to the 3' end of the first strand cDNA using RNA ligase. This enabled priming to occur specifically at the anchor site, and the PCR reaction to occur at the optimal annealing temperature.

The secondary structure of the mRNA proved to be a harder problem to solve. The majority of the cloned RACE products ended near the 5' end of the cDNA clone A06-4 (isolated from library screening), immediately 3' to the location of a hairpin loop structure. A large number of clones had to be sequenced before identifying one that extended the sequence of FBN2 further 5' to the secondary structure. New PCR primers were

synthesized and used to clone what the primer extension result had indicated to be the 5' end of the FBN2 transcript. Given the high GC content in the 5' region of the gene, we are aware that the primer extension product itself might have been an artifactual termination caused by secondary structure. Thus, the identity of the start site of transcription still needs to be further verified by S1 nuclease protection assays and additional primer extension experiments.

Since the RACE clones lack an in-frame stop codon 5' to the putative first methionine codon, there is also uncertainty regarding the transcription start site. However, we believe the ATG identified at position 1 is the actual start site of translation for two major reasons. First, the ATG codon resides within the context of a good translation initiation consensus particularly at the more critical -3 and +4 positions (Kozak, 1991). Second, the first methionine is followed by a sequence that resembles a signal peptide (Pealman and Halvorson, 1983). Additionally, the relative position of the ATG of FBN2 is the same as the translation initiation codon of FBN1 (Pereira et al., 1993). Thus, the results of the cloning experiments provided strong, if not conclusive, evidence for having determined the primary structure of the Fib2 protein.

II. Fibrillin Is a Small Gene Family

The cloned cDNAs of FBN2 cover a 10.4 kb transcript that can translate into a 314-kDa polypeptide. The protein has an amino acid profile of a secreted acidic protein with the same building blocks as Fib1, namely the EGF-like, EGF-CB, TGFβ-bp and the Fib repeats arranged in the same fashion as in Fib1. Consistent with the structural data inferred from the cloning experiments, a 350-kDa Fib2 protein was found in tissue culture media and in the ECM of several tissues.

Although the theoretical translation of Fib2 bears an overall 81% amino acid homology to Fib1, there is one region in Fib2 that greatly diverges from the corresponding proline-rich region of Fib1. This glycine-rich region of Fib2 is the most significant

structural difference between the two proteins, and this difference was used to generate Abs specific to each fibrillin.

The anti-fib2 pAb immunoprecipitated from the cell culture media a protein of the same size as Fib1. Moreover, this immunoprecipitate did not crossreact with Ab-f1C on Western blot analysis. Together with the size predicted from the cDNA sequence, these observations confirmed that the FBN2 transcript translates into a distinct protein product. Using Ab specific to Fib2, we subsequently demonstrated that, like Fib1, Fib2 is an ECM protein localized to microfibrils in a wide variety of tissues. Furthermore, preliminary gene structure data indicate that the repeats of Fib2 are encoded by single exons as previously reported for FBN1 (Pereira et al., 1993). In light of the structural homology, evolutionary kinship, and ultrastructural co-localization, we propose that the fibrillins are a small family of distinctive ECM proteins with related functions. Incidentally, another fibrillin-like protein, FLP, has been partially cloned and shown to be microfibril associated (Gibson and Mecham, personal communication). It will be interesting to eventually elucidate the evolutionary and functional relationships of FLP and the two fibrillins.

In analyzing FBN2 expression, there was a notable discrepancy between the relative level of FBN2 messenger RNA and Fib2 protein. The Northern analysis showed equivalent amounts of steady state mRNA for both fibrillins in the MG63 cell line. The data was verified with highly specific 3' UTR probes, thus excluding the possibility of cross-hybridization. In contrast, the Fib2 protein immunoprecipitated from MG63 cell culture media was estimated to be between 8 to 10 times less abundant than the Fib1 immunoprecipitate. Moreover, the level of Fib2 protein expression detected in tissues seemed much lower than that of Fib1, especially in adult tissues where virtually no Fib2 could be identified with our reagents.

Several possibilities may account for the low detection of the Fib2 protein. First of all, the discrepancy between the level of FBN2 transcript and Fib2 protein may result from less efficient translation. The 200 nucleotide long 5' leader sequence of FBN2 message is

highly GC-rich (68%) and prone to secondary structure. The secondary structure around the AUG codon may be responsible for the proposed inefficiency in translation of the FBN2 transcript. Truncation of such GC-burdened, highly structured leader sequences has been shown to dramatically improve the expression of some regulatory and house-keeping proteins, such as INT-2 (fibroblast growth factor-related oncoprotein, Dixon et al., 1989), human θ-globin (Leung et al., 1989), rat ornithine decarboxylase (Manzella and Blackshear, 1990), and c-sis (platelet-derived growth factor 2, Rao et al., 1988).

If the translation efficiency of the FBN2 mRNA is not impaired, two other possibilities must be considered. First, lower antibody affinity could contribute to the apparent low detection of the Fib2 protein. This seems unlikely, since pAbs developed against other regions of Fib2 have consistently shown much less detection of Fib2 than Fib1 in tissue cultures and histological samples (Mecham, personal communication). Finally, masking or degradation of the epitope may be leading to decreased detection. Since immunoprecipitation of Fib2 from cell culture media measures the soluble protein available before it forms insoluble matrix, faster incorporation of Fib2 protein into the matrix could make the epitope unavailable and result in under-detection. Similarly, a faster protein turnover could explain the absence of Fib2 in adult tissues. Until a more comprehensive understanding of fibrillin metabolism is attained, these considerations remain hypothetical. A possible cause of Fib2 epitope masking is the process of elastic fiber assembly and maturation. Deposition of elastin on microfibril bundles buries some of the fibrils within elastin. If Fib2 is primarily represented in these embedded fibrils, it could be hard to detect without prior removal of elastin. Overall, we believe that the lower efficiency of FBN2 mRNA translation in conjunction with epitope masking contribute to the lower amount of Fib2 in cell culture media and to decreased detection of this fibrillin in tissue samples.

III. Differential Spatial and Temporal Distributions of Fibrillins

The homology between human and murine Fib1 is 90% at the amino acid level and 80% at the nucleotide level. The murine FBN2 clones we isolated are similarly homologous to the corresponding human FBN2 regions (96% and 75% at the amino acid and nucleotide levels). Comparison of the two murine fibrillin genes shows a similar amino acid homology (78.8%) as their human counterparts in this region (76%). We are therefore quite confident that our clones represent the murine FBN2 transcript. We chose the highly divergent 3'UTR of the two genes as our in situ hybridization probes to ensure specificity. The equivalent length and similar GC content of the probes enabled us to compare the hybridization signals, and estimate the relative amount of each mRNA present in a given tissue at a particular developmental stage.

Although in situ analysis provides detailed information on when and where gene expression takes place, it does not necessarily reflect protein production, particularly when the translation efficiency might be limited. Immunostaining studies could theoretically solve this problem by giving a direct evaluation of the protein deposition. Unfortunately, our pAbs were raised in rabbits, and rabbit IgG caused a high background staining in murine tissues that interfered with the interpretation of the results. Nevertheless, immunohistochemical data obtained from human tissues supported and supplemented in situ data in defining the spatial and temporal pattern of fibrillin expression.

These data clearly demonstrated that FBN2 and FBN1 are differentially expressed genes. They consequently implied that morphologically similar microfibrils may differ in their fibrillin content in different tissues and at different developmental stages. Such findings may help us understand the function of Fib1 and Fib2, and the etiology of MFS and CCA. Following is a detailed discussion of the data with particular emphasis on the pathogenic implications. When discussing the in situ results in murine embryos, we will use the terms FBN1 and FBN2 in reference to mRNA, while the terms Fib1 and Fib2 will refer to proteins detected immunologically in tissues of the 20-week human fetus.

Musculoskeletal system

Growth of long bones is influenced by tension or pressure across the growth plates. Periosteum, as an elastic membrane, is believed to generate the tension regulating bone growth. Releasing the tension by circumferential section of the periosteum results in acceleration of bone growth, whereas longitudinal incisions have no effect (Crilly R. G., 1972; Warrell et al., 1979). Both immunohistochemical and in situ analyses have shown Fib2 expression in the perichondrium of the developing long bone, and in the periphery of the hyaline cartilage where dividing chondrocytes are located. Fib1 was uniformly distributed in the cartilaginous matrices with an elevated detection of both RNA and protein in the more differentiated hypertrophic zones. Increasing expression of FBN1 RNA was seen in perichondrium parallel to embryo development. When cartilage calcifies into bone, perichondrium becomes periosteum. The presence of defective fibrillin proteins in this structure may decrease the periostial tension, thus possibly explaining why abnormally long bones are seen in both MFS and CCA. The presence of Fib1 in the more differentiated parts of cartilage and bone is consistent with its increased appearance at later developmental stages. It also indicates that it might provide additional tension from within the bone.

The integrity of joints is provided by the ligaments connecting one bone to the other. Fib1 is readily detected in adult ligaments but not in the 20-week fetal ligaments. FBN1 transcription can be seen in ligamental fibroblasts of 16.5 d.p.c. mouse embryos. Defects in FBN1 gene may cause weakening of the ligaments which manifests itself as hyperflexibility of the joints, a feature often described in MFS patients (Pyeritz and McKusick, 1979). While we did not detected the Fib2 protein in either adult or fetal ligaments, FBN2 was expressed at an apparent higher level than FBN1 gene in mouse ligamental fibroblasts as early as 13.5 d.p.c. We believe that the Fib2 protein must therefore be present in the ligament at some point during development, and its function may

be different from Fib1 in order to explain why joint contractures rather than hypermobility occurs in CCA. Impairment of the tendon may also be involved in contractures. Although there was no detectable Fib2 in adult or 20 week fetal tendon tissues, substantial FBN2 accumulation was seen in tendon fibroblasts of both 13.5 and 16.5 d.p.c. mice. Only a low signal of FBN1 expression was detected at those stages of development, whereas the Fib1 protein was easily seen in adult tissue. The high expression of FBN2 in fetal tendon and the lack of FBN1 transcripts may explain why congenital contractures are usually observed in CCA patients and only seen in the more severe cases of infantile MFS.

While previous reports advocated the presence of microfibrils in elastic cartilage (Ishihara et al., 1973; Sanzone and Reith, 1976; Nielsen, 1976), others disputed this finding and were particularly skeptical of "peripheral elastin-associated" microfibrils in mature elastic cartilage (Serafini-Fracassini and Smith, 1974; Quintarell et al., 1979; Kostovic-Knezevic et al., 1981). The report from Quintarell et al. (1979) indicated that in rabbit ear cartilage, elastic tissue was formed by fusion of amorphous elastin into bundles of 3-4 nm filaments absent at the periphery of mature elastic fibers. They also found these fine filaments within purified elastin produced by chondrocytes in tissue culture. Kostovic-Knezevic et al. (1981) confirmed that microfibrils could not be demonstrated in adult rat ear cartilage, but they did show the presence of microfibrils adjacent to the chondrocytes in the boundary zone and perichondrium. Their result was confirmed immunologically by Prosser et al. (1984) using a pAb raised against microfibrillar extract of bovine nuchal ligament. The authors attributed the failure to detect a positive microfibrillar signal in the elastic cartilaginous core to epitope masking by proteoglycans. Our data of in situ hybridization in epiglottis and cuneiform cartilage, and of immunohistochemistry in ear cartilage strongly suggest that Fib2 is the predominant fibrillin in elastic cartilage microfibrils. Our findings clarify the apparent failure to detect microfibrils in the elastic cartilaginous core. They also explain the origin of the characteristic crumbled ear of CCA patients. We think that the pAb raised by Prosser et al. (1984) is probably directed against

Fib1 epitopes, and therefore stains only the microfibrils at the perichondrium as did our Fib1 specific pAb. The preferential expression of FBN2 in elastin-rich tissues is also seen in the elastic ligamentum flava which is the equivalent of ligamentum nuchae in ruminants. This issue will be further discussed in the context of the data suggesting functional differences between fibrillins.

Although long and thin extremities are present in both MFS and CCA patients, muscular hypoplasia is particularly noted in individuals with CCA (Epstein et al., 1968; Ramos et al., 1985). Our in situ results suggest a molecular basis for this clinical difference. While FBN1 expression is seen in the fibroblasts of perimysium (where Fib1 accumulation was confirmed with anti-Fib1 Ab), FBN2 is expressed by myocytes. This is true not only for skeletal myocytes but also for cardiomyocytes. This and the muscular hypoplasia typical of CCA patients suggest a functional role for Fib2 in muscle development.

Cardiovascular system

Similar to skeletal muscle, expression of Fib2 is seen primarily in the myocardium layer of the heart. The epicardium and endocardium cells express Fib1, which is also present in the fibroblast of the cardiac skeleton later in development (13.5 d.p.c.). The immunohistochemical data, as well as the in situ results clearly showed that Fib1 is present throughout the full thickness of the aortic wall, whereas Fib2 is primarily located in the aortic media. This gives another example of Fib2 being more intimately associated with elastin, since the media layer contains most of the elastic fibers. It is known that the adventitia layer sustains the bulk of the stress and pressure in aorta (Tilson et al., 1990). Therefore it is conceivable to speculate that defects in Fib1 might cause weakening of the adventitia, thus leading to dilatation and rupture of the vessel. A load bearing structural function of Fib1 is clearly indicated in this case. Fib2 appears not to be a major component of the adventitia. Consistent with this finding, CCA is not characterized by aortic dilatation

and aneurysm. The function of Fib2 may be more related to elastic fiber formation, a concept also supported by its higher expression at earlier stages of vessel morphogenesis. It is also interesting to note that Fib2 is expressed mostly in the smooth muscle media layer of the vessel. This is the equivalent layer of the myocardium of the heart. FBN1 transcription, on the other hand, dominates in the intimal and adventitial cells which correspond to the endo- and pericardial cells, respectively. This finding may suggest a cell lineage selectivity in fibrillin expression. The active expression of the FBN1 gene in the endothelial cells of the heart and vessels seem to coincide with the previous observations of microfibrils in the atherosclerotic plaques (Haust, et al., 1967; McCullagh, 1973). It is possible that this protein also has some involvment in plaque formation during injury.

Mitral valve prolapse (MVP) is often seen in MFS patients and has the tendency to worsen with age (Pyeritz, 1990), whereas MVP or any other cardiovascular deformities are not usually associated with CCA. Although both fibrillins are expressed in tissues that will form atrio-ventricular septa, the pathology in MFS and its absence in CCA suggest that they may have distinct functions. Fib1 may function more as a structural component; in contrast, Fib2 might be more important in the formation of a structure rather than in sustaining it therefore its impairment may tend to be lethal. Additionally, the preponderance of Fib1 expression in the cardiovascular system is demonstrated by its substantial presence in the arterioles of different organs, where Fib2 is scarce. Altogether, the data indicate that Fib1 is the major fibrillin component in the microfibrils of cardiovascular system.

Respiratory system

Although spontaneous pneumothorax, bullous emphysema, reduced total lung capacity and residual volume are all documented in MFS patients, it is unclear whether these pulmonary problems are directly caused by the genetic defect. For example, reduced lung vital capacity in MFS patients is often attributed to the thoracic cage deformities, such

as kyphoscoliosis and pectus excavatum (Pyeritz et al, 1990). Our studies have identified the expression of FBN1 in the developing lung parenchyma, and the presence of Fib1 protein in alveolar connective tissues, bronchioles, interlobular septa and pleura (Sakai et al, 1986; Zhang et al 1994). These findings provide a histological basis to include the congenital lung abnormalities of MFS patients as part of the primary symptoms of the disorder. The possibility that a defective Fib1 protein is associated with spontaneous pneumothorax and bullous emphysema suggests that Fib1 may have a structural role in withstanding the expansile force upon inhalation. Mutations may also interfere with the normal development of the lung parenchyma itself, which results in reduced lung capacity.

If pulmonary involvement is not commonly recognized as part of the clinical spectrum of MFS, it is very rarely seen in association with CCA. In fact there is only one documented case of CCA with respiratory problems, in addition to the typical CCA manifestations. The patient had also generalized osteopenia and underdevelopment of the musculature, and died suddenly at 2.5 years of age. He was probably the most severe CCA case ever reported (Epstein et al., 1968). Autopsy results found a narrowed inlet of the patient's larynx and a prominent epiglottic curvature. The cause of death was determined to be suffocation from laryngeal obstruction. Pulmonary atelectasis and focal edema was noticed microscopically, although there is no detailed description (as most of the attention was devoted to the skeletal abnormalities). Atelectasis could be caused by chronic suffocation resulting from the narrowed laryngeal inlet. We demonstrated high expression of the FBN2 gene in elastic cartilage at both the RNA and protein level. Malformation of the laryngeal elastic cartilages is not a surprising finding in CCA patients, as abnormally shaped elastic cartilage of the ear is one of the characteristic signs of this condition.

Strong and specific in situ signals of FBN2 in the bronchial epithelia indicated the potential importance of Fib2 in the formation of the respiratory tract. Elastogenesis is believed to play a role in lung morphogenesis and growth (Loosli and Potter, 1959; Emery, 1969). This is indirectly supported by the concurrence of elastogenesis and cavity

formation of bronchi, respiratory bronchioles and alveoli (Collet and Biens, 1974; Amy et al., 1977). It is not clear whether elastogenesis initiates the program of lung morphogenesis or is itself part of the program. Nevertheless, elastogenesis of the lung seems to be synchronized with the development of the airways. In primary and secondary bronchi, elastic fibers can be seen by the 14th day in chick embryos (total incubation time 20 days, Jones and Barson, 1971), and by the 16th day in rat embryo (total gestation period 23 days, Collet and Biens, 1974). In the bronchioles (tertiary bronchi), active elastogenesis starts at day 18 for chick embryos and day 19 for rat embryos. Alveolar elastic tissue appears postnatally at the second or third day in mice as primary saccules develop into alveoli (Amy et al, 1977).

We looked into the expression of the two fibrillin genes at 10.5, 13.5, 16.5 d.p.c. of mouse embryogenesis. We found that while FBN1 is made by lung mensechymal cells but not bronchiolar epithelial cells, FBN2 is prominently expressed in these epithelial cells. FBN2 expression is also restricted temporally to a period when the bronchi (10.5 and 13.5 d.p.c.) or bronchioles (16.5 d.p.c.) are forming, and is turned off afterwards. Since Fib1 is expressed throughout the lung mesenchyme, but elastogenesis only appears around the bronchiolar tree where Fib2 is presumably abundant, we think Fib2 protein plays a special role in directing elastic fiber formation. Collet and Biens (1974) observed that "microfilaments", likely to be microfibrils, are often located between the epithelial basal lamina and the underlying smooth muscle cells, and around the smooth muscle cells. Both of these areas are sites of subsequent elastin deposition. We speculate that these microfibrils probably have a different biochemical composition from those located in other parts of the lung. Although this hypothesis could not be corroborated by immunohistochemical data, there is in the literature experimental evidence that microfibrils in rat tracheal lamina propria have different enzymatic susceptibility from that observed in typical microfibrils (Bodley and Wood, 1971). While there are other possible explanations, this observation may indicate differences in biochemical composition or

physical accessibility of the microfibrils. This subgroup of microfibrils may be specialized for initial elastin deposition, and thus may well be buried within the elastic fiber bundles and less accessible to enzymatic digestion.

The fact that there is little or no pulmonary involvement in CCA patients may, on the contrary, indicate the importance of Fib2 in elastogenesis and lung morphogenesis. Most Fib2 defects may cause pulmonary malformation too severe to be compatible with survival. CCA patients may just be a small viable fraction of FBN2 mutations that cause no serious effects on lung morphogenesis. Aside from re-emphasizing the importance of Fib2 during early lung morphogenesis, this hypothesis may also explain why the incidence of CCA is so much lower than MFS.

Ocular system

One of the key features that differentiates CCA from MFS is the lack of ocular manifestations, principally ectopia lentis. Microfibrils in the zonule fibers clearly contain Fib1 protein (Sakai et al., 1986). In line with the CCA phenotype, one would expect little or no Fib2 expression in zonules. Unfortunately we could not verify this point as our tissue samples did not have well preserved zonule fibers. We did however identify both fibrillin proteins in the sclera and the Descemet's membrane of the cornea. There is indication that the Fib1 deposition is somewhat enhanced in the outer layer of the sclera and the inner vascular choroid layer. Interestingly, expression of FBN2 precedes that of FBN1, since its message can be detected in the mensenchymal cells of the sclera at 13.5 d.p.c. when no FBN1 message is detected. Both genes eventually reach equivalent levels of mRNA accumulation at 16.5 d.p.c. This is another example suggesting that microfibrils of the same tissue can change composition over time, in addition to varying in different tissues.

Other tissues and organs

Microfibrils are present in the mesangial region of the renal glomeruli without association to immunogenic elastin (Hsu and Churg, 1979; Kumaratilake et al., 1989). Both MAGP and Fib1 have been localized to the mesangial microfibrils (Kumaratilake et al., 1989; Sakai, et al., 1986). We have now added Fib2 to the list of the microfibrillar components in the glomerular and peritubular connective tissue. The in situ data suggest a developmentally regulated pattern of expression of the two fibrillin genes during renal morphogenesis. While FBN1 transcription is primarily taking place in the mesenchymal cells of the peritubular and extraglomerular regions, FBN2 expression is mostly seen in the developing glomeruli. Although hard to determine by light microscopy, we believe that the cells actively transcribing FBN2 in the developing renal corpuscle are mesangial cells. These cells have characteristics of smooth mucle cell such as producing smooth muscle actin and being contractible (Johnson et al., 1991). It is possible that these cells have other characteristics of smooth muscle cells, including production of fibrillin. Although we did not examine stages later than 16.5 d.p.c., the immunostaining data of Sakai et al. (1986) imply that FBN1 becomes actively expressed in the renal glomeruli later in development.

The submucosal layer of the intestines contains microfibrils associated with small amount of elastin (Kumaratilake et al., 1989). Our in situ data indicate that both smooth muscle cells and mesenchymal cells of the submucosa are active producers of fibrillins. FBN2 message was selectively detected in the mesenchymal cells of the lamina propria of the intestines. Additional sites of fibrillin expression were the muscle cells of the stomach and the bladder, and the mesenchymal cells of the thymic capsule and septa. The latter in situ results confirm the light microscopic findings of elastic tissue and oxytalan fiber in the periphery of the opossum thymus (Savino, 1982).

Overall, this tissue survey demonstrated that Fib2 protein is made by a wide variety of cells including mesenchymal cells, epithelium, muscle cells (smooth, skeletal, and

cardiac), and chondrocytes. It also confirmed that morphologically similar microfibrils of different tissues, as well as those of the same tissue at different developmental stages, can be biochemically different due to changes in the ratio of the two fibrillin proteins. It remains to be determined whether or not the fibrillins assemble together in the same fibril. Electron microscopic double-immunolabeling assays of individual microfibril molecules need to be performed to answer this question.

Fib2 was accidentally discovered by cloning experiments without prior biochemical evidence suggesting its existence. In retrospect, it is not surprising that the immunobiochemical studies missed this protein. The highly insoluble nature of the microfibrils together with the immunological method used for identifying the microfibrilar components contributed to Fib2 being overlooked. The amniotic membrane used to prepare anti-microfibrilar antibodies may have low Fib2 content and, as a result, antibodies generated might have all been against Fib1. Futhermore, affinity purification of Fib1 was carried out using fibroblast culture media which contains very little Fib2 protein.

IV. Differential Functions of the Fibrillins

In broad terms, microfibrils appear to perform two major functions. First, there is the function of directing elastogenesis. This widely recognized role is based on the indirect observation that microfibrils appear first in the form of presumptive elastic fibers in developing elastic tissues and in in vitro culture systems (reviewed by Cleary and Gibson, 1983). Second, they seem to have a force-bearing structural function with limited extendibility which provides strength to elastic fibers. This function can be inferred from the tissue distribution and ultrastructural characteristics of the microfibrils. Based on the spatial and temporal pattern of gene expression, we suggest that each of the fibrillins plays predominantly one of the two postulated roles.

As extensively discussed in the previous section, Fib2 shows a preferential distribution in elastic tissues, such as elastic cartilage, the tunica media layer of the aorta,

and along the bronchial tree. During embryogenesis, transcription of FBN2 seems to start earlier than FBN1 and is sometimes limited to a window of time just before elastogenesis. This is best exemplified by the fibrillin expression during pulmonary development. Although we did not examine the expression of fibrillins in all developmental stages we observed that Fib2 expression tends to decrease with time. We therefore speculate that this transient pattern of FBN2 expression holds true in other elastic tissues. Assuming that our hypothesis is correct, it is likely that the major functional role of Fib2 is to direct elastic fiber assembly.

A few other observations support our prediction. Anti-Fib2 Abs seem to bind to the microfibrils within the amorphous elastin more often than Fib1 Abs (Davis, personal communication). Microfibrils are present during elastic cartilage morphogenesis of the ear, and later they are buried within elastin leaving the mature elastic fibers without visible peripheral microfibrils (Sanzone and Reith, 1976; Seratini-Fracassini and Smith, 1974; Quintarelli et al., 1979). Both our immunohistochemical and in situ data suggest that these microfibrils are made mostly of Fib2. Others have also noted that the microfibrils initially laid out by cultured chondrocytes are morphologically different from those that appear later (Davis, personal communication). It is interesting to note that tropoelastin binds preferentially to these morphologically distinct early microfibrils. Although the true identity of these microfibrils should be verified immunologically, we speculate that they are made of Fib2 given the transient and earlier expression pattern of FBN2.

Additional evidence that points to an intimate relationship between Fib2 and elastin comes from the co-regulation of FBN2 and tropoelastin gene expression. Tropoelastin steady state mRNA level is post-transcriptionally inhibited by TPA (12-0-tetradecanoylphorbol-13-acetate) and $VitD_3$ (1,25-dihydroxyvitamin D3) (Parks et al., 1992; Pierce et al., 1992). These two reagents greatly decrease the FBN2 message in cultured chondrocytes without decreasing FBN1 (Mecham, personnal communication). Even though the mechanism of TPA and $VitD_3$ regulation of FBN2 expression remains to

be clarified, the co-repression of FBN2 and tropoelastin provides another indirect link between these two components of the elastic fiber.

The predominance of Fib1 in stress and load bearing structures like aortic adventitia, suspensory ligament of the lens and skin, suggests that this fibrillin may be mostly responsible for the structural function of the microfibrils. Consistent with this conclusion is the fact that symptoms of MFS patients show clinical signs of a premature wearing-out of a defective load-bearing structure, including aortic aneurysm and ectopia lentis. The observation that elastic cartilage, the only elastic tissue existing in a stress-free condition, contains little Fib1 further reinforces our hypothesis.

Is there any evidence of a basis in the protein structure for the predicted differential function? As already mentioned, the most striking difference between the two proteins is the proline-rich region for Fib1 and the glycine-rich region for Fib2. While the proline-rich region does not show any recognizable relationships to elastin, the glycine-rich region is about 40% homologous to multiple segments of the tropoelastin amino acid sequence (NCBI, BLAST network service). The glycine rich sequences of both Fib2 and tropoelastin form β-sheets or β-turns that are believed to promote protein aggregation through interdigitation of the hydrophobic side chains (Robson et al., 1993; Mac Vector). Tropoelastin and the glycine-rich region of Fib2 have abundant hydrophobic amino acid residues for side chain interactions. Thus, it is conceivable that this unique region of Fib2 provides critical interaction with elastin during the assembly of the elastic fibers. This is consistent with the predominant or exclusive deposition of this fibrillin at earlier stages of development and in elastin-rich tissues.

V. Future Research Plans

In summary, the work presented in this thesis has demonstrated the existence of fibrillin-2, a new ECM glycoprotein and a distinct component of the elastin-associated microfibrils. It has also elucidated the structure of this protein and the spatiotemporal

pattern of gene expression during embryogenesis. Results from these studies have provided the basis for several hypothesis concerning the function of fibrillin-2. Accordingly, we speculate that fibrillin-2 plays a critical regulatory role during the early assembly of the elastic fiber. This hypothesis and several other unresolved points constitute the new set of questions to be addressed by future investigations.

Metabolic labeling assays will elucidate the biosynthetic steps of the Fib2 protein. This information will help explain the observed discrepancy between levels of FBN2 message and Fib2 protein. It will also determine the fate of Fib2 protein, once it is assembled into microfibrils and elastic fibers. For the later purpose, immuno-electronmicroscopy in conjunction with enzyme digestion assays will help clarify whether or not Fib2 is embedded in the amorphous elastic core, or is simply degraded after serving its purpose.

In situ hybridizations at developmental stages later than those described here will increase our knowledge of the differential spatiotemporal pattern of expression of the two fibrillin genes. The proposed function of Fib2 as an organizer of fiber assembly makes this gene product more important than Fib1 during embryogenesis. However, the levels of expression of FBN1 and FBN2 at the developmental stages analyzed in this study do not explain the abundance of Fib1 and the near absence of Fib2 in adult tissues. Although study of translation efficiency may shed light on this point, it will still be necessary to assess gene transcription at later post-natal stages in order to answer the question more directly.

Additionally, it will be more informative if we could correlate the message level to the actual accumulation of the protein in mouse embryos. The high background staining of our rabbit pAbs in murine tissues has unfortunately hampered these experiments. Preliminary results showed that the same affinity purified antibodies stain rat tissue with little unspecific signal (Panetta, personal communication). Thus, these same reagents could

be used to study the relation between protein deposition and mRNA accumulation in this animal model.

We have shown that FBN2 is a developmentally regulated gene. Preliminary data also suggest that the regulation is related to tropoelastin gene regulation. It will be interesting to explore the relationship between the Fib2 and elastin expression to understand the program of clastogenesis. Experiments examining the transcriptional mechanisms of the two genes may identify common regulatory pathways.

In vitro systems in which the expression of the FBN2 gene is altered, can be used to test the proposed function of Fib2 as the organizer of elastic fiber. In cultured cells that form an elastic fiber matrix, FBN2 gene expression could be abrogated by the ribozyme techniques (Forster and Symons, 1987, Uhlenbeck, 1987). One could observe the consequence of such an action on chondrocytes which normally express tropoelastin and both fibrillins, and which form elastic fibers. Additionally, Abs against specific regions of Fib2 (such as the glycine-rich region C) can be introduced into the culture media to identify the element(s) involved in elastic fiber formation. Alternatively, forced expression of the FBN2 gene product (or a portion thereof) in cells that produce tropoelastin, but do not form fibers may also provide information about the role of Fib2 in elastogenesis. The technique of homologous recombination in embryonic stem cells (Capecchi, 1989) could be employed to substitute the glycine-coding exon of Fib2 with the proline-coding exon of Fib1. The introduction of structural and regulatory mutations in transgenic mice will be a definitive assay for studying the function of Fib2 and its role in development.

Abbreviation Table

Ab	antibody
Ab-f1C	anti-fibrillin 1-antibody
Ab-f2C	anti-fibrillin 2-antibody
AMP	associated microfibril protein
bp	base pair(s)
CCA	congenital contractive arachnodactyly
d.p.c.	days post coitus
ECM	extracellular matrix
EGF	epidermal growth factor
EGF-CB	epidermal growth factor Ca^{++} binding subtype
Emilin	elastin microfibril interface located potein
FBN1	fibrillin 1 gene locus
FBN2	fibrillin 2 gene locus
Fib1	fibrillin 1 (protein)
Fib2	fibrillin 2 (protein)
IP	immunoprecipitate
kDa	kilo-Dalton
LOD (score)	logarithm (to base 10) of the odds
mAb	monoclonal antibody
MAGP	microfibrillar associated glycoproteins
MFS	Marfan syndrome
nt	nucleotide(s)
ORF	open reading frame
pAb	polyclonal antibody
RACE	rapid amplification of cDNA ends
TGFβ-bp	transforming growth factor-β-binding protein
Tm	melting temperature
UTR	untranslated region

BIBLIOGRAPHY

Amy, R. W. M., Bowes, D., Burri, P. H., Haines, J., and Thurlbeck, W.M. (1976). Postnatal growth of the mouse lung. J. Anat., 124, 131.

Andrikopoulos, A., Suzuki, H.R., Solursh, M., and Ramirez, F. (1992). Localization of Pro-α2(V) collagen transcripts in the tissues of the developing mouse embryo. Dev. Dynamics, 195, 113.

Barondes, S.H., 1988. Bifunctional properties of lectins: Lectins redefined. Trends in Biochem. Sci., 13, 480.

Beals, R. K., and Hecht, F. (1971). Congenital contractural arachnodactyly: a heritable disorder of connective tissue. J. Bone Joint Surg., 53, 887.

Bodley, D. H., and Wood, R. (1971). Ultrastructural studies on elastic fibers using enzymatic digestion of thin sections. Anat. Rec., 172, 71.

Breathnach, S. M., Pepys, M. B. and Hintner, M. (1989). Tissue amyloid P component in normal human dermis is non-covently associated with elastic fiber microfibrils. J. Invest. Dermatol., 92, 53.

Bressan, G. M., Castellani, I., Colombatti, A., and Volpin, D. (1983). Isolation and characterization of a 115,000-dalton matrix-associated glycoprotein from chick aorta. J. Cell Biol., 258, 13262.

Bressan, G.M., Argos, P., and Stanley, K.K. (1987). Repeating structures of chick tropoelastin revealed by complementary DNA cloning. Biochemistry, 26, 1497.

Bressan, G. M., Daga-Gordini, D., Colombatti, A., Castellani, I., Marigo, V., and Volpin, D. (1993). Emilin, a component of elastic fibers preferentially located at the elastin-microfibrils interface. J. Cell Biol., 121, 201.

Brown, P. L., Mecham, L., Tisdale, C., and Mecham, R. P. (1992). The cysteine residues in the carboxy-terminal domain of tropoelastin form an intrachain disulfide bond that stabilizes a loop structure and positively charged pocket. Biochem. Biophys. Res. Commun., 186, 549.

Bruggemann, E.P., Chaudhary V., Gottesman M.M., and Pastan I. (1991). Pseudomonas exotoxin fusion proteins are potent immunogens for raising antibodies against P-glycoprotein. Biotechniques, 10, 202.

Capecchi, M.P. (1989). The new mouse genetics: altering the genome by gene targeting. Trends Genet, 5, 70.

Cheah, K. S. E., Lan, E. T. , An, P. K. C., and Tam, D. P. L. (1991). Expression of the mouse a 1 (II) collagen is not restricted to cartilage during development. Develop., 111, 945.

Cleary, E. G., and Gibson, M. A. (1983). Elastin-associated microfibrils and microfibrillar proteins. Int. Rev. Connect. Tissue Res., 10, 197.

Collet, A. J., and Des Biens, G. (1974). Fine structure of myogenesis and elastogenesis in the developing rat lung. Anat. Rec., 179, 343.

Corson, G. M., Chalberg, S.C., Dietz, H.C., Charbonneau, N.L., and Sakai, L.Y. (1993). Fibrillin binds calcium and is coded by cDNAs that reveal a multidomain structure and alternatively spliced exons at the 5'end. Genomics, 17, 476.

Cotta-Pereira G., Guerra Rodrigo F., and Bittencourt-Sampaio, S. (1976) Oxytalan, elaunin, and elastic fibers in the human skin. J. Invest. Dermatol., 66, 143.

Cotta-Pereira G., Guerra Rodrigo F., and David Ferreira J. F. (1978). Comparative study between the elastic system fibers in human thin and thick skin. J. Biol. Cell, 31, 297.

Crilly, R. G. (1972). Longitudinal overgrowth of chicken radius. J. Anat., 112, 11.

Dahlbäck, B., Hildebrand, B., and Linse, S. (1990). Novel type of very high affinity calcium-binding sites in β-hydroxyasparagine-containing epidermal growth factor-like domains in vitamine K-dependent protein S. J. Biol. Chem. 265, 18481.

Darnell, J.E., Lodish, HJ., and Baltimore, D. (1990). In: Molecular Cell Biology. Scientific American Boos, Inc., pp.399.

Davis, C. (1990). The many faces of epidermal growth factor repeats. New Biologist, 2, 410.

Deak, S.B., Pierce, R.A., Belsky, S.A., Riley, D.J., and Boyd, C.D. (1988). Rat tropoelastin is synthesized from a 3.5 kilobase mRNA. J. Bio. Chem. 263:13504-13507.

Dempsey, E. W., and Lansing, A. I. (1954). Elastic Tissue. Intern. Rev. Cytol., 3, 436.

Dietz, H. C., Pyeritz, R.E., Hall, B.D., Cadle, R.G., Hamosh, A., Schwartz, J., Meyers, D.A., and Francomano, C.A. (1991a). The Marfan syndrome locus: confirmation of assignment to chromosome 15 and identification of tightly linked markers at 15q15-q21.3. Genomics, 9, 355.

Dietz, H. C., Cutting, G.R., Pyeritz, R.E., Maslen, C.L., Sakai, L.Y., Corson, G.M., Puffenberger, E.G., Hamosh, A., Nanthakumar, E.J., Curristin, S.M., Stetten, G., Meyers, D.A., and Francomano, C.A. (1991b). Marfan syndrome caused by a recurrent de novo missense mutation in the fibrillin gene. Nature, 352, 337.

Dietz, H. C., Saraiva, J.M., Pyeritz, R.E., Cutting, G.R., and Francomano, C.A. (1992a). Clustering of fibrillin (FBN1) missense mutations in Marfan syndrome patients at cysteine residues in the EGF-like domains. Hum. Mut., 1, 366.

Dietz, H. C., Pyeritz, R.E., Puffenberger, E.G., Kendzior, R.J., Corson, G.M., Maslen, C.J., Sakai, L.Y., Francomano, C.A., Cutting, G.R. (1992b). Marfan phenotype variability in a family segregating a missense mutation in the EGF-like motif of the fibrillin gene. J. Clin. Invest., 89, 1674.

Dietz, H. C., McIntosh, I., Sakai, L.Y., Corson, G.M., Chalberg, S.C., Pyeritz, R.E., and Francomano, C.A. (1993a). Four novel FBN1 mutations: significance for mutant transcript level and EGF-like domain calcium binding in the pathogenesis of Marfan syndrome. Genomics, 17, 468.

Dietz, H. C., Valle, D., Francomano, C.A., Kendzior, F.J., Pieritz, R.E., and Cutting, G.R. (1993b). The skipping of constitutive exons in vivo induced by nonsense mutation. Science, 254, 680.

Dixon, M., Deed, R., Acland, P., Moore, R., Whyte, A., Peters, G. and Dickson, C. (1989). Detection and characterization of the fibroblast growth factor-related oncoprotein INT-2. Mol. Cell Biol., 9, 4896

Dumas, J.B., Edwards, M., Delort, J., and Mallet, J. (1991). Oligodeoxyribonucleotide ligation to single-stranded cDNA: A new tool for cloning 5' ends of mRNAs and for constructing cDNA libraries by vitro amplification. Nucleic Acids Res. 19:5227-5232.

Emery, J. (1969). Connective tissue and lymphatics. In: The anatomy of the developing lung. J. Emery, Ed. William Heinemann Medical Books Ltd., pp.49.

Epstein, C. J. , Graham, C. B., Hodgkin, W. E., Hecht, F., and Motulsky, A. G. (1968). Hereditary dysplasia of bone with kyphoscoliosis, contractures and abnormally shaped ears. J. Pediatr., 73(3), 379.

Fanning, J. C., and Cleary, E. G. (1985) Identification of glycoproteins associated with elastin-associated microfibrils. J. Histochem. Cytochem., 33(4), 287.

Fanning, J. C., Yates, N. G., and Cleary, E. G. (1981). Elastin-associated microfibrils in aorta: species differences in large animals. Micron, 12(4), 339.

Farquhar, M. G., Wissig, S. L., and Palade, G. E. (1961). Glomerular permeability: I. ferritin transfer across the normal capillary wall. J. Exp. Med., 113, 47.

Fleischmajer, R., Contard, P., Schwartz, E., MacDonald II, E.D., Jacobs II, LLoydstone, and Sakay, L.Y. (1991). Elastin-associated microfibrils (10 nm) in a three-dimensional fibroblast culture. J. Invest. Dermat., 4, 638.

Forster, A. C., and Symons, R. H. (1987). Self-cleavage of virusoid RNA is performed by the proposed 55-nucleotide active site. Cell, 50, 9.

Foster, J. A., Bruenger, E., Rubin, L., Imberman, M., Kagan, H., Mecham, R., and Franzblau, C. (1976). Circular dichroism studies of an elastin cross-linked peptide. Biopolymers, 15, 833.

Frederickson, R. G., and Low, F. N. (1971). High-volatage electron microscopy of extracellular fibrillogenesis. Amer. J. Anat., 130, 347.

Frohman, M. A., Dush, M.K., and Martin, G.R. (1988). Rapid amplification of full-length cDNAs from rare transcripts: Amplification using a single gene-specific oligonucleotide primer. Proc Natl. Acad. Sci. U.S.A., 85, 8998.

Fullmer, H. M., Lillie, R. D. (1958). The oxytalan fiber: A previously undescribed connective tissue fiber. J. Histochem. Cytochem., 6, 425.

Gawlik, Z. (1965). Morphological and morphochemical properties of the elastic system in the motor organ of man. Folia Histochem. Cytochem., 3, 233.

Gibson, M. A., and Cleary, E. G. (1985). CL glycoprotein is the tissue form of type VI collagen. J. Biol. Chem., 260, 11149.

Gibson, M. A., Hughes, J. L., Fanning, J. C., and Cleary, E. G. (1986). The major antigen of elastin-associated microfibrils is a 31-kDa glycoprotein. J. Biol. Chem., 261, 11429.

Gibson, M. A., Kumaratilake, J.S., and Cleary, E.G. (1989). The protein components of the 12-nanometer microfribils of elastic and non-elastic tissues. J. Biol. Chem., 264, 4590.

Gibson, M. A., Sandberg, L.B., Grosso, L.E., Cleary, E.G. (1991). Complementary DNA cloning establishes microfibril-associated glycoprotein (MAPG) to be a discrete component of the elastin-associated microfibrils. J. Biol. Chem., 266, 7596.

Godfrey, M., Menashe, V., Weleber, R.G., Koler, R.D., Bigley, R.H., Lovrien, E., Zonana, J., and Hollister, D.W. (1990). Cosegregation of elastin-associated microfibrillar abnormalities with the Marfan phenotype in families. Am. J. Hum. Genet., 46, 652.

Goldberg, B., and Rabinovitch, M. (1988). In: Cell and Tissue Biology, A Text Book of Connective Tissue. L. Weiss, Ed., Urban & Schwarzenberg, Inc., Baltimore, MD. USA, pp. 168.

Godfrey, M., Vandemark, N., Wang, M., Velinov, M., Wargowsli, D., Tsipouras, P., Han, J., Becker, J., Robertson, W., Droste, S., and Rao, V.H. (1993). Prenatal diagnosis and a donor splice site mutation in fibrillin in a family with Marfan syndrome. Am. J. Hum.Genet., 53, 472.

Gosline, J.M. (1978).The temperature dependent swelling of elastin. Biopolymers, 17, 697.

Gosline, J.M., French, J. (1979). Dynamic mechanical properties of elastin. Biopolymers, 18, 2091.

Gotte L, Giro GM, Volpin D, Horne RW. (1974). The ultrastructural organization of elastin. J. Ultrastruct Res., 46, 23.

Greenlee, T. K., Jr, Ross, R., and Hartman, J.L. (1966). The fine structure of elastic fibers. J. Cell Biol., 30, 59.

Gribskov, M., and Burgess, R.R. (1986). Sigma factors from E. Coli, B. Subtilis, phage SPO1 and phage T4 are homologous proteins. Nucleic Acids Res. 14, 6745.

Hall, D. A., Reed, R., and Tunbridge, R. E.(1952). Nature, 170, 264.

Hall, D. A., Reed, R., Tunbridge, R. E. (1955). Electron microscopic studies of elastic tissue. J. Exp. Cell Res., 8, 35.

Handford, P. A., Baron, M., Mayhew, M., Willis, A., Beesley, T., Brownlee, G.G., and Campbell, I.D. (1990). The first EGF-like domain from human factor IX contains a high affinity calcium binding site. EMBO J, 9, 475.

Haust, M. D., More, R. H., Bencosme, S. A., and Balis, J. U. (1967) Electron microscopic studies in human atherosclerosis extracellular elements in aortic dots and streaks. Exp. Mol. Path., 6; 300-313.

Hay, E. (1978). Fine structure of embryonic matrices and their relation to the cell surface in ruthenim red-fixed tissues. Growth, 42, 399.

Hewett, D. R., Lynch, J.R., Smith, R., and Sykes, B.C. (1993). A novel fibrillin mutation in the Marfan syndrome which could disrupt calcium binding of the epidermal growth factor-like module. Hum. Mol. Genet., 2, 475.

Hinek, A., Wrenn, D. S., Mecham, R. P., and Barondes, S. H. (1988). The elastin receptor is a galactoside binding protein. Science, 239, 1539.

Hollister, D. W., Godfrey, M., Sakai, L.Y., and Pyeritz, R.E. (1990). Marfan syndrome:immunohistologic abnormalities of the elastin-associated microfibrillar fiber system. N. Engl. J. Med., 323, 152.

Hoeve, C. A. J. (1974). The elastic properties of elastin. Biopolymers, 13, 677.

Horrigan, S. K., Rich, C. B., Streeten, B.W., Li, Z., and Foster, J.A. (1992). Characterization of an associated microfibril protein through recombinant DNA techniques. J. Biol. Chem., 267 (14), 10087.

Hsu, H.-C. H., and Churg, J. (1979). Glomerular microfibrils in renal disease: A comparative electron microscopic study. Kidney Int., 16, 497.

Indik, Z., Yeh, H., Ornstein-Goldstein, N., Sheppard, P., Anderson, N., Rosenbloom, J. C., Peltonen, L., and Rosenbloom, J. (1987). Alternative splicing of human elastin

messenger-RNA indicated by sequence analysis of cloned genomic and complementary DNA. Proc. Natl. Acad. Sci. USA, 84, 5680.

Inoué, S. and Leblond, C.P. (1986). The microfibrils of connective tissue: I. ultrastructure. Amer. J. Anat., 176, 121.

Ishihara, T., Iwata, T., Furutani, F., Uchino, F., Maeda, S., Mogu, G., and Honjo, S. (1973). Relapsing polychondritis - report of a case with ultrastructural findings of the ear cartilage. Acta. Pathol. Jpn., 23, 577.

Johnson, R.J., Lida, H., Alpers, C.E., Majesky, M.W., Schwartz, S.M., Pritzi, P., Gordon, K., and Gown, A.M. (1991). Expression of smooth muscle cell phenotype by rat mesangial cells in immune complex nephritis. α-smotth muscle actin is a marker of mesangial cell proliferation. J. Clin. Invest., 87, 847.

Jones, A.W., and Barson, A.J. (1971). Elastogenesis in the developing chick lung: a light and electron microscopical study. J. Anat., 110, 1

Kagan, H. M., Vaccaro, C.A., Bronson, R.E., Tang, S.S., and Brody, J.S. (1986). Ultrastructural immunolocalization of lysyl oxidase in vascular connective tissue. J. Cell Biol., 103, 1121.

Kainulainen, K., Pulkkinen, L., Savolainen, A., Kaitila, I., Peltonen, L. (1990a). Location of chromosome 15 of the gene defect causing Marfan syndrome. N. Engl. J. Med., 323, 935.

Kainulainen, K., Savolainen, A., Palotie, A., Kaitilia, I., Rosenbloom, J., and Peltonen, L. (1990b). Marfan syndrome: exclusion of genetic linkage of five genes coding for connective tissue components in the long arm of chromsome 2. Hum. Genet., 84, 233.

Kainulainen, K., B. Steinmann, F. Collins, H. C. Dietz, C. A. Francomano, A. Child, M. W. Kilpatrick, D. J. H. Brock, M. Keston, R. E. Pyeritz, I. Peltonen. (1991). Marfan syndrome: no evidence for heterogeneity in different populations and more precise mapping of the gene. Am. J. Hum. Genet., 49, 662.

Kainulainen, K., Sakai, L.Y., Child, A., Pope, M.F., Puhakka, L., Ryhanen, L., Palotie, A., Kaitila, I., and Peltonen, L. (1992). Two mutations in Marfan syndrome resulting in truncated polypeptide chains of fibrillin. Proc. Natl. Acad. Sci. U.S.A., 89, 5917.

Kainulainen, K., Karttunen, L., Puhakka, L., Sakai, L., and Peltone, L. (1994). Mutations in the fibrillin gene responsible for dominant ectopia lentis and neonatal Marfan syndrome. Nature Genet., 6, 64.

Kanzaki, T., Olofsson, A., Moren, A., Wernstedt, C., Hellman, U., Miyazono, K., Claesson-Welsh, L., Heldin, C.H. (1990). TGF-β1 binding protein: a component of the large latent complex of TGF-β1 with multiple repeat sequences. Cell, 61, 1051.

Karrer, H. E. (1958). The fine structure of connective tissue in the tunica propria of bronchioles. J. Ultrastruct. Res., 2, 96.

Karrer, H. E., and Cox, J. (1961). Electron microscope study of developing chick embryo aorta. J. Ultrastruct.Res., 4, 420.

Keene, D. R., Maddox, B.K., Kuo, H.J., Sakai, L.Y., and Glanville, R.W. (1991). Extraction of extendable beaded structures and their identification as fibrillin-containing extracellular matrix microfibrils. J. Histochem. Cytochem., 39, 441.

Kelley, M. R., Kidd, S., Deutsch, W.A., and Young M.W. (1987). Mutations altering the structure of epidermal growth factor-like coding sequences at the Drosophila Notch locus. Cell, 51, 539.

Kewley, M. A., Steven, F. S., and Williams, G. (1977a). Preparation of a specific antiserum towards the microfibrillar protein of elastic tissues. Immunology, 32, 483.

Kewley, M.A., Steven, F.S. and Williams, G. (1977b). Immunofluorescence studies with a specific antiserum to the microfibrillar protein of elastic fibres. Location in elastic and non-elastic connective tissues. Immunology, 33, 381.

Kobayashi, R., Tashima, Y., Masuda, H., Shozawa, T., Numata, Y., Miyauchi, K., and Hayakawa, T. (1989). Isolation and characterization of a new 36-kDa microfibril-associated glycoprotein from porcine aorta. J. Biol. Chem., 264, 17437.

Kostovic-Knezevic, L., Bradamante, Z., and Svajger, A. (1981). Ultrastructure of elastic cartilage in the rat external ear. Cell Tissue Res., 218, 149.

Kozak, M. (1991a). Structural features in eukaryotic mRNAs that modulate the initiation of translation. J. Biol. Chem., 266, 19867.

Kozak, M. (1991b). An analysis of vertebrate mRNA sequences: intimations of translational control. J. Cell Biol., 115, 887

Kumaratilake, J. S., Gibson, M. A., Fanning, J.C., and Cleary, E.G. (1989). The tissue distribution of microfibrils reacting with a monospecific antibody to MAGP, the major glycoprotein antigen of elastin-associated microfibrils. Eur. J. Cell Biol., 50, 117.

Labat-Robert, J., Bihari-Varga, M., Robert, L. (1990). Extracellular matrix. FEBS 268, 386.

Lee, B., Godfrey, M., Vitale, E., Hori, H., Mattei, M.G., Sarfarazi, M., Tsipouras, P., Ramirez, F., and Hollister, D.W. (1991). Linkage of Marfan syndrome and a phenotypically related disorder to two fibrillin genes. Nature, 352, 330.

Lefevre, M., and Rucker, R. B. (1980). Aorta elastin turnover in normal and hypercholesterolemic Japanese quail. Biochim. Biophys. Acta, 630, 519.

Leung, S., Whitelaw, E., and Proudfoot, N. J. (1989). Transcriptional and translational analysis of the human θ globin gene. Nucleic Acids Res., 17, 8283.

Loosi, C. G., and Potter, E. L. (1959). Pre- and post-natal development of the respiratory portion of the human lung. Amer. Rev. Resp. Dis., 80 Part II (suppl), 5.

Low, F. N. (1962). Microfibrils: fine filamentous components of the tissue space. Anat. Rec., 142, 131.

Maddox, B. K., Sakai, L.Y., Keene, D.R., and Glanville, R.W. (1989). Connective tissue microfibrils; isolation and characterization of three large pepsin-resistant domains of fibrillin. J. Biol .Chem., 264, 21381.

Manzella, J. M. and Blackshear, P.J. (1990) Regulation of rat ornithine decarboxylase mRNA translation by its 5' untranslated region. J. Biol. Chem., 265, 11817

Maslen, C. L., Corson, G.M., Maddox, B.K., Glanville, R.W., and Sakai, L.Y. (1991). Partial sequence of a candidate gene for the Marfan syndrome. Nature, 352, 334.

Mayer, B. W., Hay, E. D., and Hynes, R. O. (1981). Immunocytochemical localization of fibronectin in embryonic chick trunk and area vasculosa. Dev. Biol., 82, 267.

McCullagh, K.G. (1973). Studies on elephant aortic elastic tissue part I. The histochemistry and fine structure of the fiber. Exp. Mol. Path., 18: 190-201

McGookey-Milewicz, D., Pyeritz R.E., Crawford E.S., and Byers P.H. (1992). Marfan syndrome:defective synthesis, secretion and extracellular matrix formation of fibrillin by cultured dermal fibroblasts. J. Clin. Invest., 89, 79.

McKusick, V. (1956). In: Heritable Disorders of Connective Tissue. 1st Ed. St. Louis: CV Mosby.

Mecham, R. P., Whitehouse, L., Hay, M., Hinek, A., and Sheetz, M. (1991). Ligand affinity of the 67kDa elastin/laminin binding protein is modulated by the protein's lectin domain: Visualization of elastin/laminin receptor complexes with gold-tagged ligand. J. Cell Biol., 113, 187.

Mecham, R. P., and Hauser, J.E. (1992). The Elastic Fiber. In: Cell Biology of the Extracellular Matrix, 2nd Edition. E. D. Hay, Ed., Plenum Publishing Co., New York, pp. 79.

Nielsen, E. H. (1976). The elastic cartilage in the normal rat epiglottis. Cell tissue Res., 173, 179.

Ohlin, A-K., Linse S., and Stenflo J. (1988). Calcium binding to the epidermal growth factor homology region of bovine protein C. J. Biol. Chem. 261, 7411-7417.

Parks, W. C., Kolodziej, M. E., and Pierce, R. A. (1992). Phorbol ester-mediated downregulation of tropoelastin expression is controlled by a posttranscriptional mechanism. Biochemistry, 31, 6639.

Pasquali-Ronchetti, I., and Fornieri, C. (1984). The ultrastructural organization of the elastin fibre. In: Ultrastructure of the Connective Tissue Matrix. A. Ruggeri and P. M. Motta, Eds., Nijhoff, The Hague, pp. 126-139, .

Paz, M.A., Keith, D.A., and Gallop, P.M.(1982). Elastin isolation and cross-linking. Methods Enzymol. 82, 571.

Pereira, L., D'Alessio, M, Ramirez, F, Lynch, J.R., Sykes, Pangilinan, T, Bonadio, J (1993). Genomic organization of the sequence coding for fibrillin, the defective gene product in Marfan syndrome. Hum. Mol. Genet., 2, 961.

Perlman, D., and Halvorson, H.O., (1983). A putative signal peptidase recognition site and sequence in eukaryotic and prokaryotic signal peptides. J. Mol. Biol., 167, 391.

Pierce, R. A., Kolodziej, M. E., and Parks, W. C. (1992). 1, 25-dihydroxyvitamine D_3 represses tropoelastin expression by a posttranscriptional mechanisim. J. Biol. Chem., 267, 11593.

Prosser, I.W., Gibson, M.A. and Cleary, E.G. (1984). Microfibrillar protein from elastic tissue: a critical evaluation. J. Exp. Biol. Med. Sci. 62, 485.

Pyeritz, R. E., and McKusick, V.A. (1979). The Marfan syndrome:diagnosis and management. N. Engl. J. Med., 300, 772.

Pyeritz.R. E. (1990). Marfan syndrom. In: Principles and Practice of Medical Genetics. A. E. H. Emery and D.L. Rimoin, D. L., Eds, Churchill Livingstone, London, pp. 820.

Quintarelli, G., Starcher, B. C., Vacaturo, A., di Gianfilippo, F., Gotte, L., and Mecham, R. P. (1979). Fibrogenesis and biosynthesis of elastin in cartilage. Connect. Tissue Res., 7, 1.

Raju, K., and Anwar, R. A. (1987). Primary structures of bovine elastin a, b, and c deduced from the sequences of cDNA clones. J. Biol. Chem., 262, 5755.

Ramos Arroyo, M., Weaver, D. D., and Beals R. K. (1985). Congenital contractural arachnodactyly, report of four additional families and review of literature. Clinical Genetics, 27, 570.

Rao, C. D., Pech, M., Robbins, K.C., and Aaronson, S.A. (1988). The 5' untranslated sequence of the c-sis/platelet-derived growth factor 2 transcript is a potent translational inhibitor. Mol. Cell Biol., 8, 284

Raviola, G. (1971). The fine structure of the ciliary zonule and ciliary epithelium. Invest. Ophthalmol., 10, 851.

Rebay, I., Fleming, R.J., Fehon, R.G., Cherbas, L., Cherbas, P., and Artavanis-Tsakonas, S. (1991). Specific EGF repeats of Notch mediate interactions with Delta and Serrate:implications for Notch as a multifunctional receptor. Cell, 67, 687.

Rees, D.J.G., Jones, I.M., Handford, P.A., Walter,S. J., Esnouf, M. P., Smith, K. J., and Brownlee, G.G. (1988). The role of β-hydroxyaspartate and adjacent carboxylate residues in the first EGF domain of human factor IX. EMBO J., 7, 2053.

Ren, Z. X., Brewton, R.G., and Mayne, R. (1991). An analysis by rotary shadowing of the structure of the mammalian vitreous humor and zonular apparatus. J. Struct. Biol., 106, 57.

Robson, P. Wright, G. M., Sitarz, E., Maiti, A., Rawat, M., Youson, J. H., and Keeley, F. W. (1993). Characterization of lamprin, an unusual matrix protein from lamprey cartilage. J. Biol. Chem., 268, 1440.

Ross, R., and Bornstein, P. (1969). The elastic fiber. I. The seperation and partial characterization of its macromolecular components. J. Cell Biol., 40, 366.

Saiki, R.K. (1989). The design and optimization of the PCR. In: PCR Technology. H.A. Erlich , Ed., New York: Stockton Press.

Sakai, L. Y., Keene, D.R., and Engvall, E. (1986). Fibrillin, a new 350-kDa glycoprotein, is a component of extracellular microfibrils. J. Cell. Biol., 103, 2499.

Sakai, L. Y., Keene, D.R., Glanville, R.W., and Bachinger, H.P. (1991). Purification and partial characterization of fibrillin, a cysteine-rich structural component of connective tissue microfibrils. J. Biol. Chem., 266, 14763.

Sambrook, J., Fritsch, E.F., and Maniatis, T. (1989). Molecular Cloning: A Laboratory Manual., 2nd Edition. Cold Spring Harbor Laboratory Press, U.S.A.

Sanger, F., Air, G.M., Barrell, B.G. (1977). Nucleotide sequence of bacteriophage Phix174 DNA. Nature 265, 687.

Sandberg, L. B., Weissman, N., and Smith, D. W. (1969). The purification and partial characterization of a soluble elastin-like protein from copper-dedicient porcine aorta. Biochemistry, 8, 2940.

Sanzone, C. F., and Reith, E. J. (1976). The development of the elastic cartilage of the mouse pinna. Am. J. Anat., 146, 31.

Sarfarazi, M., P. Tsipouras, M. Boxer, M. P. O'Connell, A. H. Child, W. Murphy. (1992). Fine mapping of the region surrounding the Marfan syndrome locus on 15q1.5->2.1. J. Med. Genet.

Savino, W. (1982). The elastic system in the thymus of the opossum Didelphis marsupialis aurita. Anat. Anz., 151, 70.

Selander-Sunnerhagen, M., Ullner, M., Persson, E., Teleman, O., Stenflo, J., and Drakenberg, T. (1992). How an epidermal groth factor (EGF)-like domain binds calcium. J. Biol. Chem., 267, 19642.

Serafini-Fracassini, A., and Smith, J. W. (1974). In: Structure and Biochemistry of Cartilage. Churchill-Livingstone, Edinburgh and London, pp.220.

Serafini-Fracassini, A., Field, J. M., Spina, M., Stephens, W. G. S., and Delf, B. (1976). The molecular organization of the elastin fibrils. J. Mol. Biol., 100, 73.

Serafini-Fracassini, A., Venterella, G., Field, M.J., Hinnie, J., Onyezili, and Griffiths, R. (1981). Characterization of a structural glycoprotein from bovine ligamentum nuchae exhibiting dual amine oxidase activity. Biochemistry, 20, 5424.

Serafini-Fracassini, A. (1984). Elastogenesis in embryonic and post-natal development. In Ultrastructure of the Connective Tissue Matrix. A. Ruggeri and P.M. Motta Eds., Nijhoff, The Hague, pp. 140.

Shapiro, S. D., Endicott, S. K., Province, M. A., Pierce, J. A., and Campbell, E. J. (1991). Marked longevity of human lung parenchymal elastic fibers deduced from prevalence of D-aspartate and nuclear weapons-related radiocarbon. J. Clin. Invest., 87, 1828.

Streeten, B. W., Licari, P. A., Marucci, A. A., and Dougherty, R. M. (1981). Immunohistochemical comparison of ocular zonules and the microfibrils of elastic tissue. Invest. Ophthalmol. Visual Sci., 21, 130.

Tilson, D.M., Elefteriades, J. and Brophy, C.M. (1990) Tensile strength and collagen in abdominal aortic aneurysm disease. In: The Cause and Management of Aneurysm. M. Greenhalgh and J.A. Mannick, Eds., Latimer Trend & Co Ltd., Plymouth, UK, pp. 97.

Tokimitsu, I., Tajima, S., Nishikawa, T., Tajima, M., and Fukasawa, T. (1987). Sequence analysis of elastin cDNA from chick aorta and tissue-specific transcription of the elastin gene in developing chick embryo. Arch. Biochem. Biophys., 256, 455.

Tsipouras, P., Borrensen, A.L., Bamforth, S., Harper, P.S., and Berg, K. (1986). Marfan Syndrome: exclusion of genetic linkage to the COL1A2 gene. Clin. Genet., 30, 428.

Tsipouras, P., Sarfarazi, M., Devi, A., Weiffenbach, B., and Boxer, M. (1991). Marfan syndrome is closely linked to a marker on 15q1.5-q2.1. Proc. Natl. Acad. Sci.U.S.A., 88, 4486.

Tsipouras, P., Del Mastro, R., Sarfarazi, M., Lee, B., Vitale, E., Child, A., Godfrey, M., Devereux, R., Hewett, D., Steinmann, B., Viljoen, D., Sykes, B.C., Kilkpatrick, M., and Ramirez, F. (1992). Linkage of Marfan syndrome, dominant ectopia lentis and congenital contractural arachnodactyl to the fibrillin genes on chromsomes 15 and 5. N. Engl. J. Med., 326, 905.

Uhlenbeck, O. C. (1987). A small catalytic oligoribonucleotide. Nature, 328, 596.

Urry, D. W. (1984). Protein elasticity based on conformations of sequential polypeptides: the biological elastic fiber. J. Prot. Chem., 3, 403.

Warrell, E., and Taylor, J. F. (1979) The role of periosteal tension in the growth of long bones. J. Anat., 128, 179.

Weis-Fogh, T., and Andersen, S. O. (1970). New molecular model for the long-range elasticity of elastin. Nature, 227, 718.

Wright, D. W., and Mayne, R. (1988). Vitreous humor of chicken contains two fibrillar systems: an analysis of their structure. J. Ultrastr. Mol. Struc. Res., 100, 224.

Yeh, H., Ornstein-Goldstein, N., Indik, Z., Sheppard, P., Anderson, N., Rosenbloom, J. C., Cicila, G., Yoon, K., and Rosenbloom, J. (1987). Sequence variation of bovine elastin mRNA due to alternative splicing. Collagen Relat. Res., 7, 235.

Yin, W., Germiller, J., Sanguineti, C., Smiley, E., Pereira, L., Ramirez, F., and Bonadio, J. (1994). Primary structure and developmental expression of *Fbn1*, the mouse fibrillin gene. J. Biol. Chem., in press.

Yu, S. Y., and Lai, S. E. (1970). Structure of aortic elastic fiber: An electron microscopic study with special reference to staining by Ruthenium Red. J. Electron Micros., 19(4), 362.

Zhang, H., Apfelroth, S.D., Hu, W., Davis, E.C., Sanguineti, C. (1994). Structure and expression of fibrillin-2, a novel microfibrillar component preferentially located in elastic matrices. J. Cell. Biol., 124, 855.